NASA/TM-2004-213010

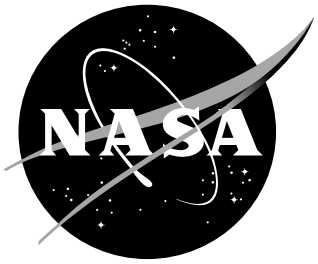

Portable Wireless LAN Device and Two-Way Radio Threat Assessment for Aircraft VHF Communication Radio Band

Truong X. Nguyen, Sandra V. Koppen, Jay J. Ely,
Reuben A. Williams and Laura J. Smith
Langley Research Center, Hampton, Virginia

Maria Theresa P. Salud
Lockheed Martin, Hampton, Virginia

March 2004

The NASA STI Program Office ... in Profile

Since its founding, NASA has been dedicated to the advancement of aeronautics and space science. The NASA Scientific and Technical Information (STI) Program Office plays a key part in helping NASA maintain this important role.

The NASA STI Program Office is operated by Langley Research Center, the lead center for NASA's scientific and technical information. The NASA STI Program Office provides access to the NASA STI Database, the largest collection of aeronautical and space science STI in the world. The Program Office is also NASA's institutional mechanism for disseminating the results of its research and development activities. These results are published by NASA in the NASA STI Report Series, which includes the following report types:

- TECHNICAL PUBLICATION. Reports of completed research or a major significant phase of research that present the results of NASA programs and include extensive data or theoretical analysis. Includes compilations of significant scientific and technical data and information deemed to be of continuing reference value. NASA counterpart of peer-reviewed formal professional papers, but having less stringent limitations on manuscript length and extent of graphic presentations.

- TECHNICAL MEMORANDUM. Scientific and technical findings that are preliminary or of specialized interest, e.g., quick release reports, working papers, and bibliographies that contain minimal annotation. Does not contain extensive analysis.

- CONTRACTOR REPORT. Scientific and technical findings by NASA-sponsored contractors and grantees.

- CONFERENCE PUBLICATION. Collected papers from scientific and technical conferences, symposia, seminars, or other meetings sponsored or co-sponsored by NASA.

- SPECIAL PUBLICATION. Scientific, technical, or historical information from NASA programs, projects, and missions, often concerned with subjects having substantial public interest.

- TECHNICAL TRANSLATION. English-language translations of foreign scientific and technical material pertinent to NASA's mission.

Specialized services that complement the STI Program Office's diverse offerings include creating custom thesauri, building customized databases, organizing and publishing research results ... even providing videos.

For more information about the NASA STI Program Office, see the following:

- Access the NASA STI Program Home Page at ***http://www.sti.nasa.gov***

- E-mail your question via the Internet to help@sti.nasa.gov

- Fax your question to the NASA STI Help Desk at (301) 621-0134

- Phone the NASA STI Help Desk at (301) 621-0390

- Write to:
  NASA STI Help Desk
  NASA Center for AeroSpace Information
  7121 Standard Drive
  Hanover, MD 21076-1320

NASA/TM-2004-213010

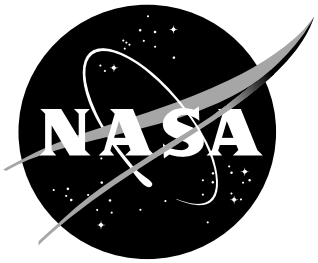

Portable Wireless LAN Device and Two-Way Radio Threat Assessment for Aircraft VHF Communication Radio Band

Truong X. Nguyen, Sandra V. Koppen, Jay J. Ely,
Reuben A. Williams and Laura J. Smith
Langley Research Center, Hampton, Virginia

Maria Theresa P. Salud
Lockheed Martin, Hampton, Virginia

National Aeronautics and
Space Administration

Langley Research Center
Hampton, Virginia 23681-2199

March 2004

Acknowledgments

The authors wish to express their gratitude to Dave Walen, John Dimtroff, and Tony Wilson of the Federal Aviation Administration for their continuing support and technical direction.

This work was funded by the Federal Aviation Administration as part of FAA/NASA Interagency Agreement DFTA03-96-X-90001, Revision 9, as well as the NASA Aviation Safety Program (Single Aircraft Accident Prevention Project)

Available from:

NASA Center for AeroSpace Information (CASI)
7121 Standard Drive
Hanover, MD 21076-1320
(301) 621-0390

National Technical Information Service (NTIS)
5285 Port Royal Road
Springfield, VA 22161-2171
(703) 605-6000

Table of Contents

Acronyms

AP	Access Point
ATCRBS	Air Traffic Control Radar Beacon System
B737, B747	Boeing 737, 747 Aircraft
BPSK	Binary Phase Shift Keying
CW	Continuous-wave
dBi	dB relative to isotropic reference pattern
dBm	dB relative to 1 milliwatt
dBμV/m	Field strength unit in dB relative to one μV/m
DME	Distance Measuring Equipment
DSSS	Direct Sequence Spread Spectrum
DUT	Device-Under-Test
EE	Emergency Exit
EMI	Electromagnetic Interference
EWI	Eagles Wings Inc.
FAA	Federal Aviation Administration
FCC	Federal Communications Commission
FHSS	Frequency Hopping Spread Spectrum
FRS	Family Radio Service
GFSK	Guassian Frequency Shift Keying
GHz	Gigahertz
GMRS	General Mobile Radio Service
GPS	Global Positioning System
GS	Glideslope
HIRF	High Intensity Radiated Fields
ICAO	International Civil Aviation Organisation
IEEE	Institute of Electrical and Electronics Engineers
ILS	Instrument Landing System
IPL	Interference Path Loss
LAP1-8	Laptop computers 1-8. See details in Table 3.2-4
LaRC	Langley Research Center
LOC	Localizer
MAX, Max	Maximum
MHz	Megahertz
Min	Minimum
MIPL	Minimum Interference Path Loss
MLS	Microwave Landing Systems

MOPS	Minimum Operating Performance Standards
NASA	National Aeronautics and Space Administration
NIC	Network Interface Card
NIST	National Institute of Standards and Technology
PCMCIA	Personal Computer Memory Card Interface Adapter
PC Card	PCMCIA Card
PDA	Personal Digital Assistant
PED	Portable Electronic Device
PLF	Path Loss Factor
PRN	Printer
PS	Ping Storm
QAM	Quadrature Amplitude Modulation
QPSK	Quadrature Phase Shift Keying
RC	Reverberation Chamber, or Mode-Stirred Chamber
RF	Radio Frequency
RTCA	RTCA, Inc.
SAC	Semi-anechoic Chamber
SatCom	Satellite Communication (Aeronautical Mobile Satellite Service)
SD	Secure Digital
StDev	Standard Deviation
TCAS	Traffic Collision Avoidance System
TCP/IP	Transmission Control Protocol/ Internet Protocol
UAL	United Airlines
UNII	Unlicensed National Information Infrastructure Band
US	United States
USB	Universal Serial Bus
VEE	Visual Engineering Environment
VHF Com	Very High Frequency Voice Communication
VHF-Com 1	VHF-Com radio no. 1
VOR	VHF Omnidirectional Range
WECA	Wireless Ethernet Compatibility Alliance
Wi-Fi	Wireless Fidelity
WLAN	Wireless Local Area Network
WPAN	Wireless Personal Area Network
Xfer	Duplex File Transfer

List of Symbols

π	Universal constant = 3.141592654
η_{Tx}	Transmit antenna efficiency factor
A	Device emission power
B	Interference coupling factor, negative of interference path loss in dB
C	Receiver susceptibility threshold
CF	Chamber Calibration Factor (dB)
CLF	Chamber Loading Factor
D_G	Directivity
E	Electric Field Intensity (V/m)
$EIRP$	Effective Isotropic Radiated Power (W)
IL	Empty chamber Insertion Loss
$L_{Chmbr(dB)}$	Chamber loss (dB), or = $-10log_{10}(CLF * IL)$
$L_{RecCable(dB)}$	Receive cable loss (dB)
$L_{XmitCable(dB)}$	Transmit cable loss (dB)
P_c	Carrier frequency power
P_{input}	Input power
P_{MaxRec}	Maximum received power measured over one paddle rotation
$P^R(2), P^R(3)$	Power received at points (2) and (3), respectively, in dBm
$P_{SAMeas(dBm)}$	Maximum receive power measured at the spectrum analyzer (dBm) over one stirrer revolution
$P^T(1),$	Power transmitted at point (1), in dBm
P_{TotRad}	Total radiated power within measurement resolution bandwidth
$P_{Xmit(dBm)}$	Power transmitted from source (dBm)
R	Distance (m)
Rx	Receive
S/I	Signal-to-Interference Ratio
TRP	Total Radiated Power (within measurement resolution bandwidth)
Tx	Transmit

Abstract

Measurement processes, data and analysis are provided to address the concern for Wireless Local Area Network devices and two-way radios to cause electromagnetic interference to aircraft Very High Frequency (VHF) Voice Communication system. In this study, spurious radiated emissions in the VHF band from various wireless network devices and two-way radios are characterized using a reverberation chamber. The results are compared against baseline measurement results from standard laptop computers and personal-digital-assistants as these devices are currently allowed for use during parts of flight. Also reported are aircraft interference path loss data and in-band on-channel interference threshold in the VHF band. From these data, interference risk is assessed for the aircraft VHF communication system.

1 Executive Summary

Wireless technologies are widely adopted in the present consumer market. Technologies such as cellular phones and wireless local area networks (WLANs) have brought a revolution in accessibility and productivity. WLANs enable consumers to have convenient access to web-browsing, email, instant messaging and numerous enterprise applications. As travelers become more dependent upon Internet access, airlines are increasingly interested in providing connectivity to their customers while traveling onboard aircraft. While WLAN equipment provided by the airlines for permanent installation on the aircraft must be properly certified, passenger carry-on products are not required to pass the rigorous aircraft radiated field emission standards.

Two-way radio communications, such as Family Radio Service (FRS) and General Mobile Radio Service (GMRS), are also becoming popular. These no-fee radio systems allow family members, friends and business associates to stay in contact during trips, shopping, or where party members may be physically dispersed. Unlike the low power FRS radios with half-watt maximum transmitted power, GMRS radio can radiate much higher power. Two-watt GMRS radio models, which require a license presently, are highly popular. Many recent models have both FRS and GMRS built-in features. While use of these radios is not presently authorized on aircraft, their low cost and popularity hint that their use by unsuspecting passengers is likely.

With the support of the Federal Aviation Administration (FAA) Aircraft Certification Office and the National Aeronautics and Space Administration (NASA) - Aviation Safety Program - Single Aircraft Accident Prevention Project, radio frequency (RF) emissions from portable WLAN devices and two-way radios were measured. In addition, results of interference path loss (IPL) measurements conducted with an airline partner are provided to quantify the attenuation levels for emission from inside the passenger cabin. These emission and path loss data are used to assess potential risks to aircraft systems.

An earlier report [1] documented the measurement of spurious emissions and the results of multiple WLAN devices and of several pairs of two-way radios. Data were reported in multiple aircraft radio

bands. Also reported were the measurements and results of aircraft interference path loss between the passenger cabin and various aircraft communication and navigation bands. From the data, interference safety margins were computed for many aircraft radio systems using interference thresholds documented in an existing standard. VHF Voice Communication (VHF-Com) band was not included in this study

At the request of the FAA, this report supplements the earlier report [1] by providing spurious emission data in the VHF-Com bands from the same WLAN devices and two-way radios. The emission results were collected using the same measurement process, equipment and test chamber as in the earlier effort. The results are also compared against emissions from standard laptop computers and Personal Digital Assistants (PDAs) in the same band. These devices are used as benchmarks since they are currently allowed for use during certain non-critical phases of flight.

This document also repeats the previously reported VHF-Com band IPL data for completeness and relevancy to the current analyses. These data were measured on the several Boeing 747-400 and Boeing 737-200 aircraft as a part of the cooperative efforts between United Airlines (UAL), Eagle Wings Incorporated and NASA Langley Research Center (LaRC). Also reported are existing data that come from other standards, references, and other previous NASA cooperative efforts. With the new emission data, the minimum IPL, and the VHF band interference threshold from an existing standard, interferece safety margins are calculated.

In this document, spurious emissions are emissions at frequencies that are outside the necessary bandwidth, and the level of which may be reduced without affecting the corresponding transmissions of information. Out-of-band emissions, or emissions at frequencies immediately outside the necessary bandwidth, are excluded.

Radiated Emission Measurement

Radiated emissions from WLAN devices and two-way radios were measured in a reverberation chamber (RC) at NASA LaRC. The WLAN devices tested include seven Institute of Electrical and Electronics Engineers (IEEE) 802.11b, five IEEE 802.11a, and six Bluetooth devices. As a result of the earlier preliminary testing, WLAN operating modes, channels, and data rates were previously identified in [1] and uniformly adopted for more extensive tests. FRS and GMRS radio operations were simple and no such preliminary testing was needed.

A preliminary set of tests [1] were also conducted, which involved selecting host laptop computers and PDAs with low emissions so they would not mask emissions from the WLAN devices under test. The screening involved emission measurement of eight laptop computers and two PDAs in various operational modes. The host laptop and PDA were selected using the criteria of having the lowest emissions in the measurement frequency band while operating in idle and file transfer modes. This screening identified a laptop computer and both PDAs, and they were chosen as a host device for the VHF-Com band.

The RC emission measurement method used was adopted from the earlier effort to assess the risk of interference from wireless phones to aircraft radio receivers [2]. The RC method was efficient, accurate, and repeatable. It also provided results directly in terms of effective peak radiated power, rather than electric field strength, so that an approximate conversion from field strengths to radiated power was not needed. Filters were used to block intentional high power transmission from the WLAN devices from reaching the receiver, preventing undesirable receiver overloading and intermodulation. Filters were also used to block spurious emissions from the WLAN AP, if any, from radiating in the chamber and contaminating the environment.

Interference Path Loss Measurement

Interference path loss (IPL) data for the VHF band is repeated from the earlier report [1] for completeness and relevancy to the analysis. IPL measurement was another major effort to help assess risks of interference to aircraft systems from passenger carry-on devices. IPL represents the attenuation to the interference signals as they propagate from the Portable Electronic Device (PED) in the passenger cabin to the aircraft system antenna and into its receivers.

As reported in [1], the measurements were conducted on four Boeing 747-400 and six Boeing 737-200 airplanes provided by UAL during three one-week trips to Southern California Aviation facility in Victorville, California. Several aircraft systems were measured, including Localizer (LOC), Glideslope (GS), Very High Frequency Omnidirectional Range (VOR), VHF-Com, Global Positioning Systems (GPS), Traffic Collision Avoidance System (TCAS), and Satellite Communication (SatCom). The measurements were conducted with a radiating antenna positioned at windows and doors, while a spectrum analyzer recorded the maximum signals coupled into aircraft antennas. The transmitting antenna was also positioned at locations other than windows and doors on two aircraft, and the end comparison indicates that the door and window measurements indeed captured the minimum IPL values. The results indicate that for the VHF-Com system, the minimum IPL is strongly affected by the antenna locations relative to an aircraft door. The measured VHF-Com IPL data are summarized in this report along with other previously available IPL data, and the all-aircraft minimum IPL values are shown.

Interference Safety Margin

Interference analysis was conducted using the WLAN and two-way radios emission results, the IPL data, and the receiver interference thresholds from a standard document. Interference safety margins were calculated for each combination of WLAN/radio device, minimum or average IPL, and the interference threshold. The resulting safety margin can be positive or negative. However, it was seen that WLAN devices have better safety margins than laptops and PDAs in the VHF-Com band due to their lower emissions.

Conclusions

Spurious emissions in the VHF-Com radio band from selected WLAN devices were lower than from laptop computers and PDAs, indicating that the WLAN devices tested are not any more threatening to the band than the common laptop computers and PDAs.

1. GMRS radio emissions are higher than from the laptops/PDAs.

2. Spurious emissions from WLAN devices are lower than Federal Communications Commission (FCC) Part 15 limits, but can be equal to or higher than (especially if directive gain is included) aircraft RTCA/DO-160D Category M emission limits.

3. Interference safety margin can be positive or negative, and can vary broadly depending on the IPL and interference threshold values used.

Recommended Future Work:

1. Additional receiver interference threshold data are needed for greater confidence level. More tests on a number of receivers from multiple manufacturers are recommended. Signal modulation and types should be considered.

2. Conduct emission measurements and interference analysis on other types of wireless devices, particularly those utilizing newly available RF bands and having multi-band capability. Some of the current and future wireless trends include 2.5G and 3G phones with GPS receiver circuitry, software-defined-radios, phones/PDAs with built-in camera and other smart features, Radio Frequency Identification (RFID) tags.

3. Assess the potential for emerging radio technologies that overlay existing spectrum (such as Ultra Wideband) to cause interference to aircraft systems.

4. Conduct additional IPL measurements on different types of aircraft where minimal data currently exists.

5. Assess impacts of multiple devices.

6. Initiate flight operational assessment of PED electromagnetic interference (EMI) to aircraft radios, addressing safety impact of EMI as affected by navigation data processing and redundancy management within specific avionics packages, including the influence of crew and air traffic control procedures.

2 Introduction

Wireless technologies have brought a revolution in personal accessibility and productivity, and have created new markets for products and services. WLANs enable convenient and affordable web-browsing, email, instant messaging and numerous enterprise applications in high-traffic public places such as restaurants, coffee shops, shopping malls, convention centers, hotels, and airports. As travelers become more dependent upon Internet access at places away from home or office, airlines are becoming more interested in providing connectivity to their customers while traveling on board aircraft.

The use of unauthorized intentional transmitters, such as WLAN devices, wireless phones and citizen's band radios are of growing concern to the FAA and to the airlines who are responsible for passenger safety. While WLAN equipment provided by the airlines for permanent installation on the aircraft must be properly certified, the passenger carry-on products are not required to pass the rigorous aircraft radiated-field emission standards. Demanding certification for use on aircraft is considered impractical due to enforceability issues that could result in poor customer relations.

FRS and GMRS are becoming popular as family members, friends and business associates desire to stay connected during trips, shopping or where members may be physically dispersed. On an aircraft, unaware passengers may attempt to use these radios to communicate with others whose seats may be assigned at different locations on the aircraft. Use of these radios by American travelers/tourists has been observed in foreign countries where their use was not yet allowed. With two watts of radiated power, GMRS radio is attractive due to extended range and increased channel capacity compared to the lower-power FRS radio. GMRS radio is readily available but requires a license to operate. However, it is unrealistic to assume that all users are aware of (or willing to comply with) the requirements of application submission and high fees. The popularity and low cost of the FRS and GMRS radios make it reasonable to assume that their use on airplanes by unsuspecting passengers is inevitable.

This report builds upon detailed threat assessments of wireless phones, portable WLAN devices, and GMRS/FRS two-way radios previously performed [1,2]. The previous NASA reports introduced a radiated emission measurement process in various aircraft communication and navigation bands. These NASA reports drew extensively from RTCA Special Committee reports published in 1988 (RTCA/DO-199 [3]) and 1996 (RTCA/DO-233 [4]), which remain the foundation for regulatory and advisory guidance for the FAA and other comparable agencies worldwide. This report extends the earlier NASA work by including the emission measurements from the WLAN devices and two-way radios in the aircraft VHF-Com band. The report is supplemented with detailed aircraft IPL and navigation radio interference threshold data from reference documents, standards and previous NASA partnerships.

The NASA efforts described in this report, as well as those documented in [1] and [2], were accomplished with the support of the FAA Aircraft Certification Office and the NASA Aviation Safety Program. Additional path loss data were measured under a cooperative agreement with UAL and EWI. These measurements were conducted for various aircraft radio receivers on four Boeing B747-400 and six Boeing B737-200 aircraft. Utilizing receiver susceptibility threshold data from RTCA/DO-199, interference safety margins were calculated and presented. The following subsections describe the objectives, the approach to measure spurious emissions, and the report organization.

2.1 Objective

The primary objectives of this report were to describe the radiated emission measurement process and test results for WLAN devices and two-way FRS/GMRS radios, to report the results of aircraft IPL measurement, and to provide interference risk assessment to aircraft VHF-Com system.

2.2 Approach

Assessment of aircraft radio receiver interference is typically accomplished by addressing the three elements of the equation:

$$A + B \geq C , \qquad \text{(Eq. 2.2-1)}$$

at any frequency in the aircraft radio navigation bands, where

"*A*" is the maximum RF emission from the offending device in dBm,

"*B*" is the maximum interference coupling factor in dB; "*-B*", in dB, is commonly referred to as the minimum IPL,

"*C*" is the receiver's minimum in-band, on-channel interference threshold in dBm.

If the minimum interference threshold, "*C*", is lower than the maximum interference signal level at the receiver's antenna port, "(*A* + *B*)", there is a potential for interference.

A primary focus of this effort was to measure the maximum RF emission, "*A*", from WLAN devices and two-way FRS/GMRS radios. In this report, the WLAN devices considered include IEEE 802.11a, IEEE 802.11b, and Bluetooth devices. Technically, Bluetooth is classified under Wireless Personal Area Network (WPAN) but it is grouped under WLAN in this report for simplicity.

The minimum IPL, "-B", for the VHF-Com band is reported for several B747 and B737 aircraft. These IPL data are summarized in this report and compared to other data previously available. The IPL data were previously reported in [1], but are repeated in this document for the VHF band due to the relevancy to the analysis.

Receiver interference thresholds "C" were not measured in this effort. Rather, test data from RTCA/DO-199 were used in evaluating interference risks to aircraft systems. DO-199 provided receiver interference threshold data on a limited number of receivers. Additional testing to include more receivers and more systems is highly desirable. Aircraft radio manufacturers are best equipped to address this issue as they should have access to multiple aircraft receivers and the in-depth knowledge of receiver operations and designs.

Sections 2.2.1 and 2.2.2 discuss in more detail the emission and path loss measurement approaches.

2.2.1 Emission Measurements of WLAN Devices and Two-Way Radios

Data in this document are reported following the same format as in [1]. In [1], emission measurements were grouped into measurement bands to simplify the process and to reduce the number of measurements. Aircraft radio bands that overlapped, or were near one another were grouped together, and emissions were measured across the entire combined band simultaneously. Five frequency groups, designated as

measurement Band 1 to Band 5, covered many aircraft radio bands of interest, including Instrument Landing System (ILS), LOC, VOR, GS, TCAS, Air Traffic Control Radar Beacon System (ATCRBS), Distance Measuring Equipment (DME), GPS, and Microwave Landing Systems (MLS).

Also of interest is the VHF-Com band, which was omitted in [1]. In this document, new emission data in the VHF-Com band are reported, along with IPL data, susceptibility threshold, and safety factor calculations. A new measurement band, designated as Band 1a, is created specifically for the VHF-Com band. In future measurements, Band 1 and Band 1a may be combined into a single measurement due to the proximity of the frequencies. Table 2.2-1 correlates the measurement bands to aircraft radio frequencies, with only Band 1a data shown in this report.

Similar to [1], it is assumed that high emissions anywhere in Band 1a would affect the entire VHF-Com band. No effort is taken to distinguish whether the emissions were on any specific VHF-Com channels.

A RC was used to measure RF emissions from a device-under-test (DUT), with the results being *total radiated power* (TRP) [5]. This method differs from the approach used in RTCA/DO-199, where the TRP was estimated from the electric field measured at a given distance from a DUT. Further details about conducting emission measurements in a RC are found in Section 3.

The measurement process began with selecting host computer laptops/PDAs for the WLAN devices. This step ensured that spurious emissions from the intended WLAN devices were not masked by emissions from a noisy host laptop/PDA. This selection involved measuring emissions from eight different laptops and two PDAs operating in various modes. The laptop/PDAs with the lowest emissions in the idle and file transfer modes in Band 1a were chosen for that band. The idle and the file transfer modes were typical laptop modes while emission measurements of the WLAN devices were being conducted. In addition, emission data of the laptop computers with all operating modes considered established an emission baseline for devices that could be used onboard an aircraft. Emissions from intentional transmitters such as WLAN devices were compared against this baseline.

Table 2.2-1: Emission Measurement Band Designations and Corresponding Aircraft Radio Bands. Only Data in Band 1a Are Reported in This Document.

Measurement Band Designation	**Measurement Freq. Range (MHz)**	**Aircraft Systems Covered**	**Spectrum (MHz)**
Band 1	105 – 120	LOC	108.1 – 111.95
		VOR	108 – 117.95
Band 1a	**116 – 140**	**VHF-Com**	**118 - 138**
Band 2	325 – 340	GS	328.6 – 335.4
Band 3	960 – 1250	TCAS	1090
		ATCRBS	1030
		DME	962 - 1213
		GPS L2	1227.60
		GPS L5	1176.45
Band 4	1565 – 1585	GPS L1	1575.42 ± 2
Band 5	5020 - 5100	MLS	5031 – 5090.7

Similar to the process reported in [1], emission measurements were conducted on five 802.11a, seven 802.11b and six Bluetooth WLAN devices. The WLAN devices were exercised through various modes, channels, and data rates during the emission measurement. Various filter combinations were used in the wireless AP antenna path to allow only the intended wireless signal to radiate for communication with the DUTs, and block spurious emissions from the APs. Additional filters were also used in the measurement path to prevent the wireless signals (from the wireless cards and the AP) from reaching the measuring instrument to cause overloading or intermodulation.

Emissions were also measured on four matched pairs of FRS radios and three matched pairs of GMRS radios. Emissions from a matched pair were measured at the same time, with each radio in turn being in transmit, receive, and idle modes. Thus, a recorded measurement trace includes the maximum emissions from both radios in all three modes. The radios were also cycled through at least two frequency channels during each measurement. Again, filters were employed to prevent overloading of the measurement receiver. For two-way FRS/GMRS radios, no host screening was needed since these devices can operate without one.

Further details are discussed in Section 3 of this report.

2.2.2 Path Loss Measurements

An earlier effort, reported in [1], supplemented existing interference path loss data with measurements on four B747-400 and six B737-200 aircraft. Three separate measurement trips were made to an aircraft storage facility in Victorville, California to measurement on VHF-Com system, along with LOC, VOR, GS, TCAS, SatCom and GPS systems (if available). The measurements were conducted at different windows along each aircraft, and the *minimum* path losses for the aircraft systems were summarized and reported. The VHF band data are repeated in this document due to relevancy to the current analysis. In addition, the measurement process is briefly described in a later section.

2.2.3 Safety Margin Calculations

With device emission "A", path loss "-B" and interference threshold "C" known, the safety margin was calculated as:

$$Safety\ Margin = C - (A + B) \qquad \text{(Eq. 2.2-2)}$$

Results of the safety margin calculations are reported in Section 5.

2.3 Report Organization

The organization of this report parallels that of [1] for ease of comparison. Measurement of emissions from WLAN devices and two-way radios is described in Section 3. The method is described in 3.2, and a summary of the results is provided in Section 3.3. Section 3.4 summarizes emission data from non-intentional transmitting laptops and PDAs. Section 3.5 compares results from all measurements reported in Sections 3.3 and 3.4. More detailed emission measurement results are shown in Appendix A for WLAN devices and two-way radios, and in Appendix B for laptops and PDAs.

Section 4 describes IPL measurements and results for Boeing 747 and 737 aircraft, and a comparison with other previously available path loss data. Section 4.1 summarizes the aircraft measurements, with detailed descriptions in 4.1.1 and results in 4.1.2. Section 4.2 shows the *minimum* and the *average* IPL for each of the measured B737 and B747 aircraft, along with similar data previously reported. Section 4.3 further condenses the data by showing the all-aircraft statistics of the minimum IPL. The lowest and the average values of the minimum IPL were used in the safety margin calculations in Section 5.

Section 5 briefly summarizes the interference threshold data from RTCA/DO-199. In this section, interference safety margins for each aircraft system of interest are calculated and reported from the emission data, the IPL data, and the susceptibility thresholds.

3 WLAN and Radio RF Emissions

3.1 Wireless Overview

IEEE 802.11a, IEEE 802.11b, and Bluetooth wireless network technologies and FRS/GMRS radios are described in this section. Table 3.1-1 lists types of devices used for this assessment with associated transmission frequency bands and operating parameters. In addition, the power used during radiated emission testing and the maximum permitted output powers, as specified by the corresponding standards or regulatory limits, are listed.

3.1.1 IEEE 802.11a

IEEE 802.11a is a very high-speed, high-bandwidth standard and a variant of the IEEE 802.11 standard. It expands on the 802.11 network standard to define WLAN operating parameters, providing access to outside networks for wireless devices, including local intercommunication. The 802.11a standard requires that data rates of 6, 12, and 24 Mbits/s must be supported; however, maximum rates of 54 Mbits/s are common. Each data rate uses a particular modulation technique to encode data. Higher data rates are achieved by employing advanced modulation techniques. Devices using 802.11a operate in the 5 GHz Unlicensed National Information Infrastructure Band (UNII). The bandwidth of 300 MHz is composed of three bands that legally operate in the US; the first band of 5.15 to 5.25 GHz uses 50 mW maximum power, the second band of 5.25 to 5.35 GHz uses 200 mW maximum power, and a third band of 5.725 to 5.825 GHz uses 800 mW maximum power [6]. The first and second bands contain eight non-overlapping 20 MHz channels. A typical application of 802.11a technology is a wireless NIC inserted into a laptop Personal Computer Memory Card Interface Adapter (PCMCIA) slot. The NIC converts the laptop, a non-intentional transmitter, to a wireless PED, capable of transmission and intercommunication with other wireless devices or APs.

3.1.2 IEEE 802.11b

The IEEE 802.11b standard provides location independent access to an outside network between wireless data devices, including intercommunication on a local scale. Primarily an extension of the 802.11 standard, it defines additional operational parameters for high-rate data transfers on WLANs while maintaining 802.11 protocols. Devices using 802.11b operate in the 2.4 GHz band, which is divided into fourteen 22 MHz channels, eleven of which legally operate in the US. Adjacent channels partially overlap, except for three of the 14, which are completely non-overlapping. The 802.11b standard utilizes a Direct Sequence Spread Spectrum (DSSS) modulation mode, as defined by 802.11, and advanced coding techniques to achieve higher data rates of 5.5 Mbit/s and 11 Mbit/s. The coding techniques

employ different modulation schemes at different data rates. The FCC allows a maximum output power of 1000 mW. However, if a power level greater than 100 mW is used, then power control must be provided by the system [6]. A distance range of 100 meters is typical, but ranges are dependent upon environmental obstacles and power. A typical application of 802.11b technology is a wireless NIC inserted into a laptop PCMCIA slot. As with 802.11a devices, a non-intentional transmitter is converted to an intentional transmitter that is capable of intercommunication with other wireless devices or APs.

After the measurements on 802.11b devices were made [1], a new IEEE 802.11g standard was introduced. This new standard has the theoretical data rate of up to 54 Mbits/s while using the same 2.4 GHz frequency allocation as the older IEEE 802.11b standard. For 802.11b compatibility, 802.11g incorportates 802.11b's Complementary Code Keying (CCK) to achieve up to 11 Mbits/s. In addition, 802.11g adopts 802.11a's Orthogonal Frequency Division Multiplexing (OFDM) for 54 Mbits/s data rate, but in the 2.4 GHz frequency range. 802.11g also comes with 22 Mbits/s speed using two optional and incompatible modes introduced by two different vendors.

802.11g devices' physical constructions are in many ways very similar to 802.11b devices. It is expected that their emission characteristics are, therefore, similar. While it is possible to have additional testing on 802.11g devices in the future, this document is restricted to reporting only the emission results from the same wireless LAN devices used in [1].

3.1.3 Bluetooth

Bluetooth is a short-range radio technology with the capability to link together different wireless devices providing for data and limited voice communication. Bluetooth uses 79 channels separated by 1 MHz each, from 2.4 to 2.48 GHz. The Bluetooth standard supports development of low cost and low power wireless devices. The specification allows for three power classes [7]. Power control is required for devices utilizing class one levels, and must be able to control and limit transmit power over 1 mW (0 dBm) [7]. Power control is optional at levels under 0 dBm, but may be employed in order to conserve power. Bluetooth units operate with a maximum data rate of 11 Mbps, and a power level up to 100 mW. The nominal distance between devices is 0.3 to 10 meters; however, greater distances are achieved with higher power. It uses Gaussian Frequency Shift Keying (GFSK) modulation combined with Frequency-Hopping Spread Spectrum (FHSS) techniques for data transmission [7]. A Bluetooth transmitter hops among 79 frequencies at a rate of 1600 hops per second.

3.1.4 FRS/GMRS Radios

FRS and GMRS radios are legal, modern, two-way communication devices in the US and Canada. These devices are more compact and more efficient than their walkie-talkie predecessors. They also have a longer communication range, less distortion, better signal reception, and more effective penetration of building structures. Both types of radios utilize 38 subcodes in each of the main channels, which enable users to achieve a semi-private conversation. A subcode is an interference filter allowing only the signals designated to a particular subcode on a channel to be heard by the users, blocking all other signals.

Several users in fairly close proximity, fewer than two miles, are able to communicate with unlicensed FRS devices. However, if communication beyond 2 miles is needed, a licensed-GMRS device may be used. GMRS regulations do not permit superficial chatter between individuals on this service, unlike the FRS radio regulations. GMRS has a larger coverage area because of the higher output power and the ability to use repeaters in the coverage area. Table 3.1-1 provides a comparison of the two radios.

Table 3.1-1: Wireless Technology Parameters

Wireless Technology	Frequency Band (GHz)	Typical Data Rates (Mbps)	Number of Channels	Maximum Output Power per Std. / per Test (mW)	Typical Range
802.11a	5.15 – 5.825	6, 12, 24, 54	12*	800 / 40 & 200	50 meters
802.11b	2.4 – 2.4835	1, 2, 5.5, 11	11*	1000 / 100	24 – 100 meters
Bluetooth	2.4 – 2.4835	1	79'	100 / < 1**	10 – 100 meters
FRS Radio	0.4625675 – 0.4677175	NA	14	500 / 500	2 miles
GMRS Radio	0.4625500 – 0.4677250	NA	23***	50000*** / 2000	5 miles

* Legal channels in US
** Less than 1 mW, varied by channel
*** FCC Part 95 Subpart E
' Utilizes FHSS over all channels

3.2 Measurement Process

This section incorporates discussions on preliminary investigations; emission testing conducted on laptop computers, PDAs, and a printer used as hosts for WLAN devices; and, device-focused tests conducted to measure radiated spurious emissions from wireless devices installed in a host. Determination of testing parameters is discussed, including procedures, RF filtering, host devices, WLAN devices, and test configurations. Several figures are included to illustrate the test environment, setup, and instrumentation. Tables are presented which include information on measurement frequency bands, measurement bandwidths, host and AP characterization, and WLAN configurations. A diagram of the test facility is presented with a discussion of NASA-LaRC High-Intensity Radiated Fields (HIRF) Laboratory RCs. The radiated emission test procedure is briefly discussed and includes calibration and emission measurement methods. Test matrices for WLAN devices and FRS and GMRS radios are presented to illustrate test modes. Finally, the data reduction process is discussed and the results are linked to data charts found in this report.

The following sections describe the measurement process by presenting the measurement method used, the types of preliminary testing conducted, the specifics of the device-focused testing on WLAN devices, and the data reduction process.

3.2.1 Measurement Method

Overview

This effort utilized the measurement process and data analysis previously developed for measuring spurious radiated emissions in aircraft communication and navigation (com/nav) receiver bands [1]. The measurement process incorporates RF measurement instrumentation, specialized data acquisition software, generation and application of calibration data, and the use of a RC. A RC was used for all emission testing in order to provide comprehensive test results and to expedite the test process. Additional advantages of using the RC method are described in the next section.

Test Facility Description

The NASA-LaRC HIRF Laboratory has three separate RCs located adjacent to one another. This facility is capable of performing radiated susceptibility tests and emission tests using either one chamber at a time or in two or three chambers simultaneously. Using multiple chambers allows for distributed testing of systems, creating different electromagnetic environments in each chamber utilized. The National Institute of Standards and Technology (NIST) has characterized the field uniformity of the NASA-LaRC RCs; details regarding their performance are located in [8]. Characterization of the chambers by NIST indicates a high degree of electromagnetic field uniformity performance within the stated usable frequencies. A chamber's lowest usable frequency is determined by its construction and geometry, and a sufficient mode density within the chamber to provide a uniform electromagnetic environment [13].

The largest chamber of the three is labeled as Chamber A. Due to its size and the lowest usable frequency, Chamber A is the only one of the three capable of conducting measurements in Band 1a. The lowest usable frequency for Chamber A is approximately 100 MHz with +/-2 dB variation [8]. Figure 3.2-1 shows the inside of the Chamber A.

Compared with the Semi-Anechoic Chamber (SAC) method, the advantages of the RC method include repeatability and speed when a large number of aspect angles in the SAC are considered. Radiated emission measurements in RCs produce results in terms of radiated power, which is preferred, rather than electric fields as in a SAC. Radiated emissions in term of power can be applied directly into Eq. 2.2-1 for interference risk assessment. In addition, the RC method does not suffer from *measurement uncertainty* caused by multipath effects (such as ground-bounce). However, establishing and maintaining connectivity with a wireless DUT can be much more difficult in a RC than in a SAC due to severe multipath interference.

Figure 3.2-1: Inside Reverberation Chamber A.

The RC method, however, may not be appropriate for measuring emission signals with very short pulse durations [10]. Due to high chamber quality factor, the chamber time-constant should not be greater than 0.4 of the pulse-width of the modulated signal. This requirement ensures that once a pulsed signal is turned on, the field environment in the chamber reaches (near) steady-state level before the pulse is turned

off. RF absorber can be added to the chamber to lower the time-constant; however, emission signal characteristics must be known in advance for all DUTs in all measurement bands. In addition, measurement sensitivity would be reduced due to higher chamber loss. Absorber was not added in this study. A method for measuring chamber quality factor and time-constant is described in [10].

The chamber time-constants vary with frequency, and are about 0.6 microsecond in Band 1a for an empty test chamber A. It is assumed that most RF emission signals measured in this effort are continuous-wave (CW), or pulse modulated signals of 1.5 microseconds (= 0.6 microseconds / 0.4) or longer.

Description of Measurement Method

Figure 3.2-2 shows the emission test setup in an RC. Tests conducted in RCs rely on several different methods to produce a statistically uniform and isotropic electromagnetic environment (field statistics measured over one stirrer revolution are isotropic and spatially uniform). Two of these methods are mode-stirred and mode-tuned [9]. Stirrers with reflective surfaces are rotated continuously during mode-stirring, or stepped at equal intervals for a complete rotation during mode-tuning. For measurements in this report, the mode-stirred method was adopted due to ease of setup, implementation, and significant speed improvements over the mode-tuned method. While the mode-tuned method can be more accurate in immunity testing applications (especially for DUTs with slow response time), the mode-stirred method is superior for most emission measurements due to speed. With a spectrum analyzer for measuring receive power, the emission measurement system can respond fast enough to the changing fields caused by the continuously rotated stirrers. Settling-time delays for stirrer stepping in mode-tuned operations are eliminated, resulting in significant speed improvements. In addition, combining mode-stirred operations with continuous frequency sweeping can further expedite the measurements.

Measurement uncertainty levels can be lowered by selecting the number of measurement points in a stirrer revolution approximately equal to the number of calibration points. In addition, the number of measurements during one stirrer revolution should be as large as possible within constraints of instrument capabilities and test time to reduce uncertainties. Using the mode-stirred method, several thousand measurements per stirrer revolution are easily achievable with a spectrum analyzer. On the other hand, the mode-tuned method with the number of measurements exceeding 100 per stirrer revolution is typically considered impractical due to excessive test time. The mode-stirred method's short calibration times also allow for frequent chamber calibrations to correct for DUT operator changes during long test times.

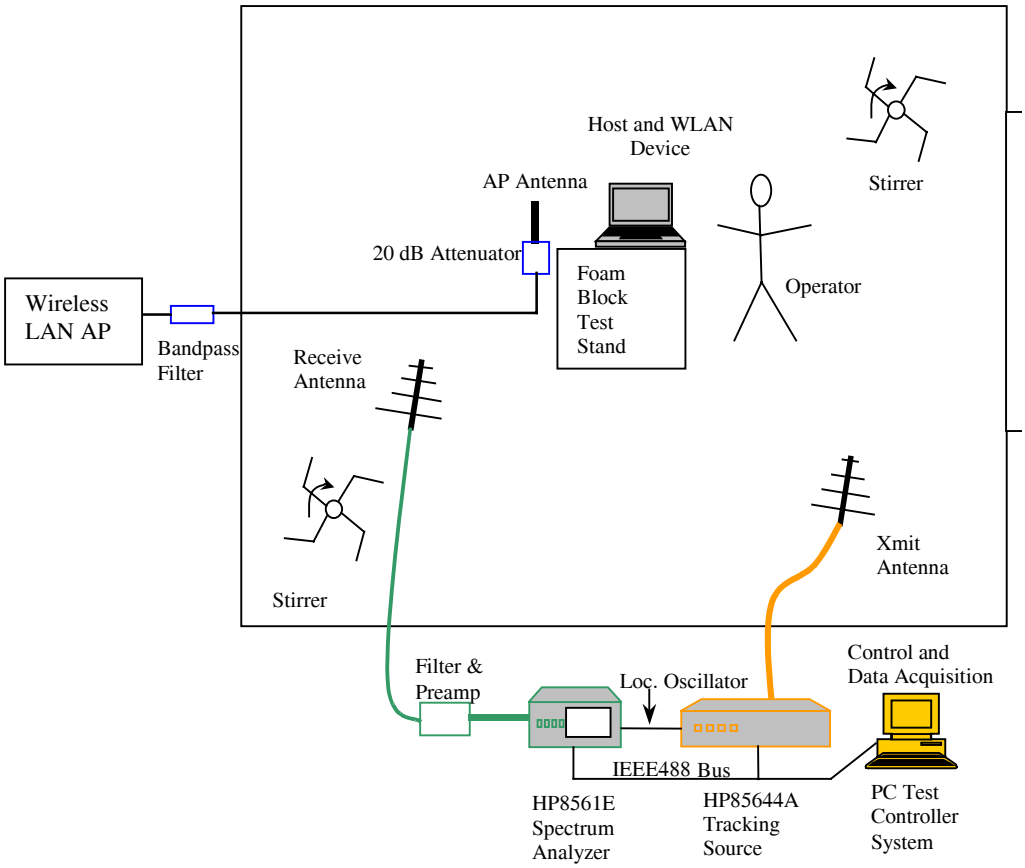

Figure 3.2-2: RC and WLAN emission test configuration.

Emission measurements using the mode-stirred method typically involve [10]:

1) Empty chamber insertion loss measurement;

2) Measurement of chamber loading, caused by the presence of a test operator and test equipment inside the chamber; and

3) Measurement of maximum receive power over a paddle rotation of the stirrer with the DUT powered on in various test modes.

The total radiated power within the measurement resolution bandwidth can be calculated using [15, appendix E]:

$$P_{TotRad} = (P_{MaxRec} * \eta_{Tx}) / (CLF * IL), \qquad \text{(Eq. 3.2-1)}$$

where

P_{TotRad} = total radiated power within the measurement resolution bandwidth,

P_{MaxRec} = maximum received power measured over one complete paddle rotation,

CLF = chamber loading factor, or the additional loading effects caused by the presence of objects or operators in the test chamber,

η_{Tx} = efficiency factor of the transmit antenna used in chamber calibration and assumed to be unity for the antennas used,

IL = empty chamber insertion loss, pre-determined during chamber calibration.

IL is measured during chamber calibration, and is defined as the ratio of the maximum receive power and the transmitted power in a stirrer revolution [15: appendix B]:

$$IL = P_{MaxRec} / P_{Input} \ , \qquad \text{(Eq. 3.2-2)}$$

where P_{MaxRec} and P_{Input} are the maximum received power and the transmit power at the antennas, respectively.

In [10], *IL* is first measured and averaged over multiple locations for improved uncertainties. *CLF* is then measured once (one location) when test objects or personnel are introduced into the test chamber. Correction for *CLF* is applied only when the values exceed a given threshold (3 dB is specified in [10]).

In this effort, a simplified one-step process was used instead: (*CLF***IL*) combination was measured together. This one-step process requires that the DUTs and DUT operator be present in the chamber during calibration. The chamber loading factor measurement is no longer needed, eliminating uncertainties about whether a correction for *CLF* should be applied. To reduce the burden on DUT operators, (*CLF***IL*) was measured at one location rather than averaged over multiple locations. The effect is an acceptable small increase in uncertainty (of about two dB or less depending on chamber field uniformity and frequency).

In an actual setup, it is often convenient to include transmit and receive path losses in the chamber calibration measurements. These path losses account for the presence of test cables, in-line amplifiers, attenuators and filters for various purposes. Transmit path losses are associated with components connecting the source output and the transmit antenna, whereas receive path losses are associated with components connecting the receive antenna and the spectrum analyzer input. As a result, chamber calibration factor (*CF*), in dB, is introduced:

$$\begin{aligned} CF &= (P_{Xmit(dBm)} - P_{SAMeas(dBm)}) \\ &= L_{Chmbr(dB)} + L_{RecCable(dB)} + L_{XmitCable(dB)} \ , \end{aligned} \qquad \text{(Eq. 3.2-3)}$$

where

CF = chamber Calibration Factor (dB),

$L_{Chmbr(dB)}$ = chamber loss (dB), or

= $-10 log_{10}(CLF * IL)$,

$L_{RecCable(dB)}$ = receive cable loss (dB),

$L_{XmitCable(dB)}$ = transmit cable loss (dB),

$P_{SAMeas(dBm)}$ = maximum receive power measured at the spectrum analyzer (dBm) over one stirrer revolution,

$P_{Xmit(dBm)}$ = power transmitted from source (dBm).

Passive losses (not to include amplifier gains) are defined to be positive in dB. The total radiated power in dBm can be computed using:

$$P_{TotRad(dBm)} = P_{SAMeas(dBm)} - L_{XmitCable(dB)} + CF . \quad \text{(Eq. 3.2-4)}$$

As shown in Figure 3.2-2, measurement instrumentation included a spectrum analyzer, a tracking source (frequency-coupled with the spectrum analyzer), a computer, a stirrer controller, transmit and receive antennas, RF filters, pre-amplifiers, and an IEEE-488 bus. The measurement procedure begins by performing a transmit path loss calibration. Transmit path losses are measured at each frequency by injecting a known power from the tracking source through the cable to the antenna connector and using a spectrum analyzer to measure the loss. Next, a chamber calibration is performed. A known level of power is delivered from the source into the chamber through the transmit antenna while the stirrer(s) are continuously rotated at a predetermined rate. The spectrum analyzer is used to record the maximum power coupled into the receive antenna (and the receive path) while performing synchronized frequency sweeps with the tracking source across the measurement bands. Eq. 3.2-3 is applied to determine the *CF* [1,11].

The source is then removed, and the transmit path connection terminated, to avoid leakage from the source into the chamber. With the DUT powered off, a radiated emission measurement is conducted to measure noise floor levels in each band. Then the DUT is powered on and a radiated emission measurement performed at each frequency with the DUT placed in each test mode. During the emission measurements, the spectrum analyzer is put on maximum hold mode while continuously sweeping over the measurement frequency band. The control software applies the equation Eq. 3.2-4 to normalize the measured power with the calibration data [2].

Figure 3.2-2 shows the position of a host and WLAN device in the center of the chamber, represented by a laptop computer on a foam block test stand. The AP antenna is also located on the same test stand. Utilizing the mode-stirred method, the two stirrers located in the corners of the chamber were continuously rotated at 5 rpm during chamber calibrations and emissions testing.

Also illustrated is the control and data acquisition system. Note the line labeled Local Oscillator Connection actually represents several connections between the tracking source and spectrum analyzer that ensure frequency synchronization. RF filters and a preamplifier are indicated in the receive path. The wireless network is illustrated outside the chamber, and includes an AP, a router, a wired laptop, and a bandpass filter inline with the AP antenna. A 20 dB attenuator is located inside the chamber at the AP antenna. This attenuator was used to improve wireless network communications by reducing signal overload caused by close proximity of the AP antenna and wireless card. The AP antenna and the wireless card were placed close to each other to overcome multipath interference. The AP antenna port that was not used was capped with a 50-ohm termination to prevent signals outside the chamber from coupling in through the AP.

3.2.2 Preliminary Testing

Overview

Much of the preliminary testing made use of the results or was performed in the same way as reported in [1]. Before radiated spurious emission measurements began, several preliminary and exploratory tests were performed. The requirements for filtering were analyzed and specific parameters were determined for selecting filters and preamplifiers. APs and WLAN devices were characterized and selected.

In addition, emissions tests were conducted on eight laptop computers and two PDAs using several different operating modes. The resulting emissions data were analyzed and compared to determine which laptop computers to use as hosts for the WLAN devices during emissions tests.

During preliminary and emission testing of WLAN devices, two tests were performed, ping storm and duplex file transfer. Ping was used to probe the target, a WLAN device, and determine if the network was functioning correctly. A network ping sends a null packet, which is a very small packet of 8 bytes, plus standard Transmission Control Protocol/Internet Protocol (TCP/IP) overhead over the network. This packet contains enough information to locate a particular receiving device or client using its IP address. The receiving device will then send a minimal response. The round-trip usually takes only milliseconds and indicates that the devices are communicating and that the network is operating correctly. A ping storm occurs when a ping is sent continuously over the network. Duplex file transfers between laptops were also conducted. A data file from a wired laptop was sent to a WLAN laptop and vice versa, simultaneously. These types of tests were performed during radiated emissions measurement testing.

Determination of Required Filtering

Tests were performed in a RC using an HP85644A sweeping source to determine if representative device emissions caused false spurious emissions within the measurement system in each measurement frequency band. These tests were conducted with required preamplifiers in place, and band-specific filters to avoid overdriving the preamplifiers. Figure 3.2-2 illustrates the receive path used during calibration and emission testing with filters and preamplifier in place. Tables 3.2-1, 3.2-2, and 3.2-3 give the designated RC, pre-amplifier, receive antennas, spectrum analyzer settings, and filters used during calibration and emission measurements for each threat type and frequency band.

Table 3.2-1: FRS/GMRS Threat Source (440 – 470 MHz)

Freq. Band	Cbr.	Pre-Amplifier Used	Receive Antenna	Spectrum Analyzer Settings	Specified filter before Pre-Amplifier
1a	A	Miteq AU-1291-N-1103-1179-WP, 60 dB; HP8491B Attenuator, 10 dB	AH SAS-200/514	HP 8561E RBW= 10kHz Atten.= 0dB	K&L 8IL40-336/U468 Lowpass Cutoff Freq. 336 MHz

Table 3.2-2: IEEE802.11b, Bluetooth Threat Source (2400 – 2500 MHz)

Freq. Band	Cbr.	Pre-Amplifier Used	Receive Antenna	Spectrum Analyzer Settings	Specified filter before Pre-Amplifier
1a	A	Miteq AU-1291-N-1103-1179-WP, 60 dB; HP8491B Attenuator, 10 dB	AH SAS-200/514	HP 8561E RBW= 10kHz Atten.= 0dB	K&L 4IL30-600/U2497 Lowpass Cutoff Freq. 600 MHz

Table 3.2-3: IEEE802.11a Threat Source (5150 – 5825 MHz)

Freq. Band	Cbr.	Pre-Amplifier Used	Receive Antenna	Spectrum Analyzer Settings	Specified filter before Pre-Amplifier
1a	A	Miteq AU-1291-N-1103-1179-WP, 60dB; HP8491B Attenuator, 10 dB	AH SAS-200/514	HP 8561E RBW= 10kHz Atten.= 0dB	K&L 6IL30-1600/U2497 Lowpass Cutoff Freq. 1600 MHz

Host Device Baseline

WLAN devices come in two different forms: 1) a removable PC card; or 2) integrated into an electronic system, which enables its host device to communicate with a mobile or fixed network using assigned radio frequencies. WLAN transmitters do not function independently and must be installed in a host device. A host is a PED that a user chooses to be mobile and linked to other PEDs in order to exchange information. A baseline of spurious radiated emissions for each possible host was measured in Band 1a. A laptop computer and a PDA with the lowest emission in Band 1A were chosen as hosts for WLAN devices, so that their emissions would not mask the WLAN emission results. Various laptop computers were used as test objects. Table 3.2-4 shows the laptops, PDAs, and a mobile printer considered. Figure 3.2-3 illustrates the configuration for a chamber with a tracking source used for calibration, a spectrum analyzer, transmit and receive antennas, a laptop computer, and an operator.

Laptop Computers

Spurious radiated emissions were recorded for Band 1a with each of the eight laptops operating in five modes. Modes are processing tasks that may be performed by a laptop while in use. Radiated emissions from the modes (idle, flowerbox screensaver, file transfer, CD, and DVD) were measured separately and then plotted with each other to achieve a maximum radiated peak envelope of the laptop, which is

discussed further in Section 3.4. The flowerbox screensaver was selected to be a large, smooth, checkerboard cube pattern that spins and blooms at maximum complexity. The file transfer mode transfers a file from the hard drive to the PCMCIA slot mounted Microdrive. Idle mode testing is conducted as a normal desktop screen is displayed. In order to exercise the video and audio cards, a CD and DVD were played. Appendix B contains results of the plotted data.

In order to determine the emissions from the WLAN devices, laptop emissions were independently measured. Combining emissions in idle and file transfer modes (typical laptop modes while WLAN devices' emissions are measured) created a baseline for each device, from which the "quietest" host was selected and used as the host for all WLAN devices of the same type. Emissions from the DUT (a WLAN device and its host) are compared against the host's emission baseline revealing the additional emission caused by the WLAN devices. From the list of devices in Table 3.2-4, LAP4 was chosen as the host for WLANs.

PDA and Printer

A PDA baseline consisted of the idle and file transfer modes. File transfer in this case was performing a backup operation to a secure digital or compact flash card.

The battery-powered printer was used as a host for a Bluetooth – USB printer adapter. The printer's baseline solely consisted of the idle mode with the unit powered on. Peak radiated emission power levels from these hosts are located in Appendix B. Host baselines are compared with the DUT emission measurements to determine how the WLAN affects the host emission levels.

Table 3.2-4: Laptop, PDA, and Mobile Printer Models

Host Designation	Manufacturer	Model
LAP1	Dell	Latitude C640
LAP2	HP	Pavilion n6395
LAP3	Sony Vaio & Dock	PCG-641R PCGA-DSM51
LAP4	Dell	Latitude C800
LAP5	Fujitsu	Lifebook
LAP6	Panasonic	Toughbook CF-47
LAP7	Fujitsu	Lifebook CP109733
LAP8	Gateway	450SX4
PDA1	Palm	m515
PDA2	Toshiba	e740
PRN	Hewlett Packard	DeskJet 350

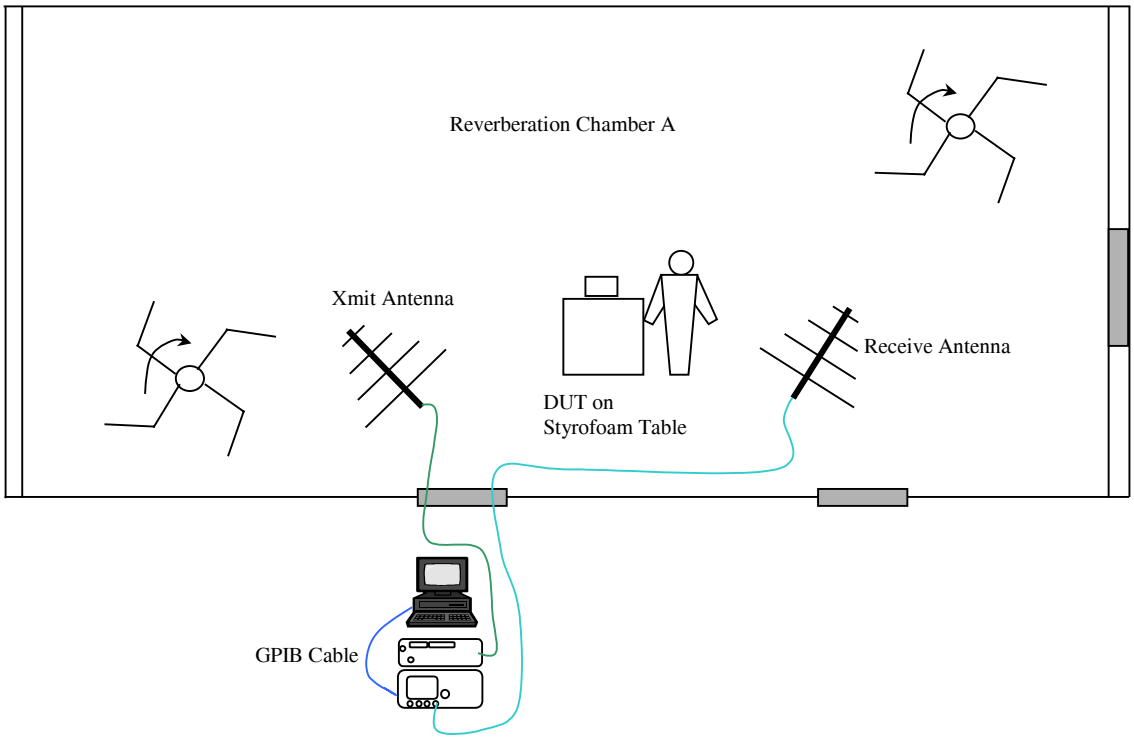

Figure 3.2-3: Setup for host baseline in RC A.

Test Set and Wireless Device Characterization and Selection

Prior to conducting radiated emission testing, WLAN APs and a Bluetooth test set were characterized to determine operating limitations, performance, and noise levels. Two 802.11a APs, two 802.11b APs, and one Bluetooth test set were evaluated. The Bluetooth test set and APs, also utilized as test sets, served as DUT controllers for setting WLAN parameters such as data rates, channels, and power. In addition, the test sets and wireless device combinations were evaluated. These characterizations were conducted in the earlier effort [1], and the results summarized below.

802.11a and 802.11b Data Rate and Channel Control

The ability of APs and WLAN devices to control data rates, channels, and power was tested and verified. Various AP and wireless PC card combinations were tested to determine interoperability and performance.

Tests were conducted to determine the data rates and channels to be used during emissions testing. For testing the capabilities and performance of APs and PC cards, a ping storm was initiated from the AP control wired laptop to the WLAN laptop while various data rates and channels were applied. Duplex file transfers between laptops were also conducted. A data file from the wired laptop was sent to the WLAN laptop with PC card and vise versa, simultaneously. Again, various data rates and channels were tested while transferring files.

Continuous operation in a RC was more difficult to maintain than in a SAC due to multipath propagation conditions. Multipath loss occurs as the RF signal bounces off the chamber walls and

rotating paddles within the chamber enroute from the AP antenna to the WLAN device. The rotating paddles are the greatest contributor to this loss. As a result, the signal can take more than one path, arriving at the WLAN device as multiple or attenuated signals. WLAN performance was significantly impacted by these losses. 802.11a device communications were more difficult to maintain in an RC than were 802.11b device communications. In these cases, the AP antenna was placed at a distance approximately one to three inches from the PC WLAN card in order to establish the network connection. Reducing the AP antenna and card distance did improve connection stability by reducing the effect of multipath signals. During emission testing, a 20dB attenuator was added at the AP antenna to prevent the WLAN card and AP antenna from overpowering each other when the two were in close proximity.

The more robust APs and cards were able to operate continuously with fewer dropouts and quicker recovery. Many of the faster data rates were difficult to sustain in this multipath environment. The selection of data rates during emission testing was determined largely by the capability of the AP/card combination to maintain association and communication and to perform in a robust manner. Data rates were selected based on the AP operability at each rate, and the desire to test as many data rates and modulation schemes as possible.

Preliminary operational testing of APs and PC cards was used to determine channel selections. Changing channels moves the transmission signal from one frequency to another within the larger operational frequency band for a particular type of device. The 802.11a WLAN devices used during testing were limited to the first two operational bands (5.15 to 5.25 GHz and 5.25 to 5.35 GHz). The availability of certain channels was further limited by equipment selected.

802.11a and 802.11b WLAN Operational Evaluation

APs were tested to identify any spurious signal emissions from the APs in the interested measurement band. While no significant spurious signals were noted, however, bandpass filters were added inline between the APs and antennas during actual emissions testing to ensure that no undesired out-of-band emissions were transmitted into the chamber.

Results of 802.11a and 802.11b Preliminary Testing

All data rates and channels allowed by the APs, test set, and cards were exercised during preliminary operational testing. The ability to control power levels proved to be very limited; therefore, PC cards were configured and maintained at maximum power levels. Power level maximums were 200 mW for 802.11a devices and 100 mW for 802.11b devices.

As the results of the earlier effort [1], two APs, one for 802.11a tests and one for 802.11b tests, were selected based on ease-of-use, overall capability, and robust behavior. The selected APs each had removable antennas, adjustable power settings, and short delays during configuration changes. The 802.11a selected data rates and associated modulation schemes are listed in Table 3.2-5, and selected channels and maximum output power are listed in Table 3.2-6. The 802.11a AP chosen for use during emissions testing had a high-speed or turbo mode capability that allowed for three additional channels. In addition to the normal channels shown in Table 3.2-6, channels 42, 50, and 58 were also used when operating in turbo mode. The 802.11b selected data rates and associated modulation schemes are listed in Table 3.2-7, and selected channels and maximum output power are listed in Table 3.2-8. Table 3.2-8 shows that the channel numbers chosen for 802.11b emissions testing were 1, 6, and 11, as these channels are non-overlapping in frequency bandwidth.

Table 3.2-5: 802.11a Selected Data Rates

Data Rate (Mbps)	Modulation**
6	BPSK
12	QPSK
24	16-QAM
36*	16-QAM

*Available in turbo mode.
**BPSK – Binary Phased Shift Keying, QPSK – Quadrature Phased Shift Keying, 16-QAM – 16 bit Quadrature Amplitude Modulation

Table 3.2-6: 802.11a Selected Channels.

Channel Numbers	Frequency (MHz)	Maximum Output Power
36	5180	40 mW
42*	-	40 mW
48	5240	40 mW
50*	-	-
58*	-	200 mW
64	5320	200 mW

* Turbo Mode Channels

Table 3.2-7 802.11b Selected Data Rates

Data Rates (Mbps)	Modulation*
1	BPSK
2	QPSK
11	QPSK

*BPSK – Binary Phased Shift Keying, QPSK – Quadrature Phased Shift Keying

Table 3.2-8: 802.11b Selected Channels

Channel Numbers	Frequency (MHz)	Maximum Output Power
1	2412	100 mW
6	2437	100 mW
11	2462	100 mW

Bluetooth Test Set Operational Evaluation and Characterization

An evaluation of an Agilent Technologies E1852B Bluetooth Test Set was conducted to determine if the operational modes of commercial-off-the-shelf Bluetooth devices could be controlled by the test set. A laptop installed with Agilent's Bluetooth test set interface software was used to send inquiry and page commands in normal mode. A communication link between the test set and a Bluetooth device occurs when the test set detects any Bluetooth device in its coverage area by using device address inquiries. The Bluetooth device address is selected to establish a connection and to implement a normal mode page communication link. A normal mode connection sends null packets with a header over the network to the

Bluetooth device, which returns a reply to the Bluetooth test set. Once a connection is made, it will remain in place until the operator releases it.

All off-the-shelf Bluetooth devices tested were unable to establish a connection through the test mode page because manufacturers remove this feature before devices reach production phase. Test mode allows a payload to be attached with the header to simulate a file transfer.

3.2.3 Device-Focused Testing

Overview

Measurements of spurious radiated emissions were conducted on WLAN devices and two-way radios for Band 1a. Devices tested include five 802.11a PC cards, six 802.11b PC cards, two PDA-based 802.11b and Bluetooth cards, and six Bluetooth devices. In addition, fourteen FRS/GMRS radios were paired and tested. Host baseline test results were used to select laptops for use during emission testing.

Several industry standards were consulted to determine and justify measurement parameters. This section includes tables listing measurement parameters, such as test measurement bands, resolution bandwidths, sweep times, dwell times, and noise floor estimates. An analysis was conducted to determine minimum test times or dwell times required in a RC in order to ensure adequate measurement sampling. Instrument and preamplifier noise measurements were conducted and combined with other losses and gains to determine the minimum measurement sensitivity for each of the five measurement bands.

The test procedure is further detailed in this section and applied for testing wireless devices. Examples of test matrices for each type of device tested are presented in order to describe the components of a typical emission test.

Included in this section are the following topics that describe the device-focused testing of WLAN devices: the selection and use of test instrumentation parameters; an analysis of measurement sensitivity; a description of the WLAN devices and radios selected for testing; radiated emission measurement test details; examples of test matrices; multipath interference issues; and, finally, the data reduction process.

Frequency Bands, Measurement Bandwidth and Scan Time

Test parameters used in spurious radiated emission testing for this report, such as measurement bandwidth and scan time, were based upon those used in [1]. To reduce test time for the mode-stirred measurements, multiple short sweeps were used instead of a single long sweep, while continuously rotating the chamber stirrers. The selected parameters are shown in Table 3.2-9.

Table 3.2-9: Measurement Bandwidths and Sweep Times for Measuring Spurious Radiated Emissions

Frequency Band Designation	Aircraft Systems	Freqquency (MHz)	Resolution Bandwidth kHz	Spectrum Analyzer Sweep Time (ms) (HP8561E)
1a	VHF-Com	116-140	10	375

Description of WLAN Devices and Two-Way Radios

The off-the-shelf wireless devices tested conformed to specified standards and interoperability criteria. Tables 3.2-10, 3.2-11, and 3.2-12 lists the brands and model numbers of devices tested in each wireless standard. Figure 3.2-4 shows the WLAN devices used in this effort.

IEEE 802.11b devices have a transmit output power range from a 5 mW to 30 mW minimum or 100 mW maximum value. When an option to adjust the transmit power level is available in the utility software, a user is able to expand or confine a transmission area with respect to other wireless devices operating nearby. Several manufacturers of NICs, universal serial bus (USB), or secure digital (SD) devices provide users with additional control options or data rates. The 11B-2, 11B-3, 11B-5, 11B12 and 11B-13 cards are among the 802.11b NICs which have the capability to control the transmit output power. The 11B-2 card was set to its maximum output power of 30 mW, whereas 11B-3, 11B-5, 11B-12 and 11B-13 were set to their maximum output power of 100 mW. The exact output powers for the other 802.11b devices were unknown, since the PC cards' utility software did not contain any feedback to display the value of the output power levels of the cards. However, 11B-7 and 11B-11 are interoperable with the other adapters, so they are accepted to be within the output power range. Several 802.11a devices contain additional data rates that are not dictated by the IEEE 802.11a standard.

Table 3.2-10: 802.11a Devices Tested

DUT Designation	Manufacturer	Model	Serial Number	Host Designation	Max Output Power Ch. Dependent
11A-1	Proxim	Harmony	052040EX3NVR	LAP4/LAP6	50 mW, 200 mW
11A-2	Proxim	Harmony	051490E0ENVR	LAP/LAP6	50 mW, 200 mW
11A-3	Linksys	WPC11	MBY2402094	LAP/LAP6	50 mW, 200 mW
11A-5	Intel	WCB5000	9009TB00C5B6	LAP/LAP6	40 mW, 200 mW
11A-6	NetGear	WAB501	WAB5A29ZC000671	LAP/LAP6	50 mW, 200 mW

Table 3.2-11: 802.11b Devices Tested

DUT Designation	Manufacturer	Model	Serial Number	Host Designation	Maximum Output Power
11B-2	Cisco	340	VMS053313RR	LAP4/LAP6	30 mW
11B-3	Cisco	350	VMS0535026D	LAP4/LAP6	100 mW
11B-5	Symbol Tech.	Spectrum 24 PCc	00A0F830E7EE	LAP4/LAP6	100 mW
11B-7	Linksys	WPC54	G3001203652	LAP4/LAP6	95 mW
11B-11	Toshiba	E740	62058024L	PDA-2	N/A
11B-12	D-Link Air	DWL-65OH	H252123003470	LAP4/LAP6	100 mW
11B-13	NetGear	WAB501	WAB5A29ZC000671	LAP4/LAP6	100 mW

Table 3.2-12: Bluetooth Devices Tested

DUT Designation	Manufacturer	Model	Serial Number	Host Designation
BLUE-2	3-Com		HHR13D2800	LAP4/LAP6
BLUE-6	TDK	Dongle	SB10008256	LAP4/LAP6
BLUE-8	Troy	Windport	FI-PCM109-68610-24A-0242	LAP4/LAP6
BLUE-10	Anycom		Prn Adap	PRN
BLUE-11	Anycom		PC Card	LAP4/LAP6
BLUE-12	Toshiba	Palm Bluetooth Card	120015892B	PDA-1 (SD Card)

Figure 3.2-4: WLAN devices in the form of NICs, a USB dongle, a SD card and integrated into the PDA.

The 802.11a standard only specifies data rates up to 54 Mbps, whereas 802.11a NIC manufacturers offer additional data rates in a turbo or 2X mode using proprietary methods. All adapters and APs with this capability were able to communicate outside the chamber with ease, and a few hindrances arose during data collection in the chamber. Table 3.2-13 lists the NICs tested with mode capability.

Table 3.2-13: 802.11a Turbo Data Rates

Manufacturer	Turbo Mode Data Rates
11A-1/11A-2	12,18,24,36,48,72, 96,108 Mbps
11A-3	Up to 72 Mbps
11A-5	N/A
11A-6	Up to 108 Mbps

During testing the data rate field was set to automatic. Rates were changed at the AP, and the NICs adjusted their rate accordingly. The AP interface software was used to enable the antenna port used during testing to transmit and receive information. Data collection for 802.11a/b had a few challenging

cases which will be discussed later in this section; but overall data were collected as expected from preliminary testing results.

Bluetooth devices, as seen in the third group of Figure 3.2-7, did not have any option controls and usually had a stable link with the test set. Usually, reseating the Bluetooth device with its host solved most of the connection failures that occurred between the Bluetooth device and test set.

FRS and GMRS radios were tested as a pair in the RC with an operator switching channels and transmitting audio. Two-way radio tests were straight forward. Table 3.2-14 lists the brands and models of devices tested. Figure 3.2-5 shows both types of paired radios used in this effort.

Figure 3.2-5: 4 pairs of FRS and 3 pairs of GMRS radios.

Table 3.2-14: FRS and GMRS Radios Tested

Pair Designation	**Manufacturer**	**Model**	**Serial Numbers**
FRS-1	Motorola	T5420	165WCB0L6H
FRS-2	Motorola	T5420	165WCB0L7T
FRS-3	Cobra	FRS 225	L201279758
FRS-4	Cobra	FRS 225	L201273388
FRS-5	Audiovox	FR-1438	112105119
FRS-6	Audiovox	FR-1438	112105121
FRS-7	Midland	75-17	00516539
FRS-8	Midland	75-17	00516537
GMR-1	Motorola	T6400	175TBWY469
GMR-2	Motorola	T6400	175TBX1332
GMR-3	Audiovox	GMRS1535	TTK0111 0019481
GMR-4	Audiovox	GMRS1535	TTK0111 0019501
GMR-5	Midland	G-11C2	15011596
GMR-6	Midland	G-11C2	15011610

Wireless Device and Two-Way Radio Radiated Emission Measurements

The test chamber configuration and test instrumentation used during calibration and emission measurements are illustrated in Figure 3.2-2. Test instrumentation consisted of an HP8561E Spectrum Analyzer, an HP85644A Tracking Source, RF filters, pre-amplifiers, transmit and receive antennas, and a

control laptop computer. A pair of in-band log-periodic antennas was used as transmit and receive antennas. RF filters and preamplifiers were included in the receive path to obtain a lower noise floor, amplify signals, and to block out-of-band signals relative to the wireless device transmission frequencies.

The previously described measurement method (Section 3.2 Measurement Method) was utilized for all calibrations and radiated emission tests. The position of a host/WLAN device and AP antenna were similar to positions indicated in Figure 3.2-2. During calibration measurements, the host and WLAN device inside the chamber and the test set outside the chamber were powered off. The operator was grounded during tests to prevent electrostatic discharge voltages from effecting the sensitive measurements. Using the control software, power measurements were normalized with the calibrated data and the results were recorded for each frequency within the test band.

Noise floor measurements were conducted to determine the ambient environment with hosts, WLAN devices, and an operator inside the chamber, but with the host/WLAN powered off and the Bluetooth test set or AP powered on. These measurements were used to verify a quiet RF environment before proceeding with radiated emissions tests.

Emission test dwell times varied depending on the number of channels accessed during a test. However, a minimum dwell time of 120 seconds was used for all tests in the RC. A dwell time is defined as the time applied for the duration of one test, which consisted of either a calibration measurement or an emission measurement where the DUT performed in a test mode, at a specific data rate and channel. RC and receive path calibration measurements were conducted for a dwell time of 120 seconds.

Figure 3.2-6 illustrates the control and data acquisition hardware located outside an RC. Pictured are the HP8561E Spectrum Analyzer and the HP85664A Tracking Source. The local oscillators and four other ports of the spectrum analyzer and tracking source were connected in order to synchronize frequencies. The picture also illustrates the receive path including cable, filters and preamplifier resting on top of the tracking source. Agilent Visual Engineering Environment (VEE) software was used to develop control and data recording software that was run on a laptop computer.

Figure 3.2-6: Control and data acquisition setup outside the RC.

The 802.11a and 802.11b APs, located outside the chamber, were used as test sets to control data transfers and switch data rates and channels while operating in ping storm (PS) and duplex file transfer (Xfer) modes. Emission tests were conducted on one WLAN device at a time. The data link between the test set and the WLAN device was exercised using three operational modes: idle, PS, and Xfer, while swiching data rates and channels. A test consisted of a mode, a data rate, and three channels. During a three-minute dwell time, channel switching was conducted at one-minute intervals. This allowed approximately one minute of test time at each channel. Host baseline test results were used to select laptops for use during emission testing of wireless devices. Selected hosts also included PDAs that operated with WLAN cards installed and a printer with wireless capabilities.

During Bluetooth device emissions testing, an Agilent Technologies E1852B Bluetooth Test Set, located outside the chamber, was used to control test modes. Bluetooth emissions tests were performed using both idle and normal paging modes. Since Bluetooth protocol uses frequency-hopping techniques, no channel switching was done. During a test, a spectrum analyzer was swept for a two-minute dwell time and then data were recorded.

FRS and GMRS radios were tested in pairs in idle mode and voice transmit/receive modes. During FRS/GMRS radio emissions testing, the operator used two radios, one in each hand, and talked into one radio while receiving with the other radio. Channels were switched every two minutes.

Test Matrix

Tables 3.2-15 and 3.2-16 are portions of the 802.11a and 802.11b test matrices used during radiated emission testing. The tables include DUT numbers, test modes and channels, and frequency band. Note that tests using idle, PS, and Xfer modes were conducted. Selected data rates and channels are indicated for PS and Xfer modes. The illustrated combination of modes, data rates, and channels was repeated for each 802.11a and 802.11b WLAN device in the measurement frequency band.

Table 3.2-15: 802.11a Test Matrix (for one device)

Device Under Test	Test Modes and Channels	Bands
11A-1	Idle	1a
11A-1	Ping Storm AP Data Rate 6 Channels 36 48 64	1a
11A-1	Ping Storm AP Data Rate 12 Channels 36 48 64	1a
11A-1	Ping Storm AP Data Rate 24 Channels 36 48 64	1a
11A-1	Ping Storm AP Data Rate 36 Turbo Channel 42 50 58	1a
11A-1	Duplex File Xfer AP Data Rate 6 Channel 36 48 64	1a
11A-1	Duplex File Xfer AP Data Rate 12 Channel 36 48 64	1a
11A-1	Duplex File Xfer AP Data Rate 24 Channel 36 48 64	1a
11A-1	Duplex File Xfer AP Data Rate 36 Turbo Channel 42 50 58	1a

Table 3.2-16: 802.11b Test Matrix (for one device)

Device Under Test	Test Modes and Channels	Bands
11B-1	Idle	1a
11B-1	Ping Storm AP Data Rate 1 Channels 1 6 11	1a
11B-1	Ping Storm AP Data Rate 2 Channels 1 6 11	1a
11B-1	Ping Storm AP Data Rate 11 Channels 1 6 11	1a
11B-1	Duplex File Xfer AP Data Rate 1 Channels 1 6 11	1a
11B-1	Duplex File Xfer AP Data Rate 2 Channels 1 6 11	1a
11B-1	Duplex File Xfer AP Data Rate 11 Channels 1 6 11	1a

Table 3.2-17 illustrates the test matrix used for radiated emissions measurements conducted on Bluetooth WLAN devices. DUT numbers, test modes, and frequency band are included. Only two modes were used, idle and normal paging.

Table 3.2-17: Bluetooth Test Matrix (for one device)

Device Under Test	Test Modes	Band
BLUE-1	Idle	1a
BLUE-1	Normal Paging	1a

Table 3.2-18 demonstrates a portion of the test matrix used during radiated emissions testing on FRS and GMRS radios. The tests required that two radios be paired for communication and transmission. The matrix illustrates the radio numbers and pairs, test modes, and frequency band.

Table 3.2-18: FRS/GMRS Radios Test Matrix (all devices)

Device Under Test	Test Modes	Band
FRS1&2	Idle	1a
FRS1&2	Xmit Voice Count, Channels 1&14	1a
FRS3&4	Idle	1a
FRS3&4	Xmit Voice Count, Channel 1&14	1a
FRS5&6	Idle	1a
FRS5&6	Xmit Voice Count, Channels 1&14	1a
FRS7&8	Idle	1a
FRS7&8	Xmit Voice Count, Channel 1&14	1a
GMR1&2	Idle	1a
GMR1&2	Xmit Voice Count, Channel 7&14&15	1a
GMR3&4	Idle	1a
GMR3&4	Xmit Voice Count, Channels 1&15	1a
GMR5&6	Xmit	1a
GMR5&6	Xmit Voice Count, Channels 1&15	1a

WLAN Device Multipath Interference

Similar to the previous efforts [1], multipath interference continued to occasionally affect communication between APs and WLAN devices during radiated emission testing in a RC. When interference occurred, it caused loss of communication between the AP and the WLAN device, making it necessary to repeat tests. Every effort was made to maintain communication for an adequate dwell time in order to collect a complete data set of measurements. Implementing one or more of the following methods removed many of the multipath interference affects:

1) The AP antenna and WLAN device were placed about one to three inches apart.

2) A 20 dB attenuator was inserted inline with the AP antenna.

3) Metal shielding was placed around the DUT, as shown in Figure 3.2-7, to avoid a direct path between the AP antenna and the stirrers.

4) Only one stirrer was used in Chamber A if communication failed after two attempts to collect data.

Other methods utilized to maintain or reestablish communication were available through the WLAN PC card. The software interfaces for each WLAN PC card provided communication status and a means to rescan for devices. When a rescan failed the NIC was reseated by ejecting it from the PCMCIA slot and then reinstalling it. While this slowed the testing process, it did allow the devices to re-associate.

Disassociation between the 802.11a/b APs and NICs occasionally occurred as a result of channel changes during testing, and recovery was sometimes difficult. If association could not be maintained during a channel change, the data collected do not contain measurements for that next channel and is, therefore, incomplete. Test log entries were made to indicate incomplete test cases and detail the problems encountered. In some cases data were collected on just one channel for three minutes. However, based on data from completed tests, changing channels during 802.11a/b device testing did not significantly alter the peak radiated emission measurements and did not affect the final results.

Table 3.2-20 provides further details on incomplete tests due to multipath interference. Details include specific device designation, data rate, and mode, and the channels not reflected in the data due to inadequate communication.

Other than the multipath interference disruptions, the data collection process proceeded with only a few technical inconveniences. The full scope of the testing is indicated in Table 3.2-19 where the total number of test cases for 802.11a/b devices is computed. About 5% of the test cases were incomplete due to multipath interference.

Table 3.2-19: Total Number of 802.11a and 802.11b Test Cases

Wireless Technology	Number of Devices	Number of Test Cases Per Device	Number of Test Bands	Total Test Cases
802.11a	5	9	1 (Band 1a)	45
802.11b	7	7	1 (Band 1a)	49

Table 3.2-20: Incomplete 802.11a and 802.11b Test Cases Due To Multipath Interference

WLAN Device	Data Rates	Test Mode	Omitted Channels	Band
11B-11	1 2 11	File Transfer	1, 6, 11	1a
11A-5	36 (turbo)	Ping Storm, File Transfer	42, 50, 58	1a

Figure 3.2-7: Metal shielding to reduce multipath interference between the WLAN card and the AP antenna.

3.2.4 Data Reduction

IEEE 802.11a, IEEE 802.11b, and Bluetooth

Figures 3.2-8 and 3.2-9 illustrate the data reduction process and results. The process was applied to the PED baseline test data set and wireless device emission data set in each frequency band. For the purpose of comparison and analysis, large amounts of data were reduced by creating data envelopes, which are representative of the maximum measurements for each PED, and each WLAN device and host combination. These data envelopes were further reduced to two composite data envelopes, a PED composite envelope and a WLAN device composite envelope, that represents the maximum magnitudes

of all PEDs and all WLAN devices. The end of the process results in data plots found in Sections 3.3, 3.4, and 3.5 comparing PED and WLAN device emissions.

A general data reduction process is illustrated in Figure 3.2-8. Implementing this process creates data envelopes from data sets by determining the maximum (MAX) magnitudes for each frequency within a frequency band. The oval shapes illustrated in the figures represent data plots produced for each of the five frequency bands. The DUT notation represents PED, host device, or combination of WLAN device and host. As input to the reduction process, DUT Data represents measurement data collected during PED/host and WLAN device testing using several operating modes. Figure 3.2-8 demonstrates the generation of DUT envelopes using measurement data and the creation of composite envelopes from individual DUT envelopes.

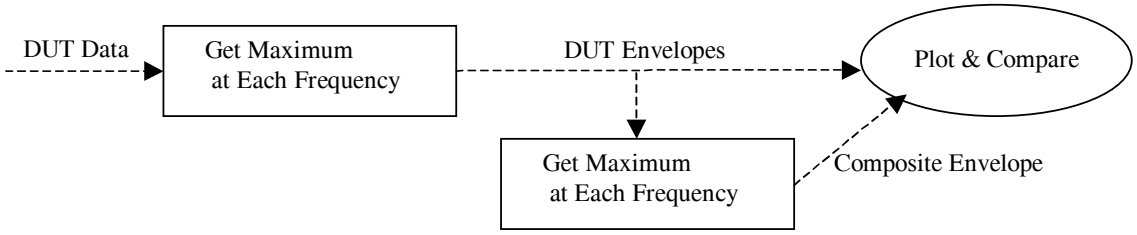

Figure 3.2-8: Data reduction process.

In this section the notation WLAN is used to refer to a WLAN device and host combination, where the host was selected based on lowest emission levels from all PEDs tested (Section 3.2.2 Host Device Baseline). WLAN and PED measurement data are illustrated in Appendices A and B, respectively. The reduction of this data followed the general process illustrated in Figure 3.2-8.

The following algorithms summarize the generation of data envelopes and use DUT to refer to PED or WLAN data.

For each frequency band, and for each DUT,

$$Max\,[DUT\ \ Emissions\ ]_{All\ \_\ Modes} \ \Rightarrow\ DUT_{Envelope}$$

For each frequency band,

$$Max\,[DUT\ \ Envelope\ ]_{All\ \_\ DUT} \ \Rightarrow\ All\ \_\ DUT_{\ Composite\ \ \_\ Env}$$

Conforming to the data reduction process, individual DUT envelopes along with their composite envelopes were generated. PED envelopes are plotted and reported in Section 3.4. WLAN envelopes are plotted and shown in Section 3.3.

Figure 3.2-9 shows the last step in the data reduction process, which plots and compares the final PED composite envelope and the final WLAN composite envelope. The two composite envelopes were plotted together for each frequency band and are reported in Section 3.5.

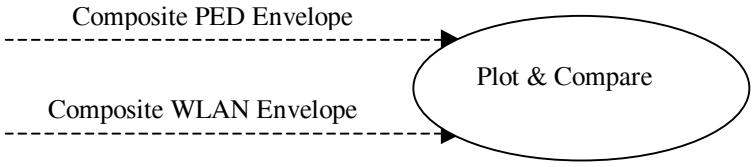

Figure 3.2-9: Composite PEDs and Composite WLAN data reduction and plot (See Section 3.5).

3.3 Test Results of WLAN Devices and Two-Way Radios

This section describes the results from the radiated emission tests conducted on WLAN devices. The following charts illustrate the WLAN devices' and two-way radios' data envelopes. This section includes data acquired during radiated emissions testing using WLAN devices, combined with a host, based on 802.11a, 802.11b, and Bluetooth standards, and FRS radios and GMRS radios.

Data presented in Figures 3.3-1 to 3.3-5 were acquired in the aircraft systems frequency band assigned to VHF-Com systems. Each figure shows envelopes for each individual WLAN device or two-way radio, and an envelope representing the maximum of all devices with data shown in that figure. Individual devices are designated with a number-letter combination, such as 11A-1, 11B-5, Blue-2, FRS1&2, or GMR3&4, whereas the envelope of all devices within a group is simply labeled 11A, 11B, Blue, for WLAN devices, and FRS or GMR for two-way radios.

The individual device envelopes were generated from measured emission data reported in Appendix A that included all test modes. For WLAN devices, these test modes include PS tests, Xfer tests, and idle mode tests. For FRS and GMRS radios, these test modes include different communication channels with the devices receiving and transmitting at maximum power. Noise floor data is also shown on charts in Appendix A.

A Devices Composite Envelope is the maximum at each frequency of all of the individual Device Envelopes. Note that the Device Composite Envelopes in figures 3.3-1 to 3.3-5 are shown in green. In all cases, the green Composite Envelope plot masks portions or all of individual device traces directly underneath, making it difficult to recognize the presence of the individual traces beneath. A description of the processes used for the reduction of data and the generation of envelopes is found in Section 3.2.4. The Composite Envelopes are also used in charts in Section 3.5.

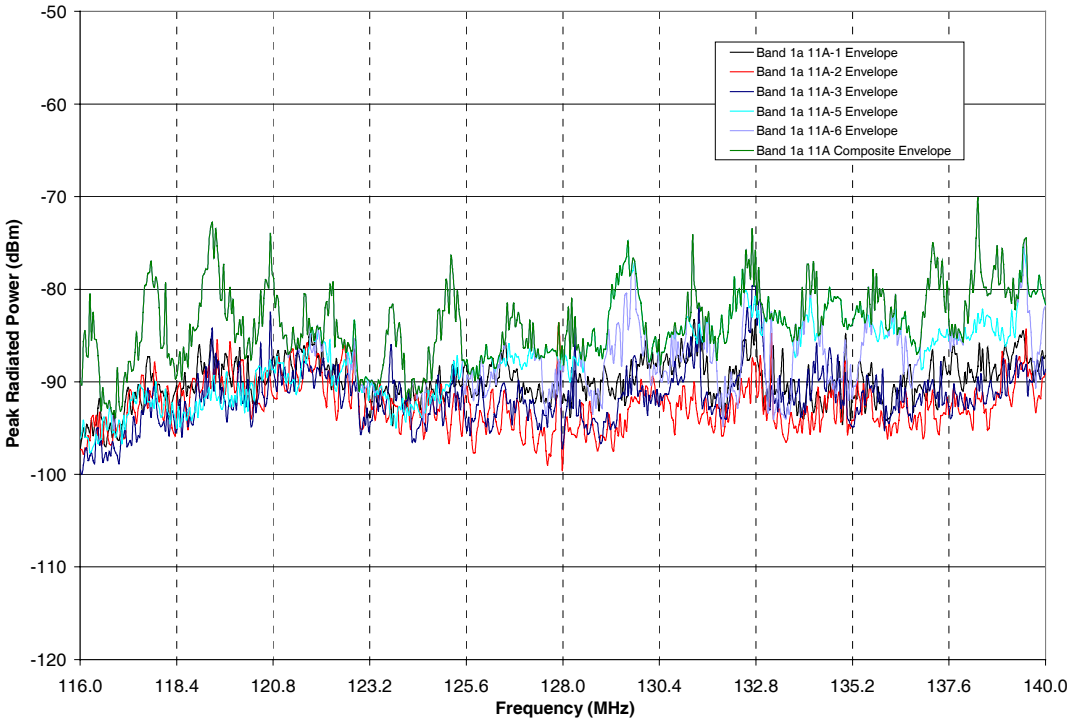

Figure 3.3-1: Individual 802.11a WLAN Device Envelopes and 802.11a WLAN Devices Composite Envelope for Band 1a.

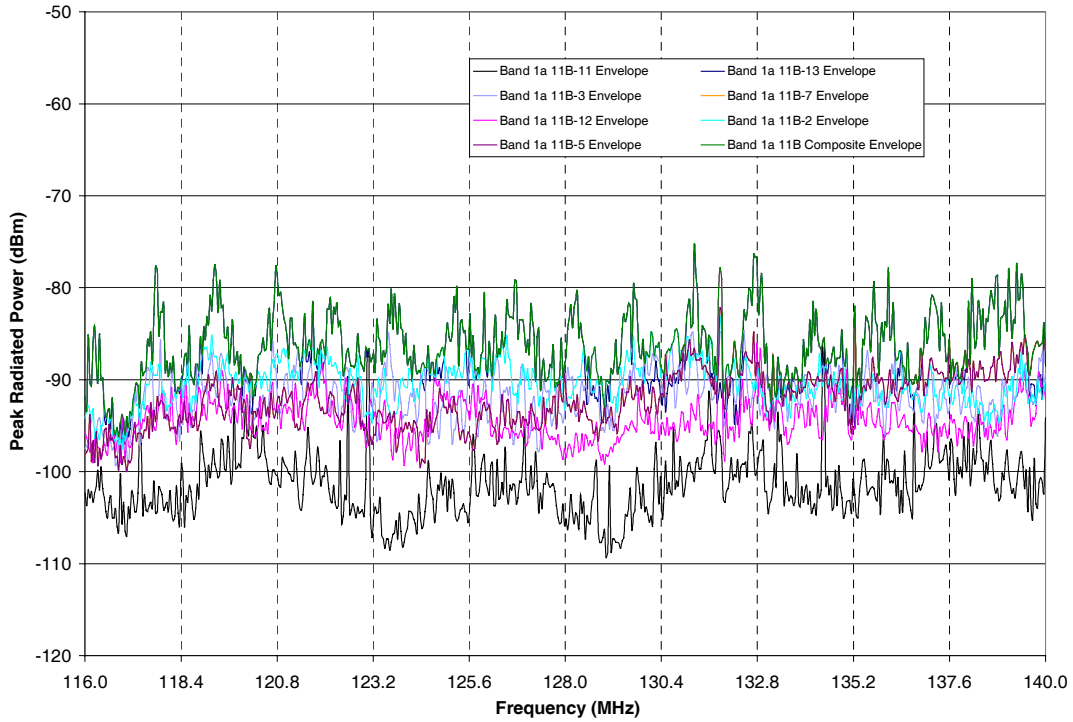

Figure 3.3-2: Individual 802.11b WLAN Device Envelopes and 802.11b WLAN Devices Composite Envelope for Band 1a.

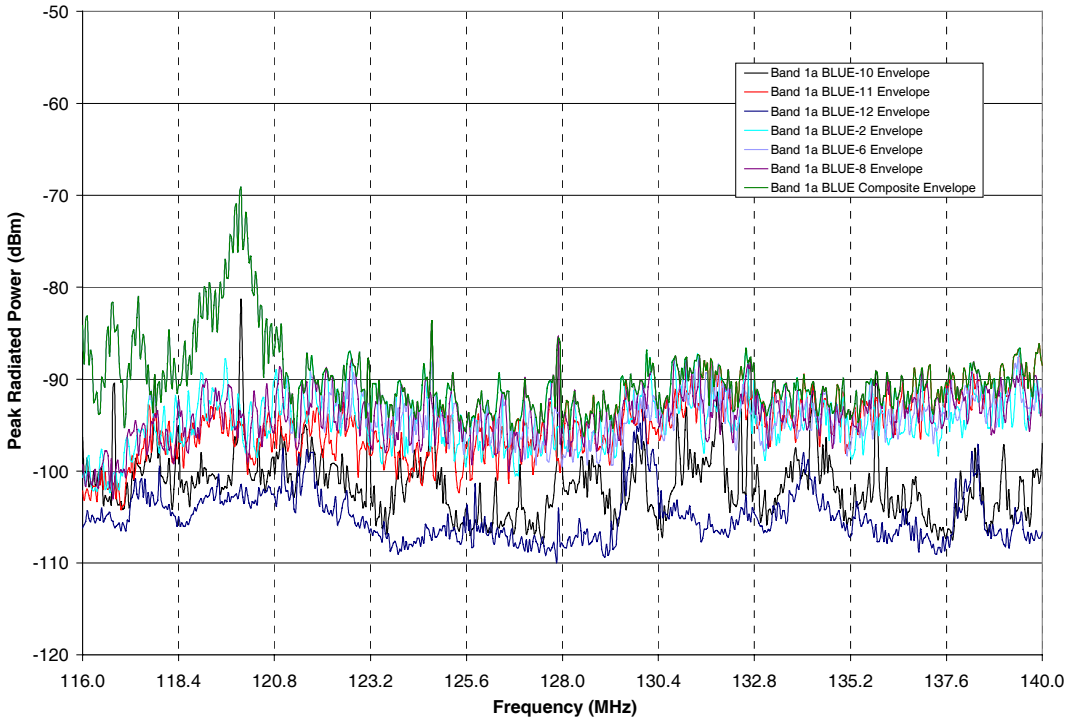

Figure 3.3-3: Individual Bluetooth WLAN Device Envelopes and Bluetooth WLAN Devices Composite Envelope for Band 1a.

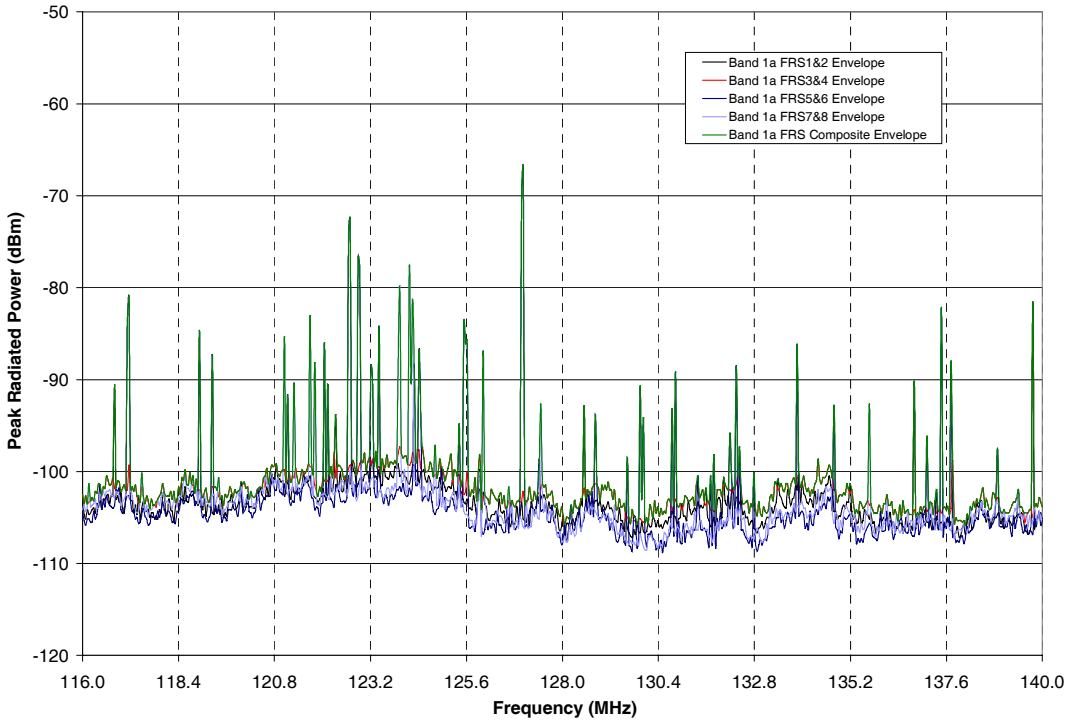

Figure 3.3-4: Individual FRS Radio Envelopes and All FRS Radios Composite Envelope for Band 1a.

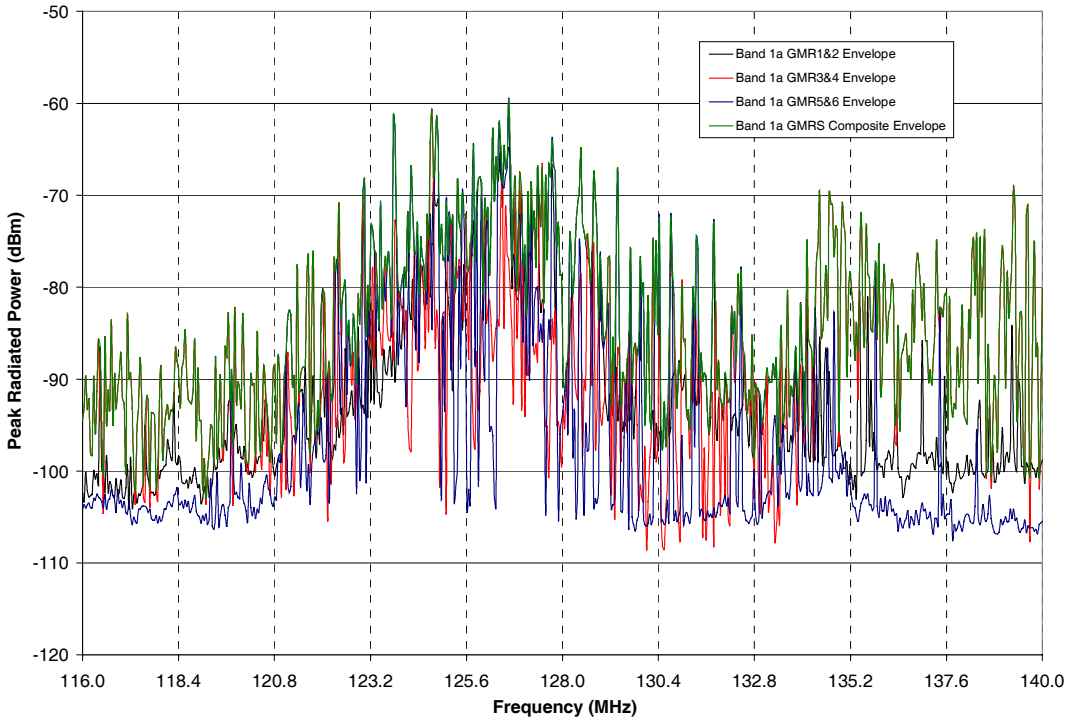

Figure 3.3-5: Individual GMRS Radio Envelopes and All GMRS Radios Composite Envelope for Band 1a.

3.4 Summary of Emission From Standard Laptops and PDAs

The following charts in this section report the PED data envelopes with all PEDs tested. The charts are the result of reduced emission data acquired using PEDs, which include various laptop computers, PDAs and a portable battery operated printer.

Each chart contains plots of all individual PED envelopes. Each individual PED envelope was generated from the measured emissions data, including idle mode and all other PED test modes as reported in Appendix B. The chart also shows a composite maximum envelope that represents the maximum emission of all devices at any given frequency. Thus, the composite maximum envelop overlays the highest individual envelopes at any frequency. A description of the processes used for the reduction of data and the generation of envelopes is found in Section 3.2.4. Noise floor data are also plotted on charts in Appendix B.

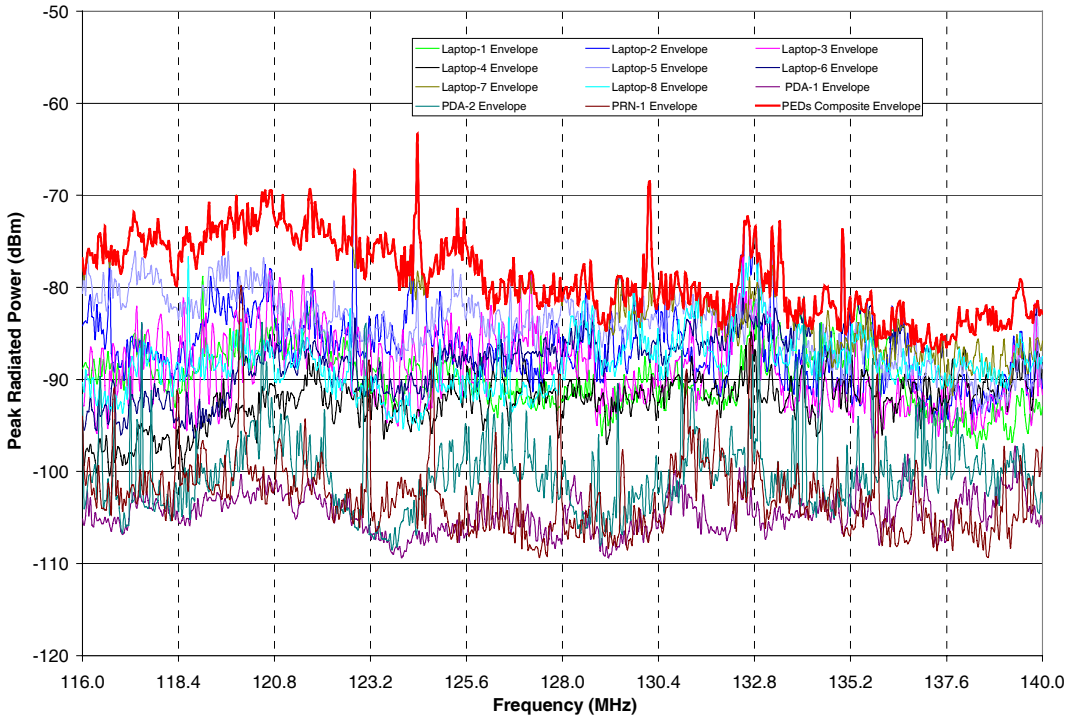

Figure 3.4-1: Individual PED Envelopes and PEDs Composite Envelope for Band 1a.

3.5 Comparison of Emissions From Intentionally- and Unintentionally-Transmitting PEDs

The following charts compare composite emission envelops of all unintentionally-transmitting PEDs, and all intentionally-transmitting 802.11a, 802.11b, and Bluetooth WLAN devices. These composite envelopes are taken from the earlier Sections 3.3 and 3.4. The reduction of the WLAN device data to a WLAN composite envelope is defined in Section 3.3 (data shown in green). The generation of PED envelopes is described in Section 3.4 (data shown in red). The envelopes for FRS and GMRS radios are also shown. A description of the processes used for the reduction of data and the generation of envelopes is found in Section 3.2.4.

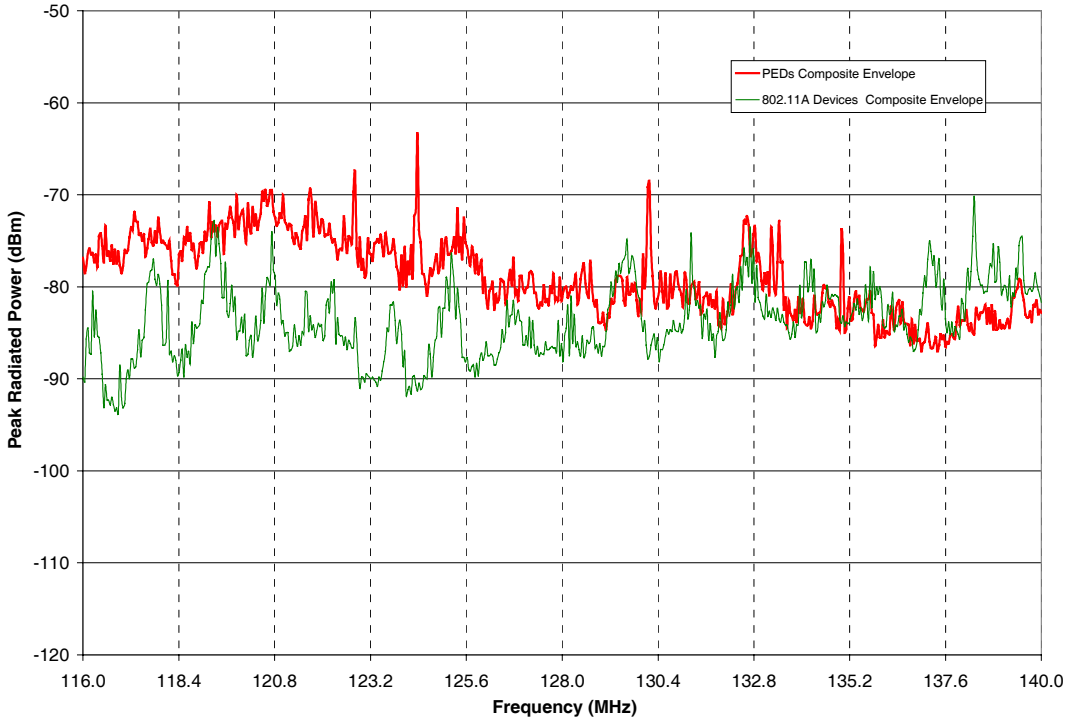

Figure 3.5-1: 802.11a Composite WLAN Devices Envelope and PEDs Composite Envelope for Band 1a.

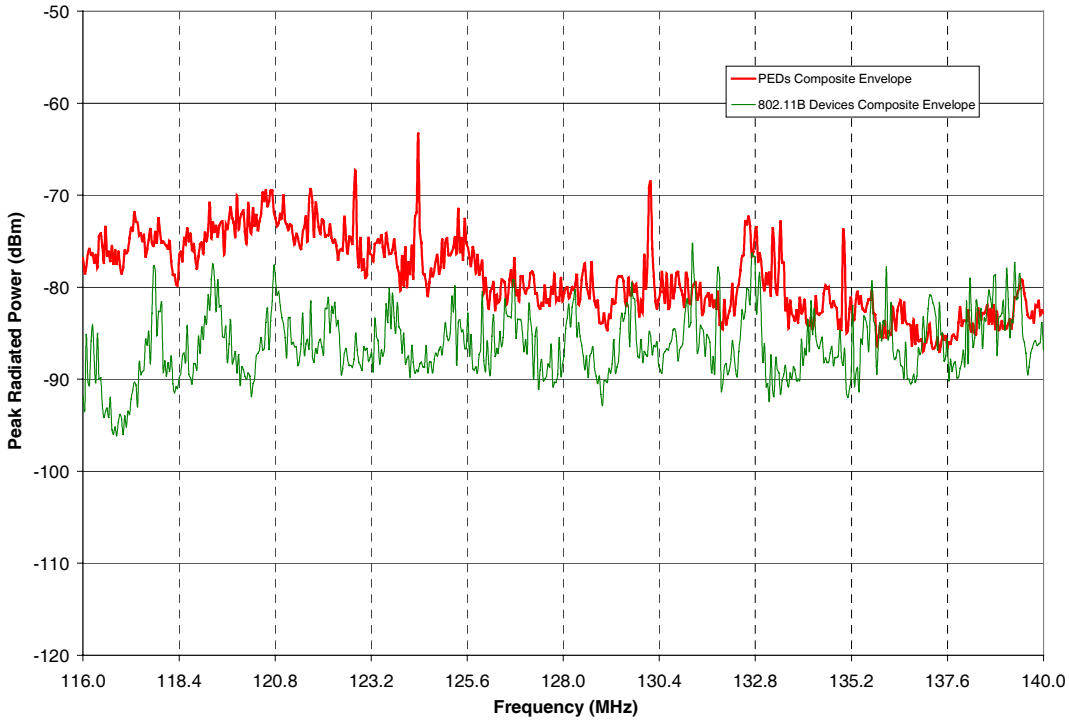

Figure 3.5-2: 802.11b Composite WLAN Devices Envelope and PEDs Composite Envelope for Band 1a.

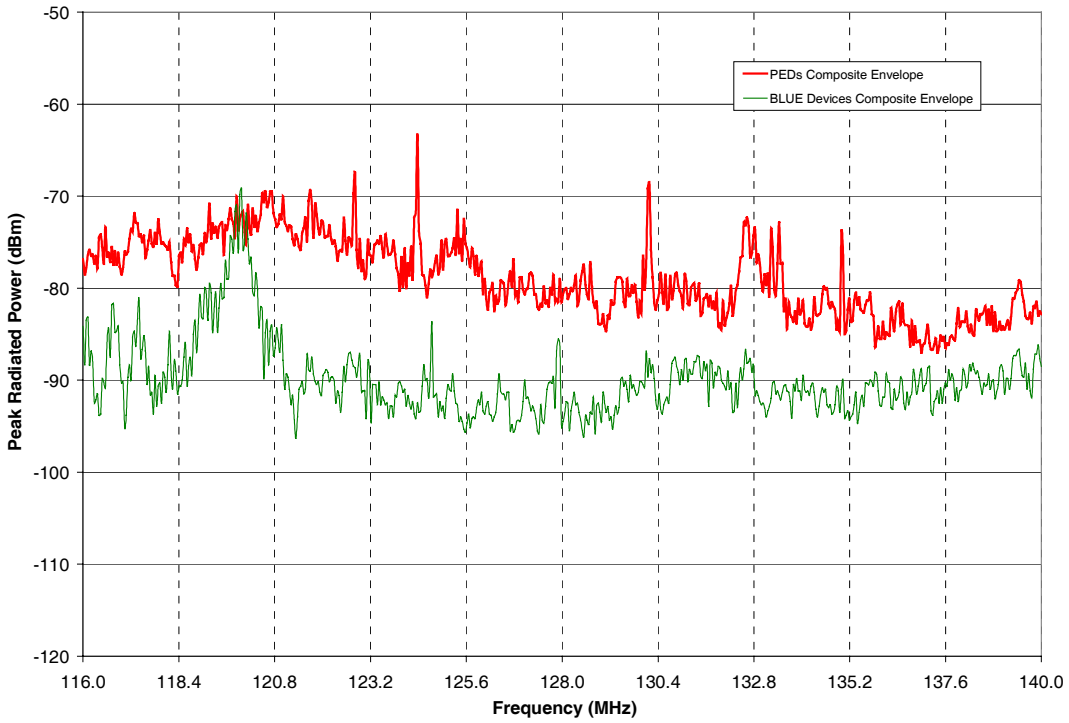

Figure 3.5-3: Bluetooth WLAN Devices Composite Envelope and PEDs Composite Envelope for Band 1a.

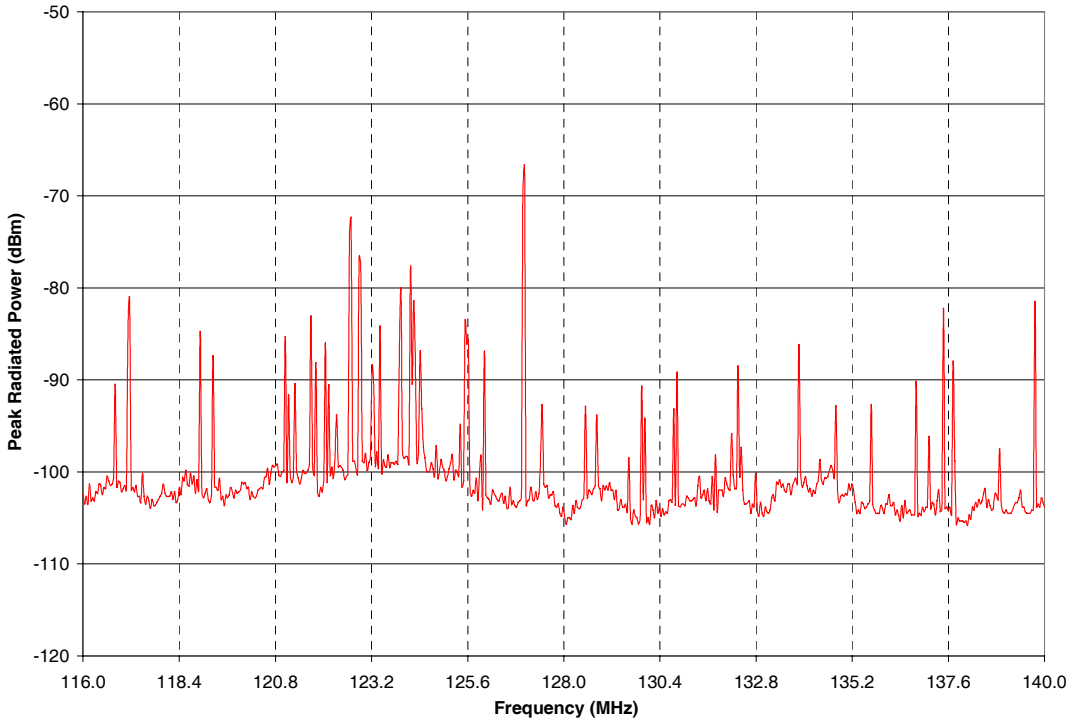

Figure 3.5-4: FRS Radios Composite Envelope for Band 1a.

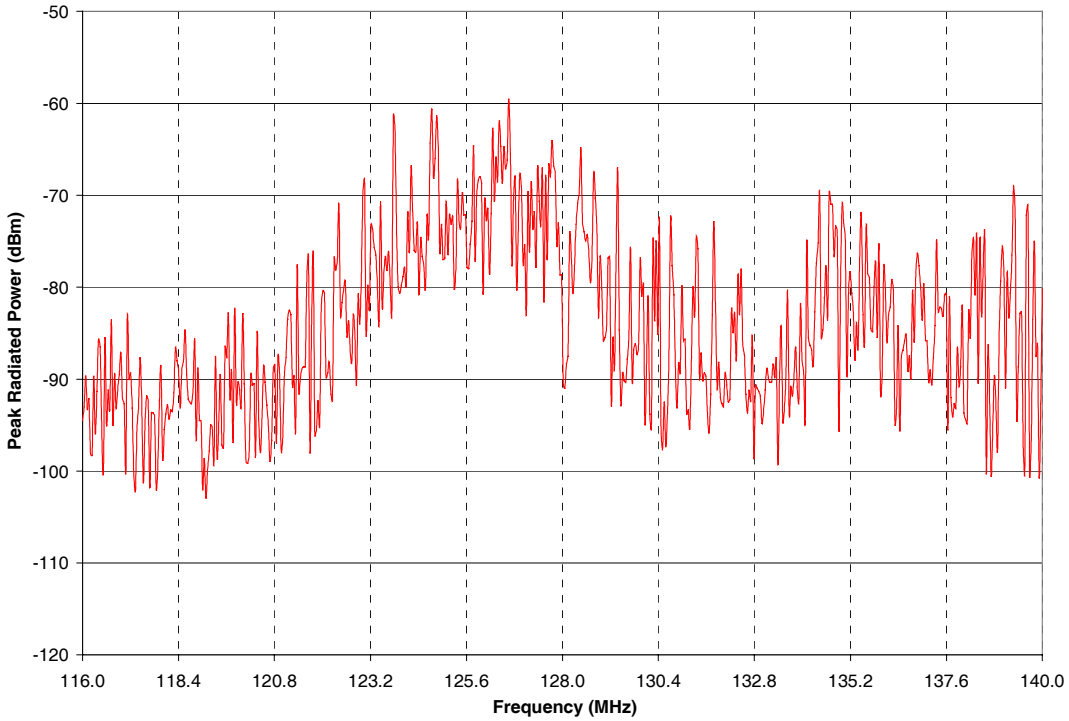

Figure 3.5-5: GMRS Radios Composite Envelope for Band 1a.

3.6 Summary of Maximum Emissions from WLAN Devices and FRS/GMRS Radios

This section summarizes maximum emission results reported in earlier sections for WLAN devices, two-way radios and computer laptops/PDAs. In addition, comparisons with corresponding FCC and RTCA/DO-160 [12] emission limits are reported.

3.6.1 Summary of Maximum Emission Results

Table 3.6-1 summarizes emission data by reporting the maximum emission value of different device groups. The device groups include 802.11b, 802.11a, Bluetooth, FRS radio, GMRS radio, and Laptop/PDAs. The new VHF-Com band emission data is reported as Band 1a. Other data in the table are the emissions results in various aircraft band for the same devices, measured in an earlier effort [1] using the same measurement process. These data are shown for comparisons and completeness.

In this table, the corresponding aircraft radio-navigation systems with frequency spectrum aligned within the emission measurement bands are grouped together as shown. These systems are potentially affected by any high emissions within the their measurement bands. These emission data from Table 3.6-1 are used in the safety margin calculations in a later section. Data in Table 3.6-1 are plotted in Figure 3.6-1.

Figure 3.6-1 also shows that the maximum emission from the WLAN devices are *lower* than the maximum emission from the laptop/PDA devices in the VHF-Com band, whereas the maximum emission from the GMRS radio is higher than from the laptops/PDA. In addition, the maximum emissions in Band 1a and Band 1 are within five dB of each other, with the exception of FRS/GMRS radios with the

difference being as much as 24 dB. Note that lines in Figure 3.6-1 are only for linking the data points at the markers; their magnitudes between the markers have no significant values.

In general, Figure 3.6-1 shows that from the WLAN devices emissions measured are lower than the laptop computers/PDA emissions, with the exception of 802.11a devices in Band 5. FRS and GMRS emissions can be as much as 30 dB higher than the laptop computers/PDAs maximum emission in Band 2, and 20 dB higher than 802.11a devices emissions in Band 5. These observations are much the same as reported in [1].

Table 3.6-1 Maximum Emission from WLAN Devices/ Two-way Radios in Aircraft Bands (in dBm)

Measurement Band	Frequency (MHz)	802.11b	Blue-tooth	802.11a	FRS Radio	GMRS Radio	Laptops PDAs	Aircraft Bands
Band 1	105 - 120	-78.2	-66.8	-74.2	-90.7	-79.3	-68.0	LOC, VOR
Band 1a	**116 - 140**	**-75.3**	**-69.2**	**-70.2**	**-67.0**	**-59.5**	**-63.3**	**VHF-Com**
Band 2	325 - 340	-75.7	-77.2	-71.8	-37.2	-28.5	-58.7	GS
Band 3	960 - 1250	-65.3	-49.7	-57.7	-43.5	-44.7	-45.7	TCAS, DME, GPS L2
Band 4	1565 -1585	-67.7	-81.7	-65.2	-60.2	-57.0	-55.8	GPS L1
Band 5	5020 - 5100	-77.7	-78.2	-52.0	-38.2	-33.0	-77.0	MLS

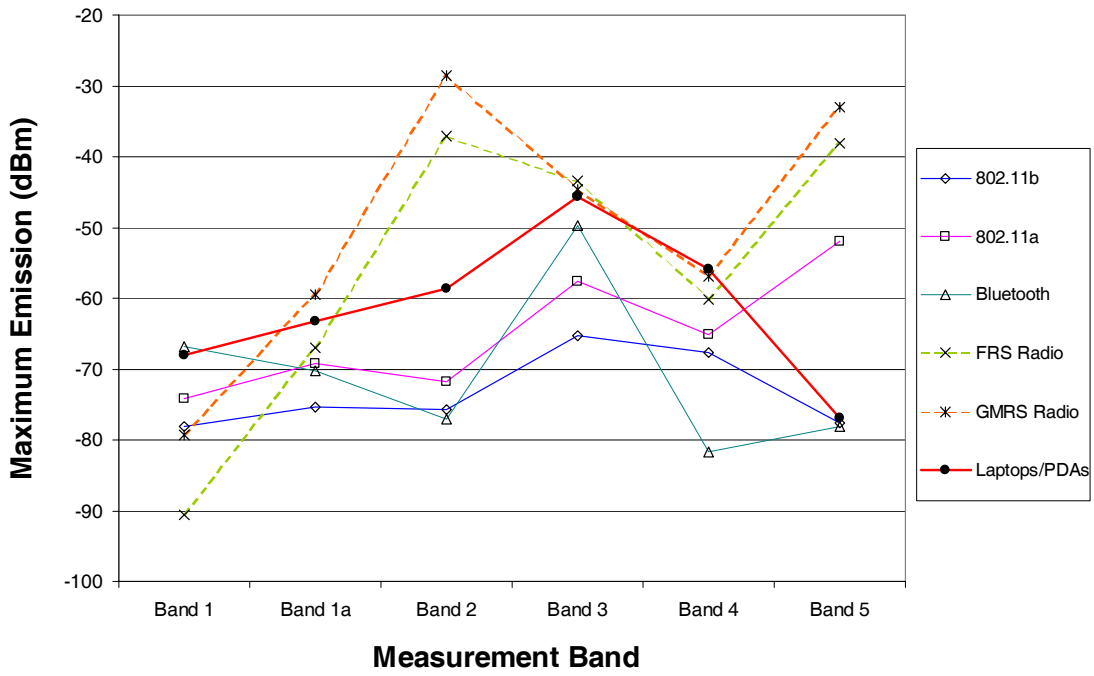

Figure 3.6-1: Maximum emission from WLAN, Bluetooth devices, FRS/GMRS radios and Laptops/PDAs. Data in bands other than Band 1a are from [1].

3.6.2 Comparison with Emission Limits

Table 3.6-2 shows the FCC Part 15.109 [13] and 15.209 [14] limits for unintentional and intentional radiators, the RTCA/DO-160 Category M limits, and the FCC spurious emission limits for FRS/GMRS radios (FCC 95.635 [15]). RTCA/DO-160 Category M emission limit is selected for comparisons with spurious emissions from passenger carry-on electronic devices since these devices can be located in the passenger cabin or in the cockpit of a transport aircraft, where apertures (such as windows) are electromagnetically significant. RTCA/DO-160 Section 21 [12] defines Category M as:

> "***Category M:***
> *This category is defined for equipment and interconnected wiring located in areas where apertures are em significant and not directly in view of radio receiver's antenna. This category may be suitable for equipment and associated interconnecting wiring located in the passenger cabin or in the cockpit of a transport aircraft*."

Table 3.6-2 below listed the FCC and RTCA emission limits in the VHF-Com Band (Band 1a) for PEDs, WLAN devices, and GMRS/FRS radios. Similar limits for other bands are also shown for comparison. In this table, the RTCA/DO-160 Category M limit for each *measurement band* is chosen to be the lowest limit for the *aircraft bands* within it. As an illustration, the emission measurement Band 3 would cover TCAS, ATCRBS, DME, GPS L2 and GPS L5. The emission limit for the whole measurement band is chosen to be the lowest limit of all the systems listed. In this case, the lowest value is 50 dBμV/m for TCAS, DME and ATCRBS since the limits for GPS L2 and GPS L5 are higher. In addition, the emission limit for each aircraft radio band is chosen to be the lowest value between its lowest and highest frequency limits.

To compare with measured emission data in dBm, the field limits in FCC Part 15 and the RTCA/DO-160 Category M are converted to the equivalent Effective Isotropic Radiated Power (*EIRP*) using Equation 3.6-1.

$$EIRP = \frac{E^2 \cdot 4\pi R^2}{120\pi} \qquad \text{(Eq. 3.6-1)}$$

where $EIRP$ = Effective Isotropic Radiated Power (*W*)

E = Electric Field Intensity at distance R (*V/m*)

R = Distance (*m*)

Ideally, *E* field measurement is taken in the direction of maximum radiation from the test device. To convert power, *EIRP,* from watts to dBm, use the expression *10 * log(1000*EIRP)*. For the RTCA/DO-160 limit given in *dBμV/m*, the unit is converted to *V/m* before applying Equation 3.6-1.

Table 3.6-2: Estimated FCC and RTCA spurious radiated emission limits.

	FCC Part 15 Limit (μV/m @ 3m)	**RTCA/DO-160 Category M Limit** (dBμV/m @ 1m)	**FCC Part 15 Limit** (*EIRP*, dBm)	**RTCA/DO-160 Category M Limit** (*EIRP*, dBm)	**FCC FRS/GMRS Radio Limit** (*TRP*,dBm)
Band 1	150	34*	-51.7	-70.8*	-13
Band 1a	150	34	-51.7	-70.8	-13
Band 2	200	52.9	-49.2	-51.9	-13
Band 3	500	50	-41.2	-54.8	-13
Band 4	500	53	-41.2	-51.8	-13
Band 5	500	71.8	-41.2	-33.0	-13

* [1] incorrectly reported DO-160 Cat. M limit one dB higher, or 35 dBμV/m @ 1m, resulting in –69.8 dBm EIRP. The corrected figures are listed above.

Emissions measured using a RC, on the other hand, provide results in "total radiated power" (*TRP*) within the measurement resolution bandwidth. *TRP* is different from *EIRP* except for antennas or devices with an isotropic radiation pattern. Rather,

$$EIRP\ (\text{dBm}) = TRP\ (\text{dBm}) + D_G\ (\text{dB}), \qquad \text{(Eq. 3.6-2)}$$

where D_G is *directivity,* or maximum *directive gain* of the test device. Directive gain of any device is a measure of radiated power as a function of aspect angle referenced to the isotropic value.

For spurious emissions, D_G is the directivity at the spurious emission frequency of interest. D_G is usually difficult to measure or calculate since maximum radiation angles and radiation mechanisms for *spurious* emissions are often not known. Maximum theoretical estimation of D_G based on device size tends to significantly over-estimate the real directivity, especially at high frequency, because the device geometry is typically not designed to radiate efficiently as an antenna as assumed in the theoretical estimation. There are other theoretical statistical developments to estimate the "expected" directivity for non-intentional radiators [19]. These developments are yet to be validated or widely accepted. Additional details on expected directivity are discussed in Section 3.6.3.

For simplicity, we assume that the WLAN devices (plus the host computer laptops/PDAs) have unity D_G for spurious emission. Thus, *TRP* is assumed to be the same as *EIRP* at all spurious frequencies of interest. This assumption introduces an uncertainty level equal to D_G, according to Equation 3.6-2. For a dipole antenna with small electrical length, D_G is close to 1.76 dBi (or dB relative to isotropic). For a half-wave dipole, D_G is close to 2.15 dBi. Thus, it is reasonable to assume for devices up to one-half a wavelength in size, the uncertainties should not be much more than 2-5 dB. This level of uncertainty is considered acceptable for a first order comparison.

Section 3.6.3 computes the "expected" directivity using formulas provided in [16]. For a device 0.5 m in size (approximately the maximum size of an open laptop computer), the expected directivity is between 5 dB near 100 MHz (near VHF-Com band) and 9 dB near 5 GHz. These expected directivity values are provided for information purposes only. The method used is yet to be proven or widely accepted.

For FRS and GMRS radios, FCC 95.635 [15] dictates the attenuation for frequency *outside* of the vicinity of the center frequency is at least $43 + 10\log(P_c)$ *dB*, where P_c is carrier frequency power in watts. For 0.5-watt FRS radios and 2-watt GMRS radios, the attenuation below carrier power is 40 dB for FRS radios and 46 dB for GMRS radios. As a result, the calculated emission limits are -13 dBm for both FRS and GMRS radios.

Figure 3.6-2 shows emissions in Band 1a from laptops/PDAs and WLAN devices are lower than corresponding FCC equivalent *EIRP* limits. However, they can approach (WLAN devices) or even exceed (laptop computers/PDAs) the RTCA/DO-160 Category M equivalent *EIRP* limits in the same band. This is especially the case if devices' directivities are considered. More about directivity can be found in section 3.6.3. From the figure, it can be argued that emissions from the measured WLAN devices in Band 1a, while approaching or exceeding the RTCA/DO-160 Cat M limits, do not pose significantly higher risk to aircraft radio receivers than emissions from standard laptop/PDA devices. Similar arguments can be made in other bands with the exception of Band 5 for MLS.

For FRS/GMRS radios, Figure 3.6-3 shows emissions are still below the FCC maximum out-of-band emission limit of –13 dBm for these devices. However, their emissions in Band 1a, and also Band 2 and 3, far exceeded the RTCA/DO-160 Cat M limits. The threat of interference from these two-way radios can be significantly higher than from the laptops/PDAs.

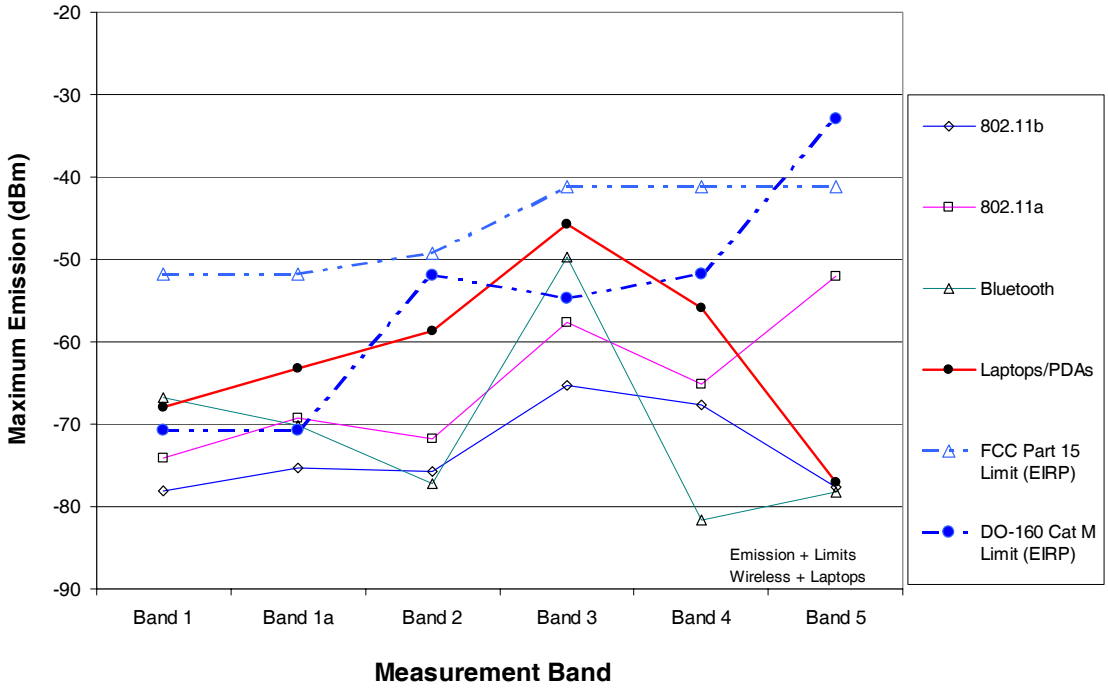

Figure 3.6-2: Maximum emissions from WLAN devices, laptops/PDAs and comparison with FCC and RTCA/DO-160 equivalent *EIRP* limits.

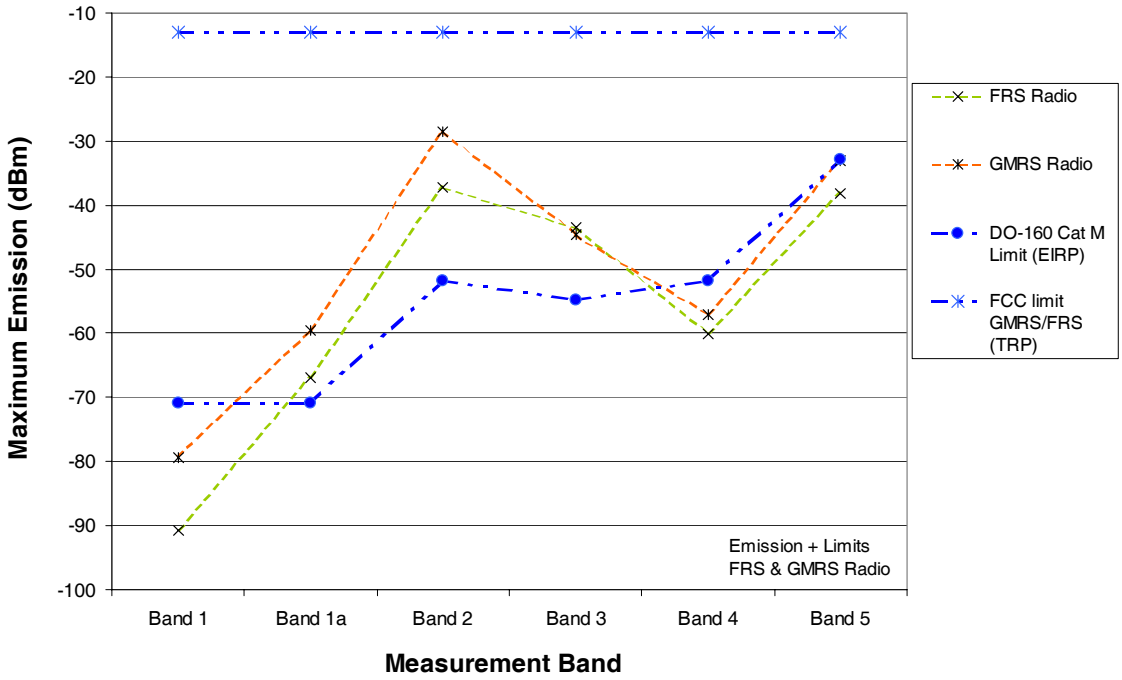

Figure 3.6-3: Maximum emission from two-way FRS/GMRS radios and comparison with FCC limits.

3.6.3 Expected Directivity Estimation

The comparisons above were between the *TRP* from the devices and the FCC Part 15 and RTCA/DO-160 Cat. M equivalent *EIRP* limits, assuming unity directivity. For devices with directivity different than unity, the limits must be adjusted downward by the amounts equal to the devices directivity in dB, which can vary with device size, frequency and geometry.

Reference [16] provides a method to estimate the *expected* directivity derived from a statistical approach. Using equations given, expected directivity of a device can be estimated if its maximum dimension is known. For a laptop computer with the maximum dimension of 0.5 m (open screen configuration), the expected directivity is shown in Figure 3.6-4. This figure shows the results of three calculations: 1) theoretical maximum directivity for a high gain antenna of the same size, 2) expected directivity for 1-planar cut measurement, and 3) expected directivity for 3-planar cut measurement. The 3-planar cut expected directivity is between five and eight dB for frequencies in Band 4 (GPS) and below, and less than nine dB in Band 5 (MLS). In Band 1a, Figure 3.6-4 shows an expected directivity of approximately 5 dB.

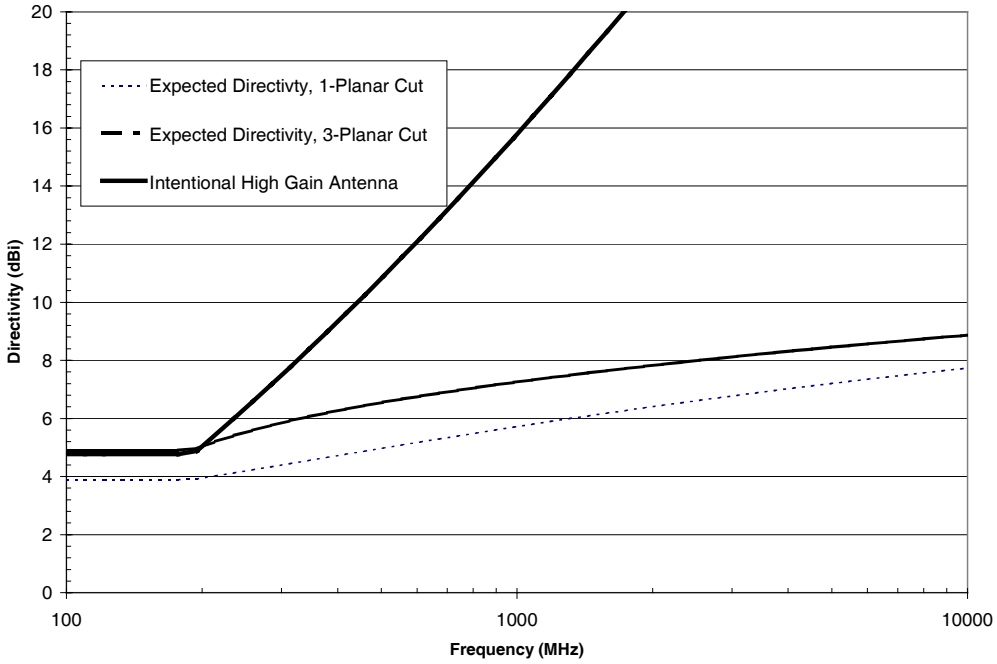

Figure 3.6-4: Expected spurious emission directivity of a device having 0.5m maximum dimension.

4 Aircraft Interference Path Loss Determination

Aircraft IPL is the second of the three major components needed for assessing the potential of interference from RF sources to aircraft receivers. There are about 35 different types of operational, commercial jet airplanes built in the US and Western Europe with a capacity of 30 seats or more. Each aircraft type and series has a unique configuration of antenna placements and radio receiver installations. These variations may result in widely different IPL values.

The following sections describe a recent effort to measure IPL on six B737s and four B747s for various radio receiver systems. The data have been previously reported in [1] and the VHF-Com band data is repeated. The results are also presented along with other existing available IPL data for comparison.

4.1 Interference Path Loss Measurements on B737s and B747s

Previous investigations [1] described the IPL measurements and results for several B737 and B747 aircraft. The measurement was a part of the cooperative effort between UAL, EWI and NASA LaRC. The IPL measurements were performed during three one-week visits to the Southern California Aviation facility in Victorville, California. UAL provided the flight-ready airplanes, along with fuel, engineering and mechanic support for this effort. These airplanes were temporarily put in storage configuration due to September 11 terrorist events that resulted in lower demand in passenger travel and an increase in surplus capacity. NASA provided measurement instrumentation, data acquisition and test control software development and support, and staff. EWI was tasked to lead the overall effort and to conduct analysis.

Measurements were conducted on six B737-200 airplanes for the VOR/LOC, VHF-Com 1, GS, TCAS, and GPS systems. The interference source, simulated with dipole and horn antennas, was positioned to radiate toward each of the windows and the door exits on one side of the aircraft. In addition, full IPL measurements were also conducted on two B737s with the transmit antenna positioned at all seat locations including locations between seats (on one side of the aircraft).

IPL measurements were also conducted on the four B747-400 aircraft for the LOC, VHF-Com 1, GS, TCAS, GPS and SatCom systems. Due to large aircraft size and the number of windows and doors, IPL was measured with the transmitting antenna positioned only at selected windows considered closest to the receiving aircraft antenna and to provide the lowest path loss values. For systems with antennas on top of the aircraft, including VHF-Com 1, these locations include all windows on one side of the *upper deck*. Figure 4.1-1 shows images of B737 and B747 aircraft at the measurement site. In these images, the VHF-1 Com antenna is visible near the over-the-wing emergency exit on a B737. On a B747, the VHF-com antenna is above the emergency exit on the upper deck, and is barely visible from the ground.

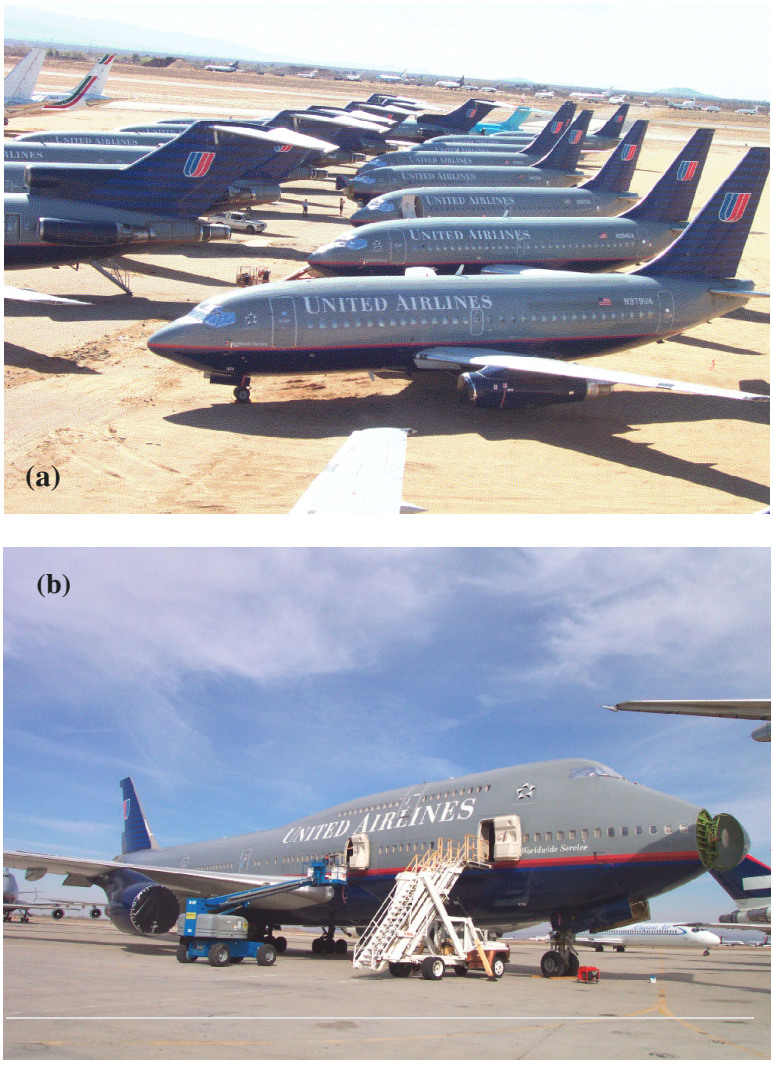

Figure 4.1-1: (a) B737-200 and (b) B747-400 aircraft at the measurement site.

The following subsections, 4.1.1 and 4.1.2, describe the measurement method and IPL results, specifically for the VHF-Com system.

4.1.1 IPL Measurement Method

It is assumed that for PEDs interference problems, the interference source is located within the passenger cabin, and the victims are aircraft radio receiver systems. A common path of PED interference is through the windows or door seams, along the aircraft body, and into the aircraft antennas. The interference signal picked up by the antennas is channeled back into the receivers to potentially cause interference if they are higher than the receiver interference thresholds.

Figures 4.1-2 and 4.1-3 illustrate typical radio receiver interference coupling paths and a setup for conducting IPL measurements. The setup shows a tracking source is used to provide RF power to the transmit antenna, and a spectrum analyzer is used to measure the signal received by the aircraft antenna. The frequency-coupled spectrum analyzer and tracking source pair allows for frequency sweeps, resulting in more thorough measurements and reduced test time. Swept CW was preferred over discrete frequency measurement, according to RTCA/DO-233. A pair of test cables is used to connect the instruments to the aircraft antenna cable and to the transmit antenna. An optional amplifier may be needed to increase the signal strength depending upon the capability of the tracking source and the path loss level. A pre-amplifier may be needed in the receive path near the spectrum analyzer for increased dynamic range. This pre-amplifier (not shown in Figure 4.1-3) may be internal to the spectrum analyzer.

In Figure 4.1-3, VHF-Com band IPL is defined to be the ratio, or the difference in dB, between the power radiated from the transmit antenna at location (1) to the power received at location (2). Or,

$$IPL = P^{T}_{(1)} - P^{R}_{(2)} \quad \text{for most systems including VHF-Com} \qquad \text{(Eq. 4.1-1)}$$

where $P^{T}_{(1)}$ is power transmitted at point (1), and $P^{R}_{(2)}$ is power received at points (2)in dBm.

A standard dipole antenna tuned to the measurement band center frequency was used as the transmit antenna. No corrections were made to account for the transmit antenna gain as performed on many data sets documented in RTCA/DO-199 and RTCA/DO-233. The proximity of the transmit antennas and their surroundings, such as walls, seats, windows, table trays, would have large effects on the true antenna gain, and that free-space antenna gain is viewed as not the appropriate correction factor. The true antenna gain is not known in the presence of the obstacles.

In earlier efforts, transmit antenna gain correction was not applied to at least one set of data in RTCA/DO-199. In this effort, it is considered best not to correct for the free space antenna gain in the definition for IPL for the reasons stated. However, the free-space antenna gain, as provided by the antenna manufacturer, is shown in Table 4.1-1 for use in factoring in the transmit antenna free-space gain, if so desired.

In the actual measurement, the test cables at (1) and (2) were connected together and a “through” swept measurement was made for the total system loss. The test cables were then reconnected at points (1) and (2) and another swept-frequency measurement was made. The instrument settings were maintained to be the same as during the “through” system loss measurement. The receive power difference between the maximum of the first measurement data and the maximum of the second measurement data gave the IPL for that particular transmit antenna location. This calculation for IPL was conducted during data post-processing.

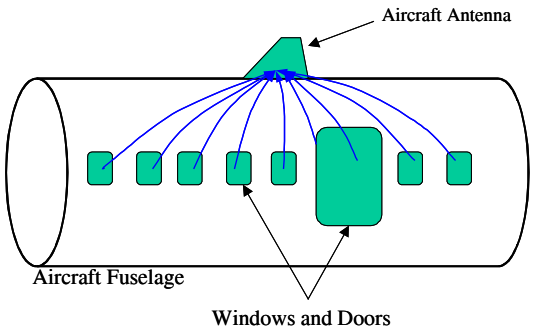

Figure 4.1-2: A typical radio receiver interference coupling path for a top mounted aircraft antenna.

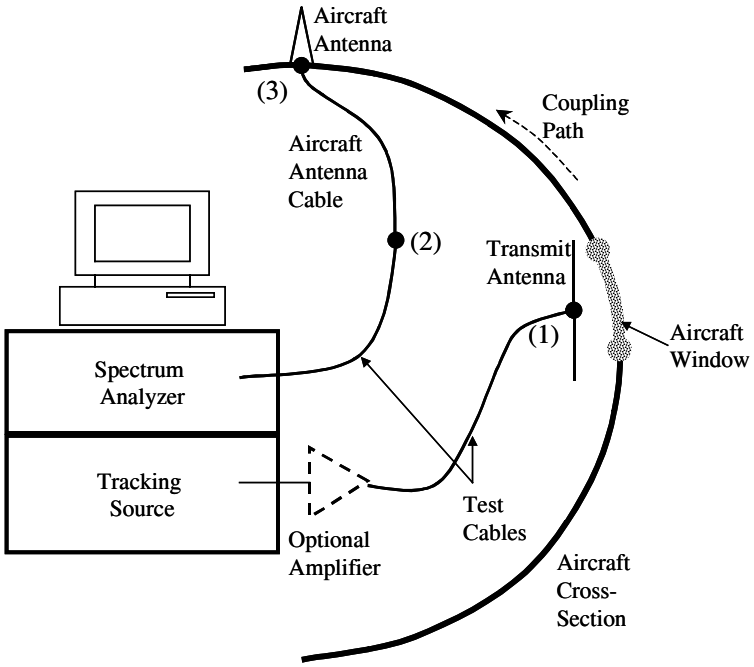

Figure 4.1-3: A typical setup for conducting an IPL measurement.

Table 4.1-1: Transmit Antenna Free-Space Gain (dBi)

Aircraft Systems	Aircraft Antenna Location	Spectrum (MHz)	Measurement Frequency Range (MHz)	Transmit Antenna Type	Free-Space Antenna Gain (dBi)
VHF-Com 1	Top	118 – 137	116-138	Dipole	2.1

As shown in Figure 4.1-3, a transmit antenna was used to simulate an interference source. The tuned dipole transmit antenna was used for the VHF-Com band.

For the VHF-Com system, IPL included aircraft cable loss, since receiver susceptibility thresholds were specified at the receiver antenna port.

The measurement process for each system on each aircraft typically involved the following steps:

1. Conduct 1-meter path loss measurement. IPL was measured with the transmit antenna positioned one meter from the aircraft antenna. This simple step established a baseline measurement and helped detect any excessive aircraft antenna cable loss. Excessive cable loss could indicate possible signs of connector corrosion in the path. These data were not needed to compute the IPL.

2. Configure the spectrum analyzer to the proper reference level, resolution bandwidth, attenuation level and desired measurement frequency band. Configure the tracking source to track the frequency sweep of the spectrum analyzer. Set the tracking source output to desired power level.

3. Measure test cable and aircraft cable "through" losses.

4. Position the transmit antenna at a desired location, typically near a window or door. Point the antenna to radiate toward a window or door seam.

5. Clear spectrum analyzer's trace. Set spectrum analyzer to "Trace Max Hold" and sweep continuously across the desired measurement band.

6. Scan the transmit antenna slowly along the door seam, while the spectrum analyzer is still set at "Trace Max Hold". No scanning was needed at the windows due to small window sizes.

7. Record trace and the peak marker value. For systems that experience narrowband peaks caused by strong local transmitters, position the marker at the peak of the broadband envelope while avoiding the narrowband peaks. Record data at this marker location.

8. Change polarization and repeat from step 2 so that both vertical and horizontal polarizations of the transmit antenna are included.

9. Relocate the transmit antenna to another window/door and repeat from step 4.

Post processing involved removing the measured system "through" loss from the total path loss data. The system loss includes the effects of test cable losses, amplifier gains, and other types of losses/gains in the measurement path.

Figure 4.1-4 shows a measurement being conducted with the transmit antenna at a window, and the computer and software used for data acquisition. Instruments and computers were located within the passenger cabin. Spurious emissions from these equipment were too low to be measurable or to affect the measurement. In contrast, the output signal from the tracking source was 10 dBm or higher depending upon whether an external amplifier was used.

Figure 4.1-4: IPL measurement at window locations. A dipole was used as transmit antenna for VHF-Com, while a computer recorded data from the spectrum analyzer (located underneath the computer).

4.1.2 Measured Interference Path Loss Results

Using the method described in the previous section, IPL was measured for several radio receivers on six B737-200 and four B747-400 aircraft, including the VHF-Com system. Table 4.1-1 shows the measurement frequency range used and the system spectrum along with the measurement frequencies. Table 4.1-2 documents the specific aircraft and their nose numbers.

Table 4.1-2: B737-200 and B747-400 Aircraft Used for IPL Measurement and Their Nose Numbers

B737-200 Aircraft UAL Nose No.	B747-400 Aircraft UAL Nose No.
1881	8173
1883	8174
1879	8188
1994	8186
1997	
1989	

The following sections report measured IPL data for the aircraft listed. Figures 4.1-5 and 4.1-6 show the VHF-Com IPL results for B737 and B747 aircraft. These plots show IPL versus window/door locations where the transmit antenna radiated. It is important to note that the window/door IPL data are similar to the data reported [17], except data in [17] were normalized to the 1-meter path loss measurement. Similar to RTCA/DO-199 and RTCA/DO-233, data in this document are not normalized to the 1-meter path loss measurement.

In addition to the window and door locations, IPL measurements were also conducted at each of the seats, including one measurement between two adjacent seats on the left half of two B737 aircraft. As a result, each full aircraft (nose number 1989 and 1997) measurement provided approximately 160 locations (times two for two transmit antenna polarizations) rather than about 36 window and door locations. Only the window and door measurements are shown in Figures 4.1-6 to 4.1-10. Statistics of the IPL data, including the minimum and the average IPL, are shown in Tables 4.2-1 to 4.2-6.

Comparing the window/door data against the full aircraft data for these two B737s (nose number 1989

to 1997), it can be recognized that the window/door measurements capture the *minimum* IPL for the systems on those aircraft. Also, the differences in *average* IPL values are not significant. This comparison validates the common understanding that the minimum IPL occurs at window and door locations, at which most measurements on other aircraft were made.

On these plots, IPL for each receiver system on each aircraft is represented by two traces for the two vertical and horizontal polarizations of the transmit antennas. The window locations are simply labeled as the n^{th} side window starting from the cockpit. The door locations are labeled as "L1" and "L2" for left side doors; "S1" and "S2" for right side doors; and "EE" for emergency exits. At the doors, a sweep was typically conducted with the transmit antenna scanning along the door seam. A door sweep at L1 is labeled as "L1 Dr Swp".

It was observed that the IPL for both B737 and B747 aircraft generally had a dip in magnitude when the transmitter was located in the vicinity of a door. The magnitude of the dip was significant, in the range of 20 to 25 dB, for the VHF Com systems. This phenomenon shows that the minimum IPL is strongly influenced by the antenna mounting locations relative to a door.

IPL for VHF on a B747 aircraft was also measured with the aircraft partially pressurized. Figure 4.1-6 indicates that by partially pressurizing the passenger cabin, IPL increases by about 10 dB for a VHF system (with the antenna mounted near a door). Thus, pressurizing an aircraft can have a positive effect by reducing RF leakage through the door, and can increase the IPL.

B737-200 IPL Results

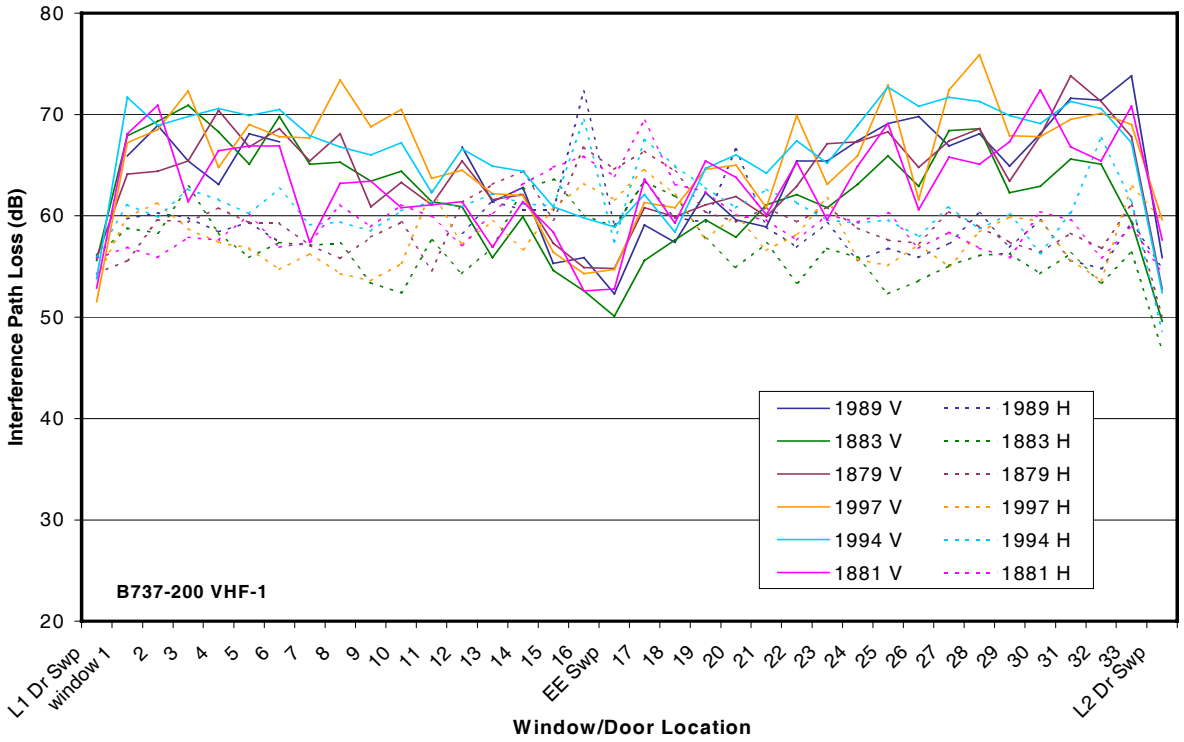

Figure 4.1-5: B737-200 VHF-Com 1 (Top) interference path loss. Left windows/doors excitation.

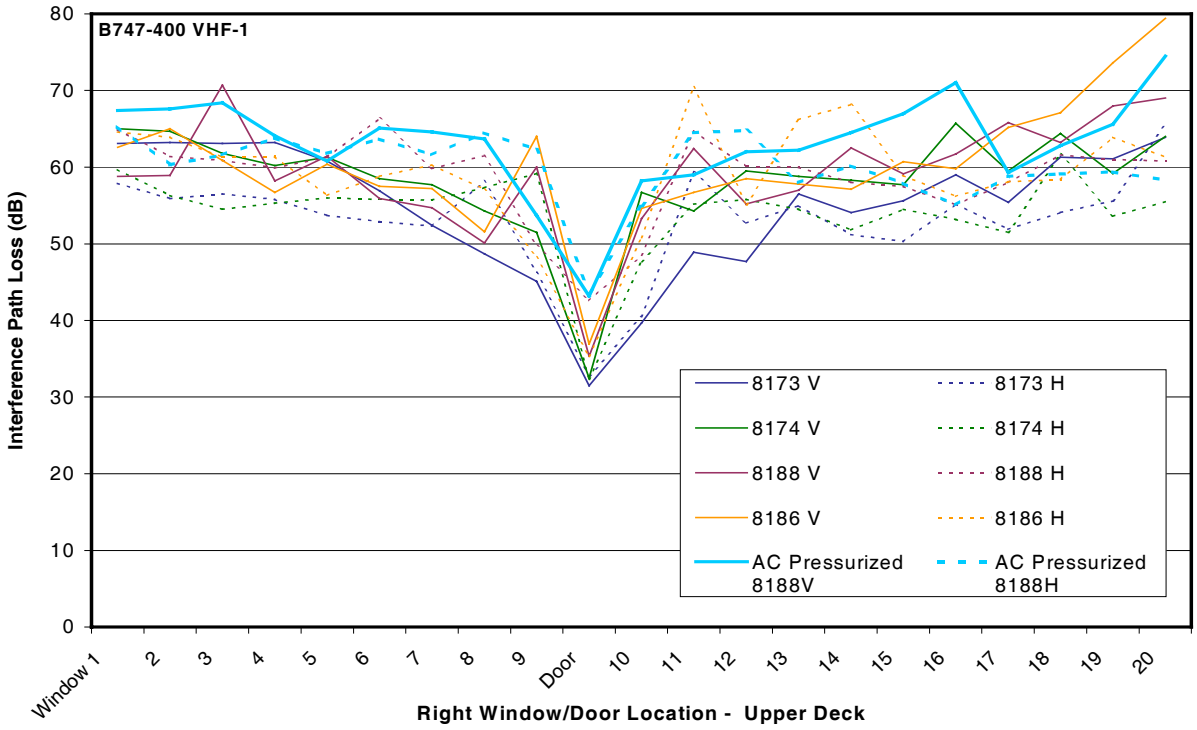

Figure 4.1-6: B747-400 VHF-Com (Top) interference path loss. Upper deck, right windows/doors excitation.

4.2 Other Interference Path Loss Data

In addition to the data previously presented, there are other VHF-Com IPL data previously reported in various documents. These documents include RTCA/DO-199 [3], DO-233 [4], a Veda [18] report, and those from the cooperative agreement between NASA and Delta Airlines [19]. Most of these data were summarized in the previous report on interference effects of cellular phones and wireless LAN [1,2]. Due to relevancy to the current problem, they are repeated in Tables 4.2-2 along with the new B747 and B737 IPL data.

The main difference between the path loss definition in this document and the definition used in parts of RTCA/DO-199 and RTCA/DO-233 is whether the transmit antenna's free-space antenna factors are included in the path loss data provided. In this document, it is assumed that the environment is far from free space and that free-space antenna factors are not valid correction factors. The true transmit antenna factors are not known, and are not included in the path loss calculations. However, free-space antenna factors for the antennas used are provided in Table 4.1-1.

In RTCA/DO-199 (Appendix A), most reported papers used the same definition for IPL as shown in Eq. 4.1-1, but with a correction for transmit antenna gain. Namely,

$$PLF = (\text{Tx Power in dBm}) - (\text{Rx Power in dBm}) + (\text{Tx Antenna Gain in dB}), \qquad \text{(Eq. 4.2-1)}$$

where

PLF is Path Loss Factor, and

Tx and *Rx* are *Transmit* and *Receive* (Antennas), respectively.

There were also test papers in RTCA/DO-199 with PLF calculated *without* the correction applied (paper SC156-110), and the transmit antenna gain factors were not provided. In these cases, the path loss definition is the same as in Eq. 4.1-1.

Boeing 757 path loss data from papers RTCA/DO-199 SC156-26, -65 and -186 are not reported in Tables 4.2-1 to 4.2-7. These papers defined transmit power in a way not directly comparable with definitions used in this document, RTCA/DO-233, and the remaining papers in RTCA/DO-199. Data from these papers resulted in unusually low path loss values and are excluded from the minimum IPL estimation in Table 4.3-1 and the interference safety margin calculations in Section 5.

In RTCA/DO-233, *PLF* calculations "may" include *Tx* antenna gain. Antenna gain values were given for a few cases but not others.

Table 4.2-1 summarizes the IPL data for VHF-Com system. Data collected under the cooperative agreement between with UAL, EWI and NASA LaRC are marked as new (even though they were reported earlier in [1]) and were computed from Figures 4.1-5 and 4.1-6. They were computed from the combined data for both vertical and horizontal polarizations. New B737 and B747 data along with existing data from other sources were grouped into large, medium, and small aircraft categories. For each aircraft measured, the minimum IPL (MIPL), the average IPL and the standard deviation (StDev) were reported if available.

The number of measurement points and measurement frequency range were also reported when available. The number of measurement points was often reported as a *number times 2*, i.e. "*26x2*". This notation indicated that both transmit antenna polarizations, vertical and horizontal, were used at each measurement location, effectively doubling the number of data points. Thus, "26x2" indicated measurements were taken at 26 locations, with vertical and horizontal polarized source antenna, resulting in 52 data points.

The statistics of the MIPL for each large, medium and small aircraft category were also reported. In addition, statistics of the MIPL calculated using ALL available data were shown at the end of each table and again in Table 4.3-1. These statistics include the lowest MIPL and the average MIPL for the safety margin calculations in Section 5.

Table 4.2-1: VHF Comm IPL

New Data	Aircraft & Model	Interference Path Loss (IPL) (dB)			No. of Meas.	Test Freq. Range (MHz)
		Min (MIPL)	Average	StDev		
	Large Aircraft					
✓	B747 8173 (UAL/EWI/NASA)	31.5	53.9	7.7	21x2	116-138
✓	B747 8174 (UAL/EWI/NASA)	32.3	56.3	6.7	21x2	116-138
✓	B747 8188 (UAL/EWI/NASA)	35.3	58.9	6.6	21x2	116-138
✓	B747 8186 (UAL/EWI/NASA)	35.3	59.5	7.9	21x2	116-138
✓	B747 8188 (UAL/EWI/NASA) (AC Pressurized)	43.2	61.5	5.9	21x2	116-138
	B747 -VHF1 (DO-233)	40.5	79.2	12.0		
	B747 -VHF2 (DO-233)	63.2	86.2	10.8		
	B747 -VHF3 (DO-233)	71.5	92.9	7.4		
	DC 10 (DO-199)	63.0	80.0		45	117-137
	L1011 -VHF1 (DO-233)	56.2	72.9	6.1		
	L1011 -VHF2 (DO-233)					
	L1011 -VHF3 (DO-233)	62.2	77.2	4.2		
	Column Minimum	***31.5***	***53.9***			
	Column Average	***48.6***	***70.8***			
	Column Maximum	***71.5***	***92.9***			
	Medium Aircraft					
✓	B737 1989 (UAL/EWI/NASA)	52.3	61.9	5.2	36x2	116-138
✓	B737 1883 (UAL/EWI/NASA)	46.8	59.3	5.2	36x2	116-138
✓	B737 1879 (UAL/EWI/NASA)	50.1	61.6	4.7	36x2	116-138
✓	B737 1997 Windows (UAL/EWI/NASA)	51.5	61.9	5.8	36x2	116-138
✓	B737 1997 Full (UAL/EWI/NASA)	51.5	65.8	4.3	173x2	116-138
✓	B737 1994 (UAL/EWI/NASA)	48.6	63.5	5.1	36x2	116-138
✓	B737 1881 (UAL/EWI/NASA)	52.6	61.2	4.5	36x2	116-138
	B737 -VHF1 (DO-233)	52.9	69.0	7.6		
	B737 -VHF2 (DO-233)	58.4	74.2	9.3		
	B737 -VHF3 (DO-233)	53.2	76.2	9.6		
	B757 -VHF1 (DO-233)	49.7	72.9	9.8		
	B757 -VHF2 (DO-233)	38.0	64.7	8.7		
	B757 -VHF3 (DO-233)	53.0	79.3	8.7		
	B757-VHF-Left (Delta/EWI/NASA)	36.3	52.8	7.4	56x2	
	B757-VHF-Right (Delta/EWI/NASA)	49.3	60.6	6.2	38x2	
	B757-VHF-Center (Delta/EWI/NASA)	50.3	64.0	6.7	55x2	
	B727 N40 -a (DO-199)	67.0	71.0		6	118-135
	B727 N40 -b (DO-199)	44.0	53.0		49	118-135
	B727 N40 -c (DO-199)	76.0	80.0		6	109

Table 4.2-1: Concluded

MD80-VHF1 (DO-233)	57.2	74.5	9.2	
MD80-VHF2 (DO-233)	64.9	81.7	10.0	
MD80-VHF3 (DO-233)	55.2	81.7	13.3	
A320 -VHF1 (DO-233)	51.5	70.0	8.4	
A320 -VHF2 (DO-233)	62.1	77.6	6.7	
A320 -VHF3 (DO-233)	55.6	76.2	7.4	
Column Minimum	***36.3***	***52.8***		
Column Average	***53.1***	***68.6***		
Column Maximum	***76.0***	***81.7***		
Small Aircraft				
CRJ VHF-L (Delta/EWI/NASA)	36.7	53.7	7.6	14x2
CRJ VHF-R (Delta/EWI/NASA)	50.9	62.3	6.0	14x2
Emb 120 -VHF-L (Delta/EWI/NASA)	28.7	47.0	7.3	12x2
Emb 120 -VHF-R (Delta/EWI/NASA)	45.0	53.5	3.7	11x2
ATR72- VHF-L (Delta/EWI/NASA)	48.4	61.3	8.2	13x2
ATR72- VHF-R (Delta/EWI/NASA)	43.5	60.0	6.3	26x2
Column Minimum	***28.7***	***47.0***		
Column Average	***42.2***	***56.3***		
Column Maximum	***50.9***	***62.3***		
All Aircraft Column Minimum	**28.7**	**47.0**		
All Aircraft Column Average	**50.4**	**67.4**		
All Aircraft Column Maximum	**76.0**	**92.9**		
All Aircraft Standard Deviation	**10.9**	**10.6**		

4.3 Summary of Minimum Interference Path Loss Data

Table 4.3-1 summarizes the MIPL shown in the tables in Section 4.2. Data in this table were taken from the "All Aircraft" summary rows at the end of the table 4.2-1. The *minimum MIPL* values shown are the *lowest* MIPL of all aircraft. Likewise, the *average MIPL* values displayed are the *average* of the MIPL of all aircraft. The minimum MIPL and the average MIPL will be used in the later calculations for interference safety margins. The maximum MIPL and the StDev of the MIPL of all aircraft are also shown. The standard deviation was calculated without assigning additional weight to any specific aircraft model or number of measurement points.

As observed, there can be a large difference in dB between the maximum MIPL and the minimum MIPL. MIPL can vary between 28.7 dB to 76 dB.

Table 4.3-1: Summary of Aircraft Minimum IPL (MIPL)

	Min MIPL (dB)	**Ave MIPL (dB)**	**Max MIPL (dB)**	**StDev (dB)**
VHF	28.7	50.4	76.0	10.9

5 Interference Analysis

In this section, receiver susceptibility thresholds are discussed and summarized from RTCA/DO-199. In addition, safety margins are calculated from the interference susceptibility thresholds, the path loss data in Section 4, and the emissions from WLAN devices and two-way radios.

5.1 Published Receiver Susceptibility Threshold

Of the three elements required for risk assessment (WLAN/PED/two-way radio emission; aircraft IPL; and receiver interference threshold), receiver interference threshold (to PED interfering signal) is the one element with the least amount of available data. International Civil Aviation Organisation (ICAO) Annex 10, Vol.1 [20] and receiver Minimum Operating Performance Standards (MOPS) did not properly address the in-band, on-channel interference. Spurious signals from PEDs and WLAN devices were too low to cause other interference, such as desensitization, addressed in these documents. As of late 2003, RTCA/DO-199 appears to be the only publicly available source with measured data for VHF-Com band. The volume of available data is far from sufficient to provide confidence in the figures provided.

In RTCA/DO-199, receiver interference levels along with test signal strengths were documented to be –107 dBm with a desired signal level of –89 dBm. The result is a signal-to-interference (*S/I*) ratio of 18 dB. In this document, the test signals were set equal to the minimum desired signals at the receivers. These signals were calculated from the minimum desired external field environments within the coverage airspace assuming an isotropic, lossless antenna, and fixed values of cable losses. To determine the minimum desired external field environments, data from several sources were considered including the FAA Standard Agency Orders and ICAO Annex 10, Vol. I, Part I. In the end, the field value from the ICAO was considered to high to be valid and was rejected.

According to observations stated in RTCA/DO-199, a disruption threshold in general tends to vary along with the signal level in such a way that the *S/I* ratio stays constant. Thus, if the *S/I* ratio for a receiver is known, the interference level can be determined if desired signal level is also known. While RTCA/DO-199 considered the desired signal to be the minimum receiver signal strength at the edge of coverage airspace, many considered it to be the sensitivity of the receiver (receivers may have much lower sensitivity level than the required). For the analysis in this report, however, only the interference level in RTCA/DO-199 is used, as they are actual measured data.

Table 5.1-1: RTCA/DO-199 Interference Thresholds

	VHF
Desired Signal at Receiver (dBm)	-89
Interference Level (dBm)	-107
Signal/Inteference (S/I) Ratio (dB)	18

5.2 Safety Margin Calculations

Knowing device emission "A", aircraft minimum path loss "-B", and receiver susceptibility threshold "C", safety margin can be computed using

$$Safety\ Margin\ = C - (A + B)$$

This section first calculates the interference signal strength at the receiver's antenna port (A +B). Safety margin can then be computed with the knowledge of "C".

Applying the minimum and the average values of MIPL ("-B") in Table 4.3-1 to the emission data ("A") in Table 3.6-1, the resulting interference signals at the receiver ("A+B") are shown in Table 5.2-1. Due to the large range of IPL "-B" values, the results of the calculation (A+B) are presented with only the maximum and the average values that are calculated from the minimum and the average path loss "-B" values.

Table 5.2-1: Interference Signal Strength at Receiver's Antenna Port (A+B). Maximum and Average values in dBm

	802.11b	**Bluetooth**	**802.11a**	**FRS/GMRS Radio**	**Laptops/ PDA**
VHF(*) (Max/Ave)	-104.0/-125.7	-97.9/-119.6	-98.9/-120.6	-88.2/-109.9	-92.0/-113.7

Comparing the maximum and the average signal strength at the receivers, (A+B), in Table 5.2-1 to the typical and the minimum susceptibility thresholds in Table 5.1-1, safety margins can be calculated. The safety margin results are 2x1 matrices.

Table 5.2-2 reports the results of the calculation with the safety margin results highlighted in **bold** for each combination of WLAN/radio device, MIPL, and interference threshold values. To determine safety

margin, one simply locates the right combinations of WLAN/PED/Radio devices, MIPL values, and interference thresholds in the tables. Thus, for the combination of a 802.11b WLAN device, a minimum MIPL (resulting in the interference signal at receiver of –104 dBm), and a VHF-Com interference threshold (-107 dBm) results in –3 dB safety margin. A large positive safety margin is desirable, whereas a large negative safety margin indicates a possibility of interference.

As observed from the tables, interference safety margins can be positive or negative depending upon the combination of MIPL and receiver interference thresholds used. WLAN devices generally have better safety margin than standard laptops and PDAs based on test data in this effort.

Table 5.2-2: VHF Safety Margin (in dB) for Different Combinations of WLAN/Radio Devices, MIPL and Interference Thresholds

	802.11b &		**BlueTooth &**		**802.11a &**		**FRS/GMRS &**		**Laptops/PDAs &**	
Interference Signal at Receiver (dBm) =	Min MIPL	Ave MIPL	Min MIPL	Ave MIPL	Min MIPL	Ave MIPL	Min MIPL	Ave MIPL	Min MIPL	Ave MIPL
	-104	*-125.7*	*-97.9*	*-119.6*	*-98.9*	*-120.6*	*-88.2*	*-109.9*	*-92*	*-113.7*
VHF-Com Interference Threshold (dBm) *-107*	**-3**	**18.7**	**-9.1**	**12.6**	**-8.1**	**13.6**	**-18.8**	**2.9**	**-15**	**6.7**

6 Summary and Conclusions

Emission measurements were conducted on WLAN devices and two-way radios. These observations were made for the VHF-Com band:

a. WLAN device spurious emissions are not any worse (not higher) than spurious emissions from computer laptops/PDAs in the VHF-Com band.

b. The emission levels from WLAN devices and laptops/PDAs are lower than the FCC limits, but they can be higher than RTCA/DO-160D Category M limits.

c. Spurious emissions from FRS and GMRS two-way radios can be 11 dB higher than RTCA/DO-160D Category M limit, and 4 dB higher than the maximum laptop/PDA emissions.

Interference threshold data are inadequate to thoroughly assess the threat from PED-type EMI. Based on the limited interference threshold data, safety margin calculations were conducted for many aircraft systems. The results show that the safety margins can be negative or positive depending upon the interference thresholds (minimum or typical) and the minimum IPL data (the lowest or the average) used.

7 References

[1] Nguyen, T. X.; Koppen, S. V.; Ely, J. J.; Williams R. A.; Smith, L. J., and Salud, M. T.: *Portable Wireless LAN Device and Two-Way Radio Threat Assessment for Aircraft Navigation Radios,* NASA/TP-2003-212438, July 2003.

[2] Ely, J. J.; Nguyen T. X.; Koppen, S. V.; Salud, M. T.; and Beggs J. H.: *Wireless Phone Threat Assessment and New Wireless Technology Concerns for Aircraft Navigation Radios*, NASA/TP-2003-212446, July 2003.

[3] RTCA/DO-199, *Potential Interference to Aircraft Electronic Equipment from Devices Carried Aboard*, September 16, 1988.

[4] RTCA DO-233, *Portable Electronic Devices Carried On Board Aircraft*, Prepared by SC-177, August 20, 1996.

[5] Hill, David A.: *Electromagnetic Theory of Reverberation Chambers*, Chapter 4, Technical Note 1506, National Institute of Standards and Technology, December 1998.

[6] IEEE Computer Society, LAN/MAN Standards Committee, *Part 11: Wireless LAN Medium Access Control (MAC) and Physical Layer (PHY) Specifications: High-speed Physical Layer in the 5 GHZ Band*, September 16, 1999.

[7] Bluetooth SIG, *Bluetooth Specification Version 1.1*, February 22, 2001.

[8] Ladbury, J.; Koepke, G.; and Camell, D.: *Evaluation of the NASA Langley Research Center Mode-Stirred Chamber Facility*, NIST Technical Note 1508, January 1998.

[9] Crawford, M. L.; and Koepke, G. H.: *Design, Evaluation, and Use of a Reverberation Chamber for Performing Electromagnetic Susceptibility/Vulnerability Measurements*, NBS Technical Note 1092, U. S. Department of Commerce/National Bureau of Standards, April 1986.

[10] International Electrotechnical Commission (IEC) 61000-4-21, 2003 (Draft).

[11] Koppen, S. V.: *A Description of the Software Element of the NASA Portable Electronic Device Radiated Emissions Investigation*, NASA Contractor Report CR-2002-211675, May 2002.

[12] RTCA DO-160D, Change No. 1, Section 20, "Radio Frequency Susceptibility (Radiated and Conducted)", *Environmental Conditions and Test Procedures for Airborne Equipment*", Prepared by SC-135, December 14, 2000.

[13] 47CFR Ch. 1, Part 15.109, "Radiated Emission Limits", *US Code of Federal Regulations,* Federal Register dated December 19, 2001.

[14] 47CFR Ch. 1, Part 15.209, "Radiated Emission Limits; General Requirements", *US Code of Federal Regulations*, Federal Register dated December 19, 2001.

[15] 47CFR Ch. 1, Part 95.635, "Personal Radio Service – Unwanted Radiation", *US Code of Federal Regulations*, Federal Register dated 10-01-98.

[16] Koepke, G.; Hill, D.; and Ladbury, J.: "Directivity of the Test Device in EMC Measurements", *2000 IEEE International Symposium on Electromagnetic Compatibility*, Aug. 21-25, 2000.

[17] Fuller, G.: *B737-200 and B747-400 Path Loss Tests, Victorville, California*. Eagles Wings Inc., Prepared for NASA LaRC under NASA PO# L-16099, Task 1, 2 and 3, 2002.

[18] Veda Inc., *CV-580 RF Coupling Validation Experiment Report*, Report #79689-96U/P30041, 11/15/1996.

[19] Delta Airlines Engineering, *ENGINEERING REPORT Delta/NASA Cooperative Agreement NCC-1-381 Deliverable Reports*, Report No. 10-76052-20, December 8, 2000.

[20] International Civil Aviation Organization (ICAO), Aeronautical Telecommunications, Annex 10, Vol. 1 (Fifth Edition – July 1996).

Appendix A: Measurement and Results of Intentional Transmitters Including WLAN Devices and Two-Way Radios

The following charts illustrate WLAN device idle, ping storm envelope, and file transfer (Xfer) envelope compared to the baseline (idle and file Xfer) of the host laptop. An equivalent measurement noise floor is included in each chart for each band to represent the instrument noise floor, but with calibration factors applied as had been done with the emission data. These charts were used to further reduce the data to the forms that are found in Sections 3.3 and 3.5 of this report. Table A-1 has details on the organization of data charts produced from each wireless communication device tested. Every device tested in a wireless technology category was grouped together by measurement bands, so that each device may be easily compared with others.

The legends in each chart list the data plots by host laptop computer number and WLAN device designation. For instance, Figure A1 displays emission data plots acquired from Laptop 4 with 802.11a WLAN device 11A-1 installed. Tables 3.2-14 to 3.2-16 list the WLAN device designations and associated manufacturers. Table 3.2-4 provides the host laptop designations and manufacturers.

Table A-1: Organization of Charts in this Section

Wireless Technology	Band 1a Figure
802.11A	A1-A5
802.11B	A6-A12
Bluetooth	A13-A18
FRS	A19-A22
GMRS	A23-A25

A.1 802.11A WLAN Devices

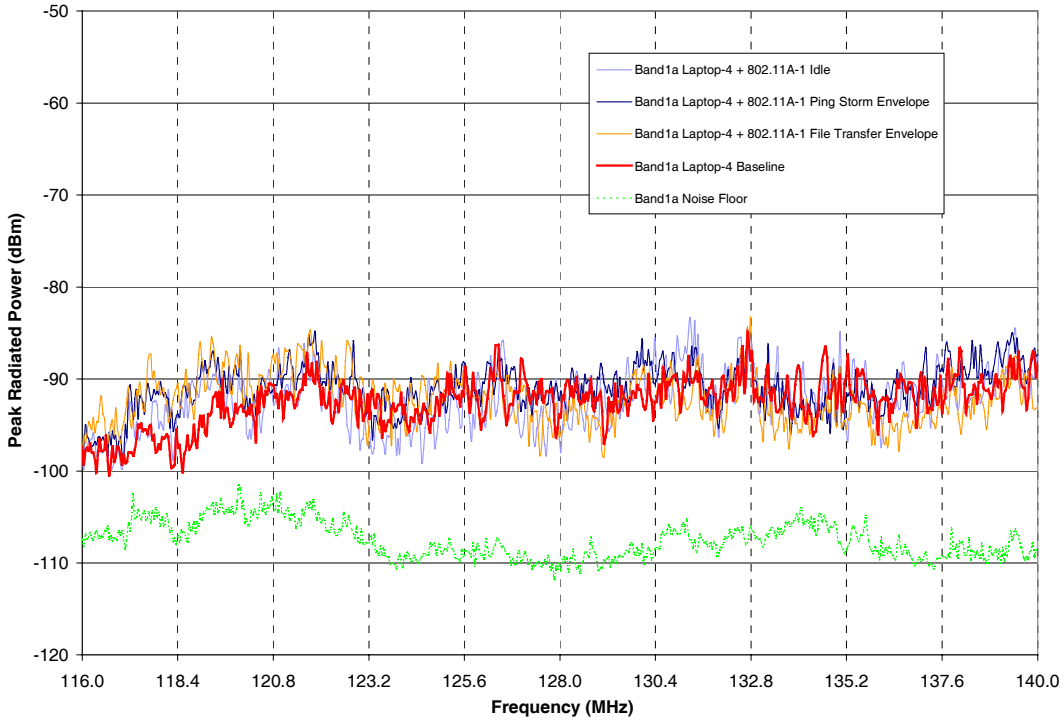

Figure A1: Laptop-4 and 802.11A-1.

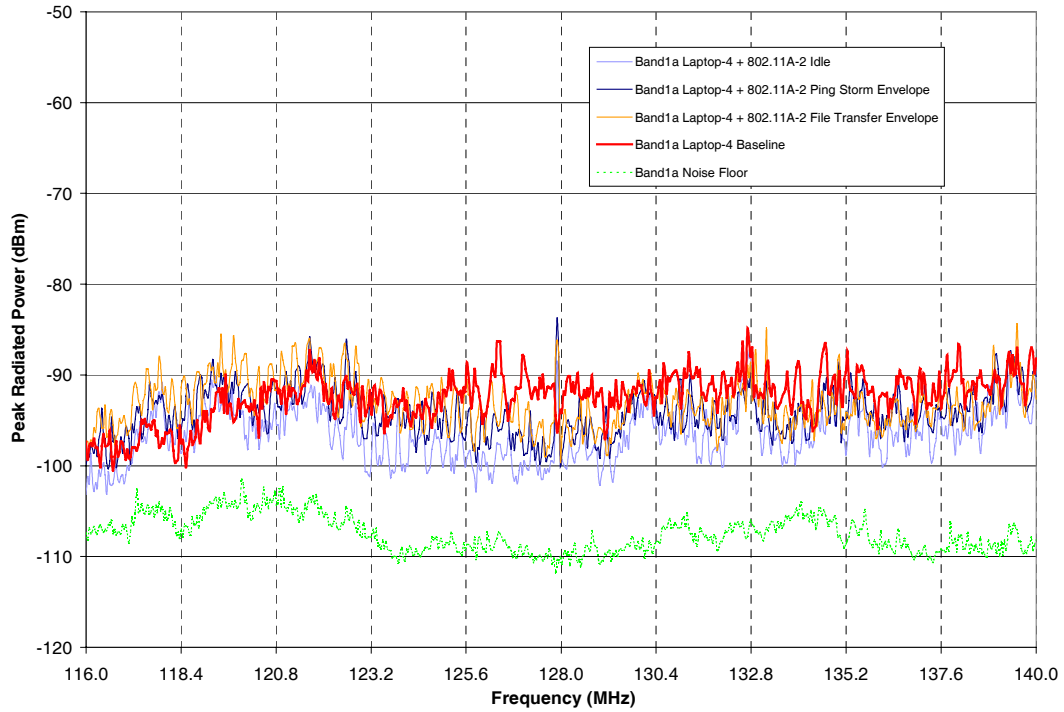

Figure A2: Laptop-4 and 802.11A-2.

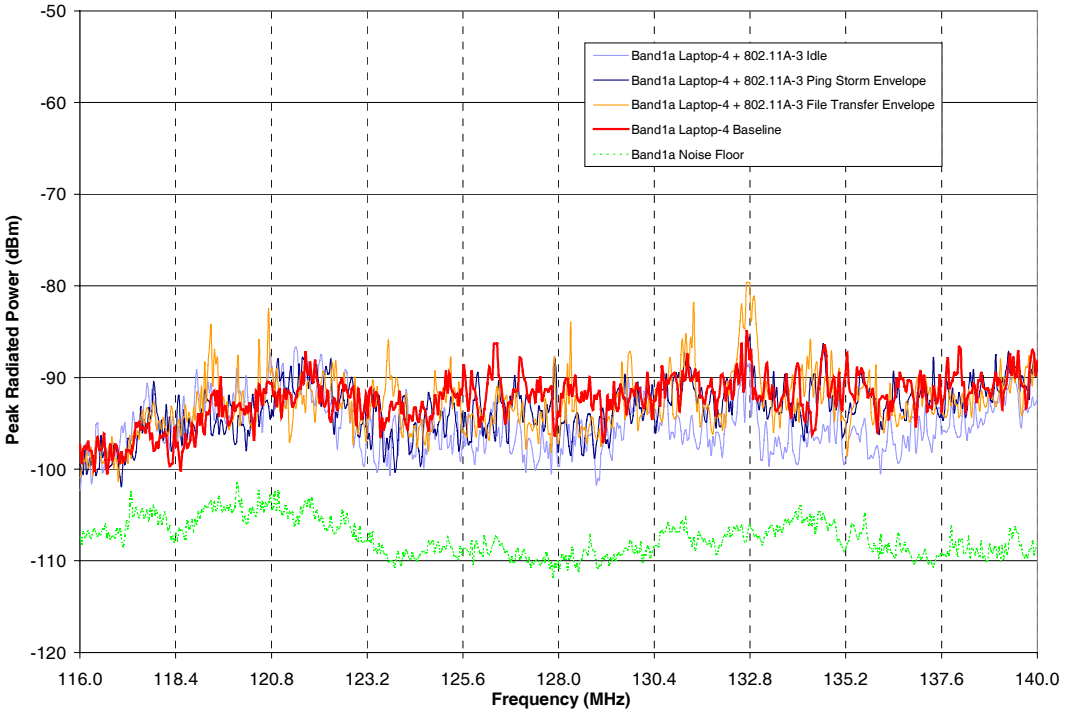

Figure A3: Laptop-4 and 802.11A-3.

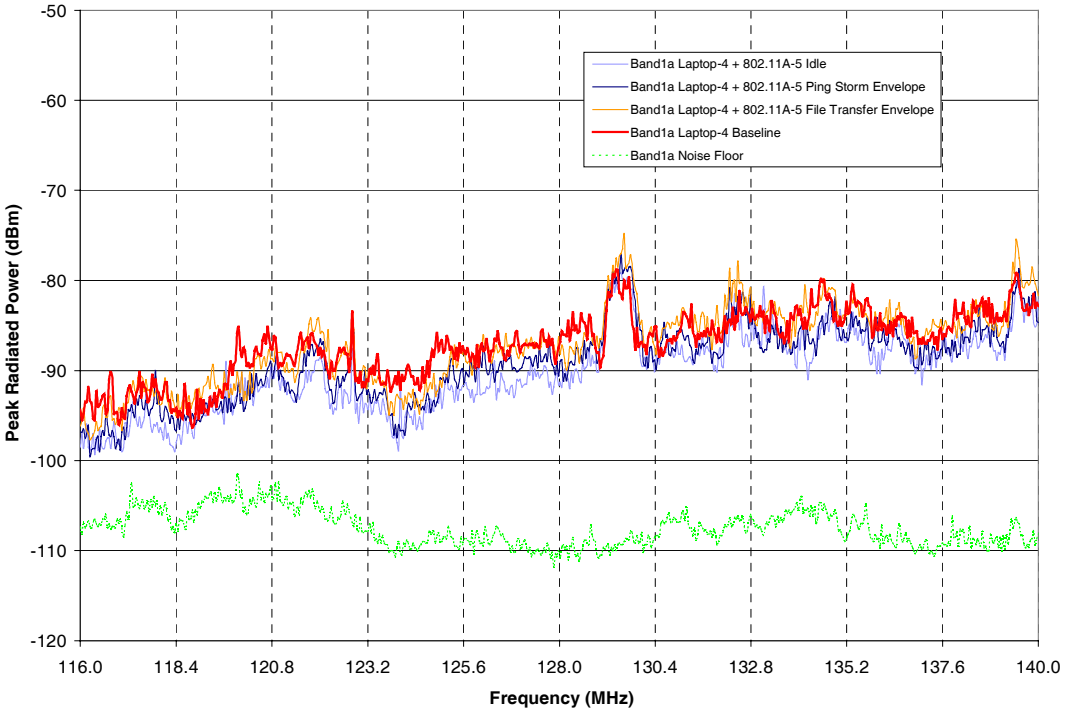

Figure A4: Laptop-4 and 802.11A-5.

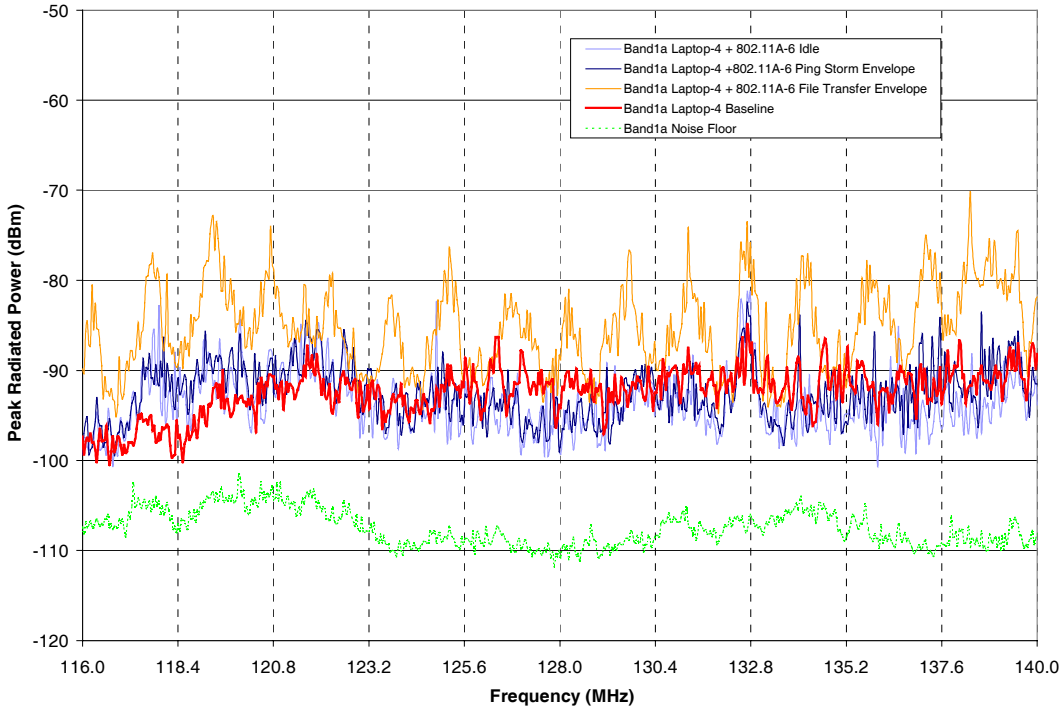

Figure A5: Laptop-4 and 802.11A-6.

A.2 802.11B WLAN Devices

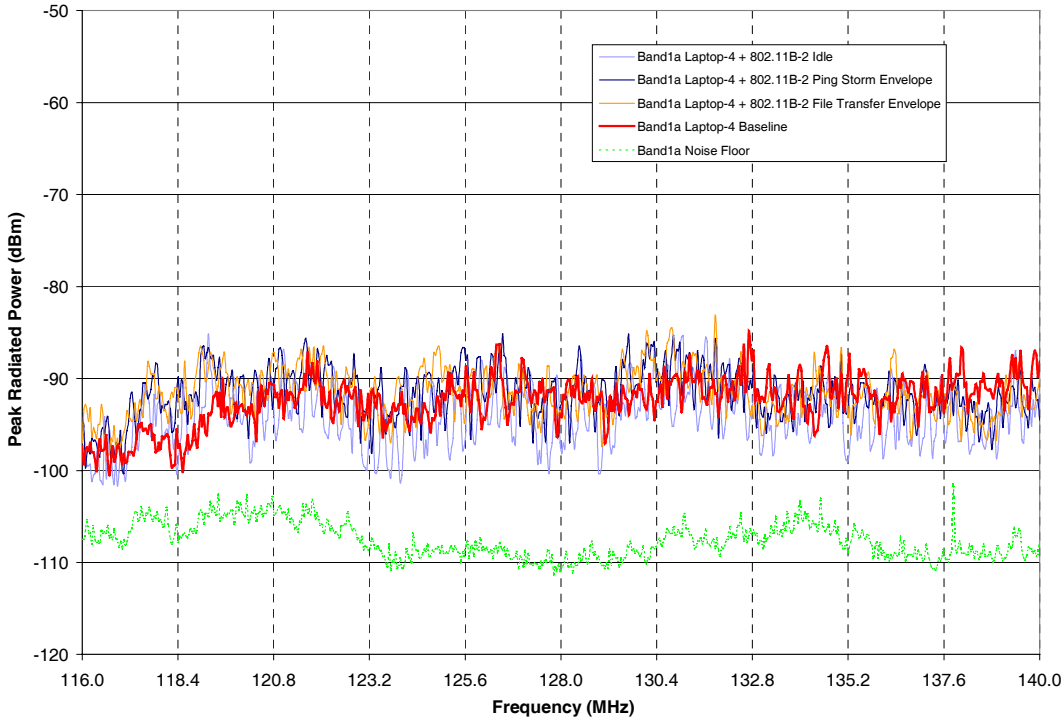

Figure A6: Laptop-4 and 802.11B-2.

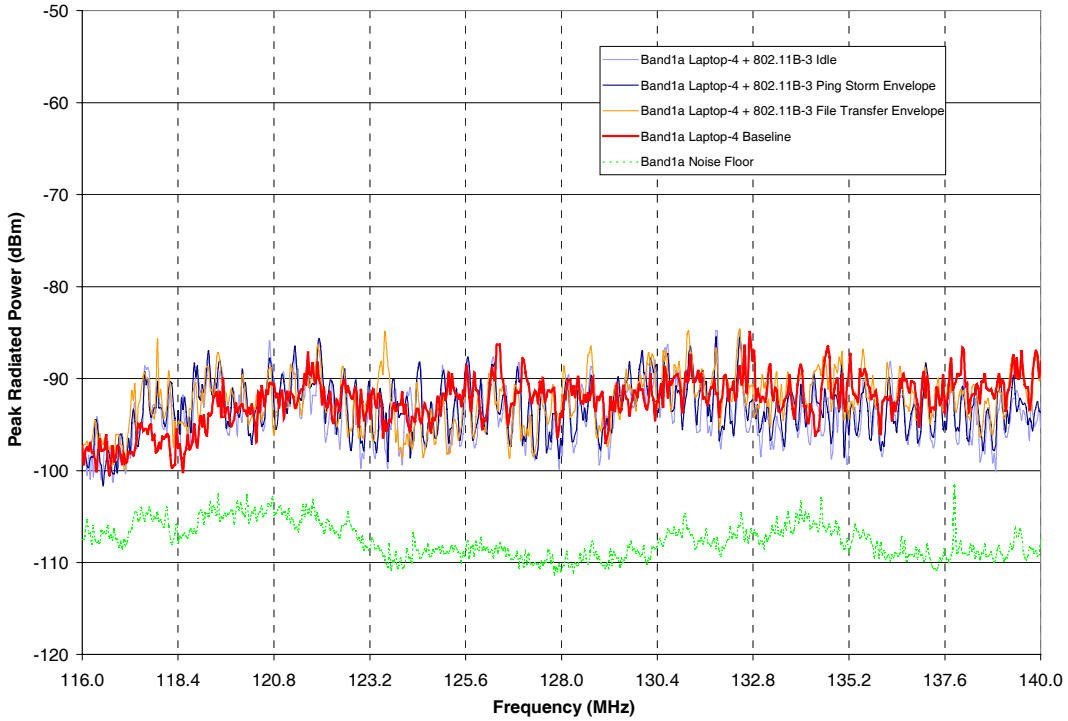

Figure A7: Laptop-4 and 802.11B-3.

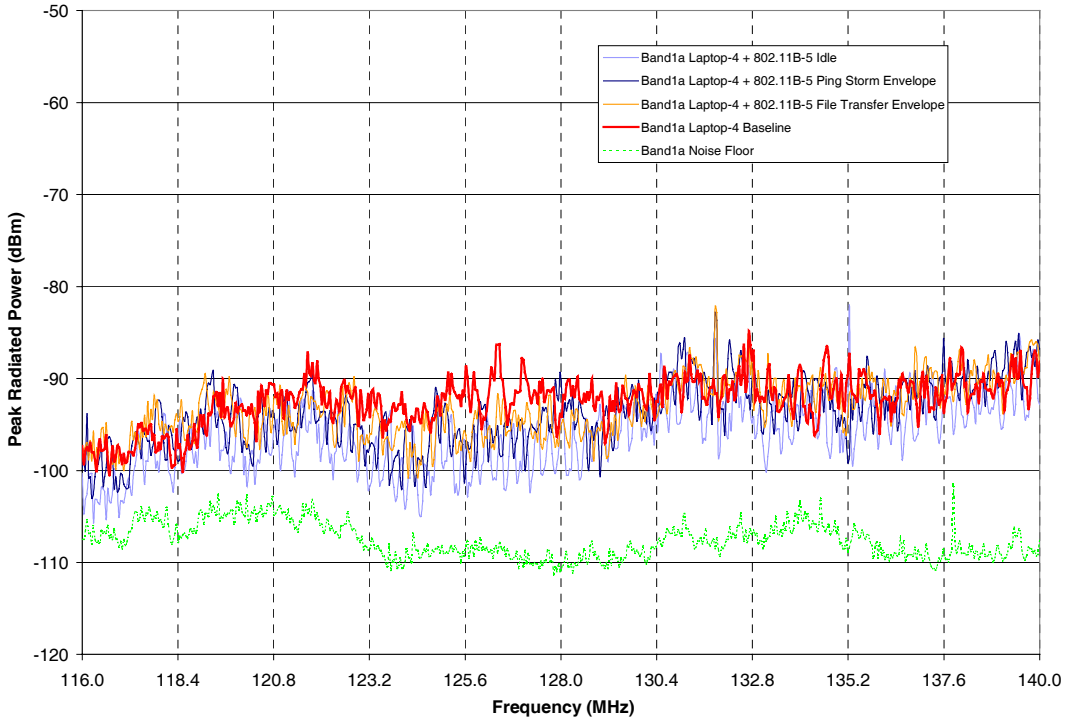

Figure A8: Laptop-4 and 802.11B-5.

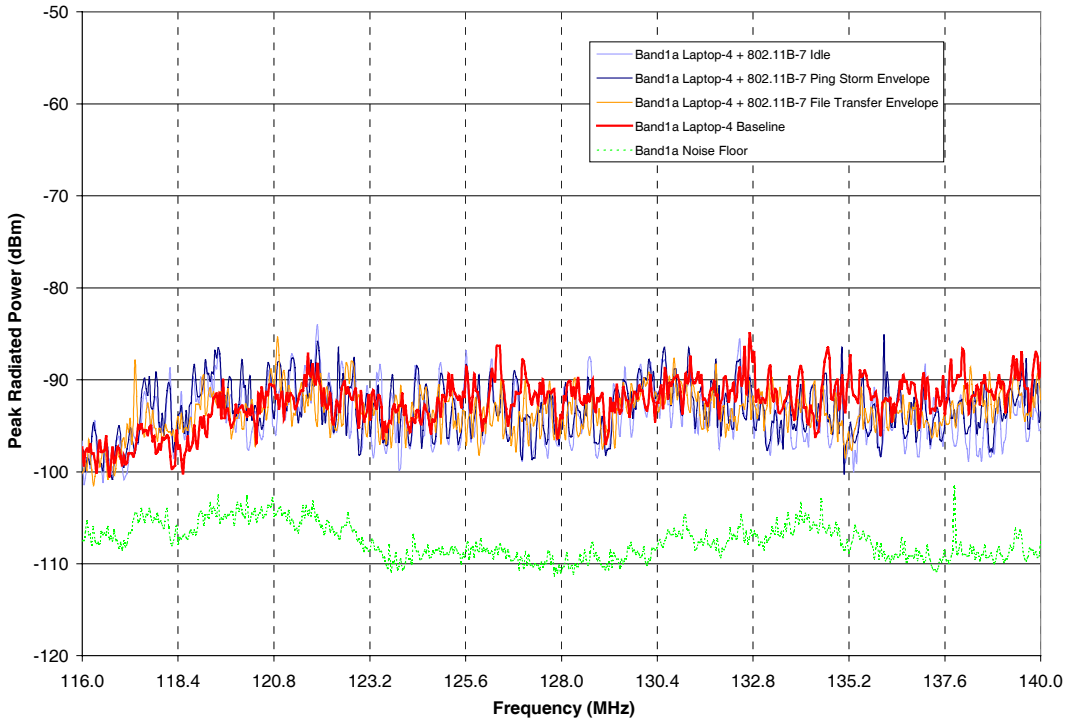

Figure A9: Laptop-4 and 802.11B-7.

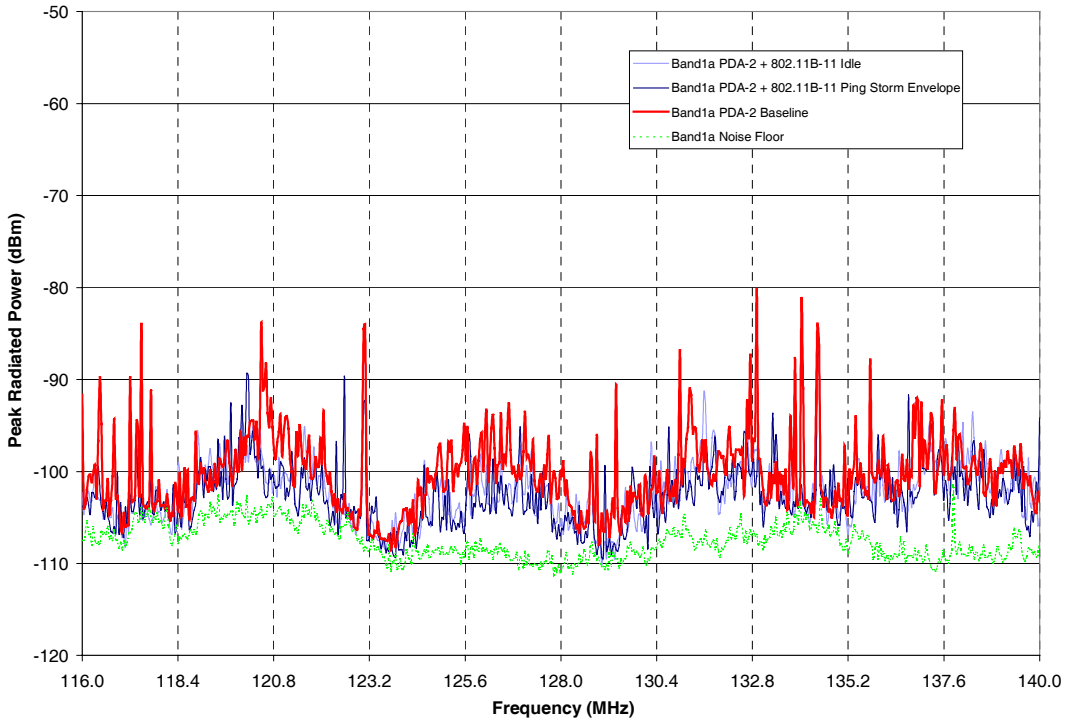

Figure A10: Laptop-4 and 802.11B-11.

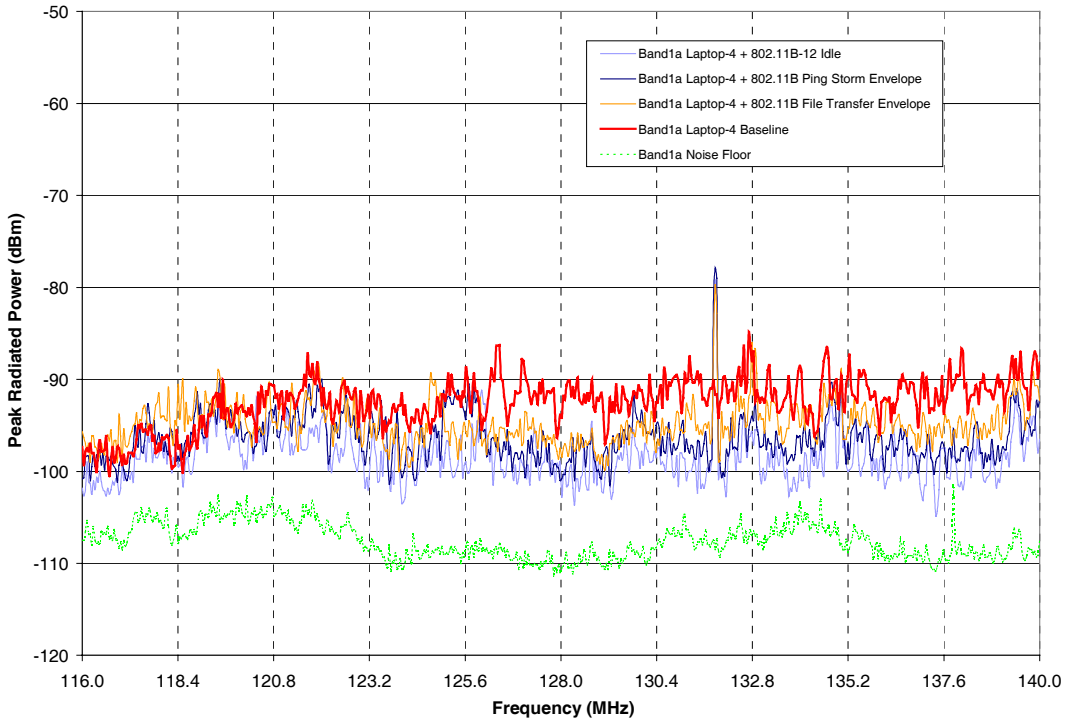

Figure A11: Laptop-4 and 802.11B-12.

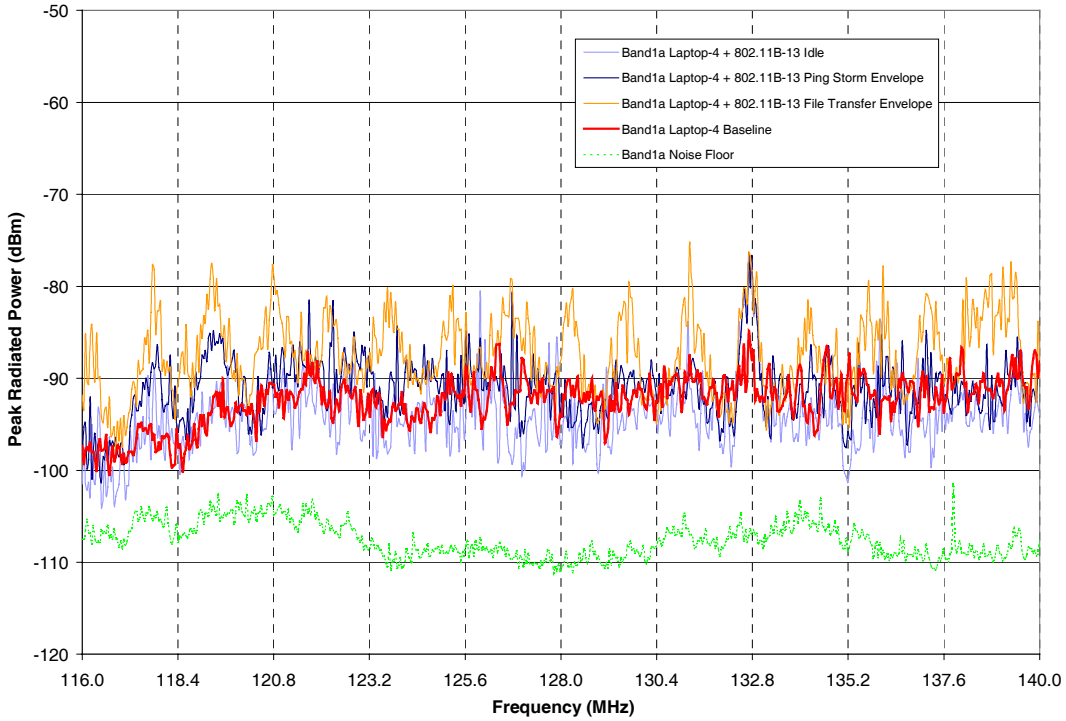

Figure A12: Laptop-4 and 802.11B-13.

A.3 Bluetooth Devices

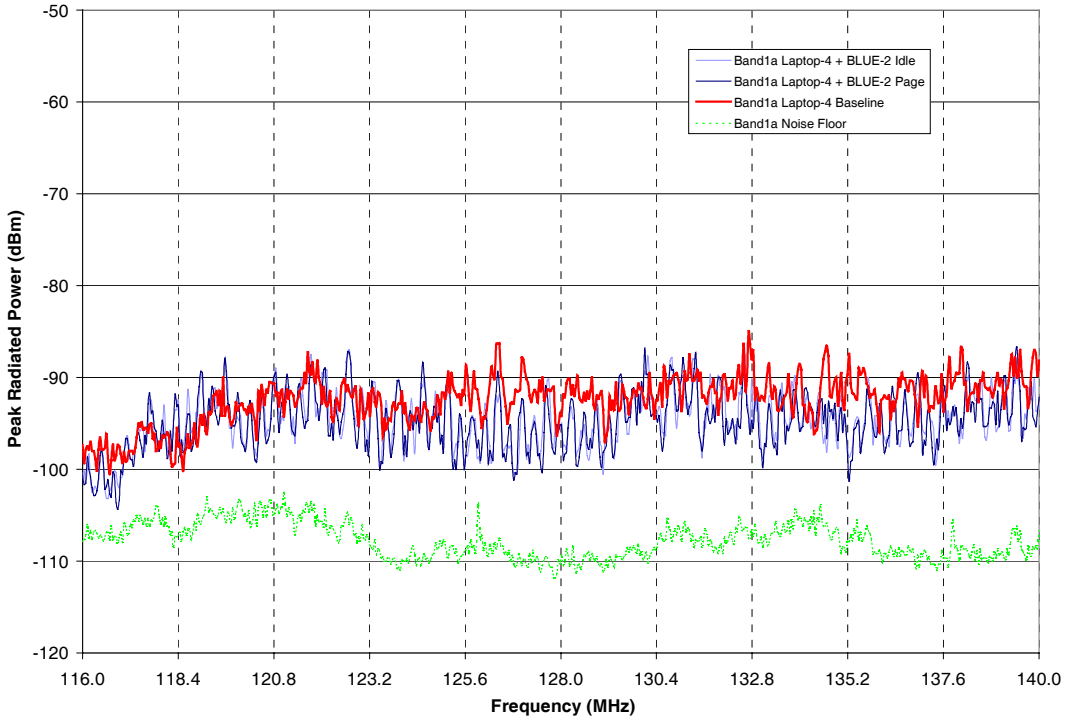

Figure A13: Laptop-4 and BLUE-2.

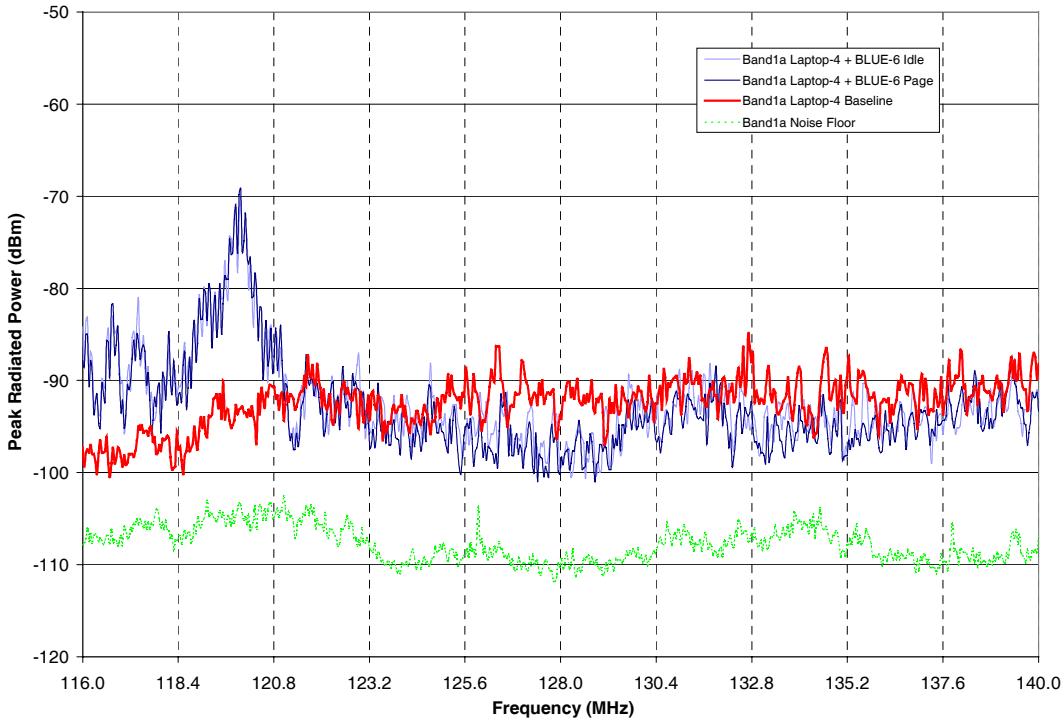

Figure A14: Laptop-4 and BLUE-6.

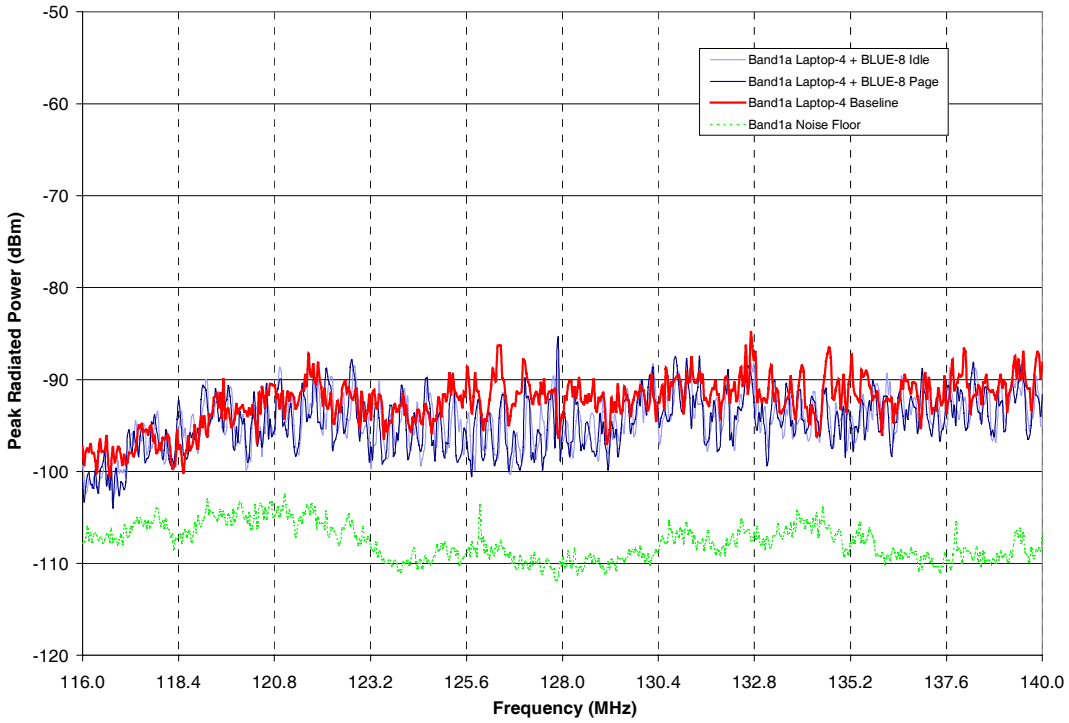

Figure A15: Laptop-4 and BLUE-8.

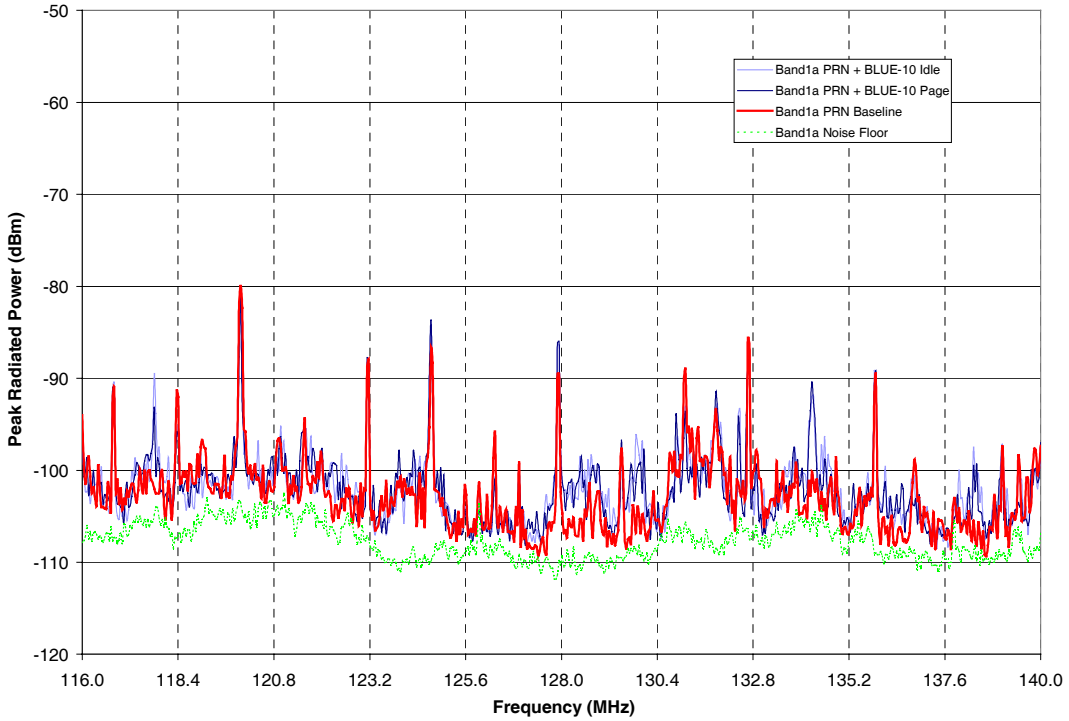

Figure A16: Printer and BLUE-10.

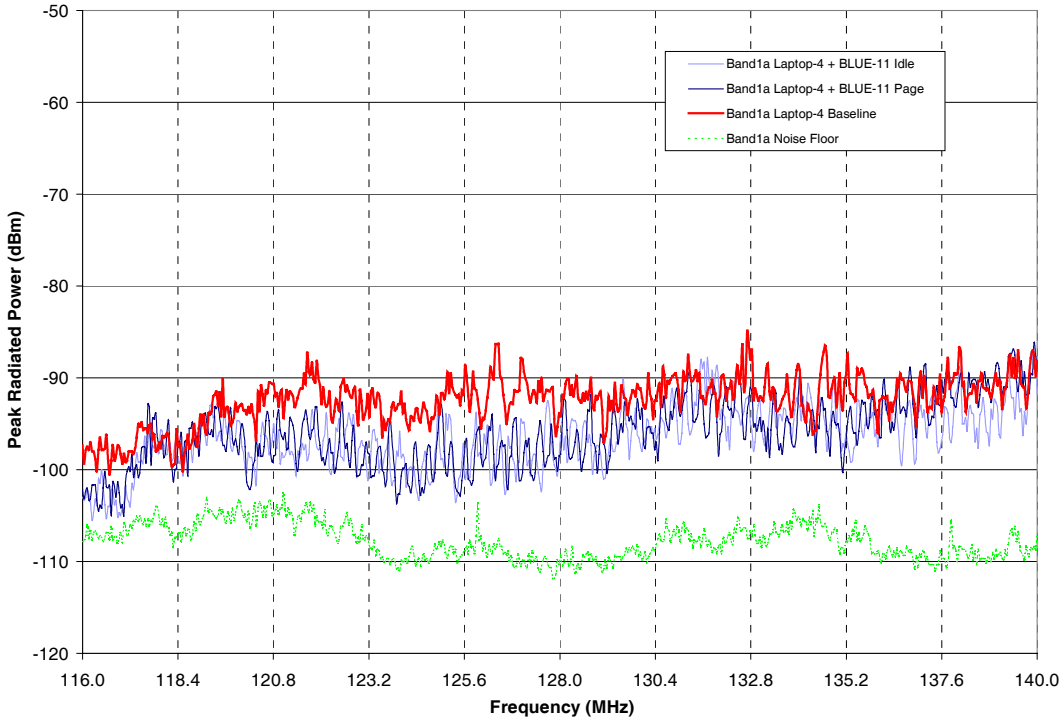

Figure A17: Laptop-4 and BLUE-11.

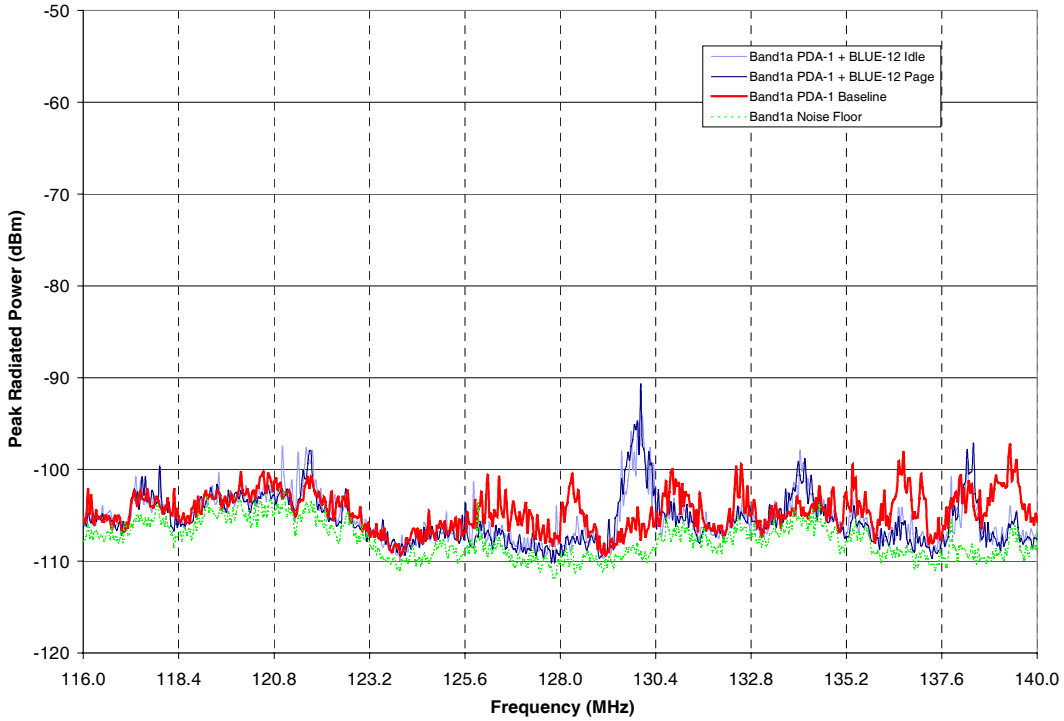

Figure A18: PDA-1 and BLUE-12.

A.4 FRS Radios

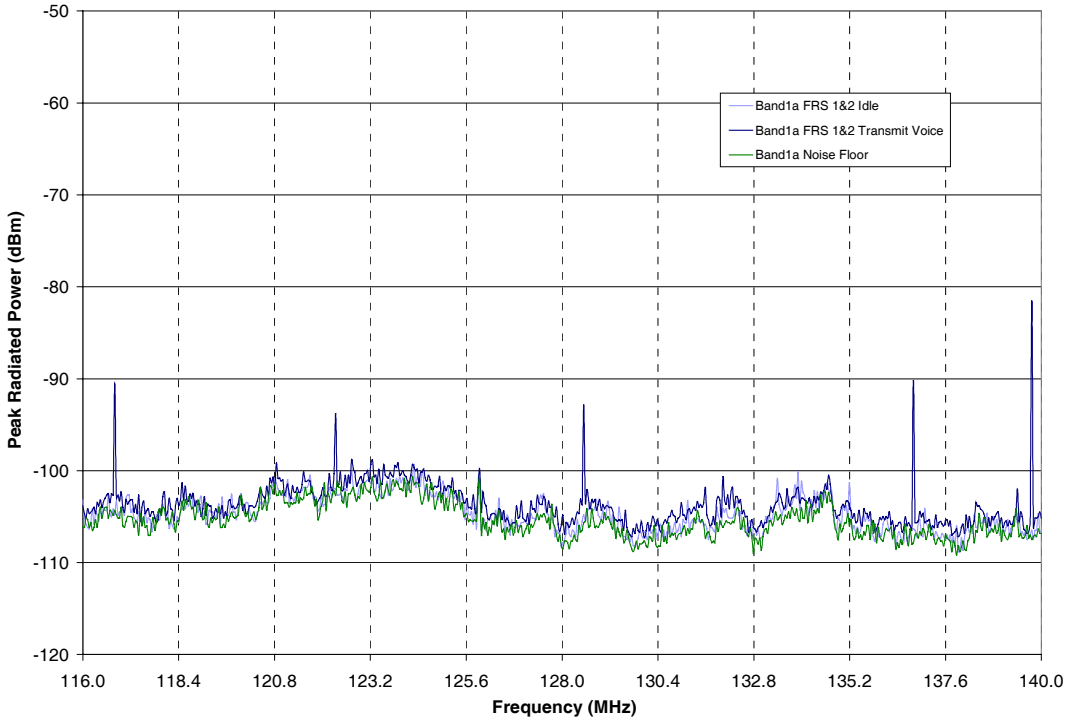

Figure A19: FRS 1 and 2.

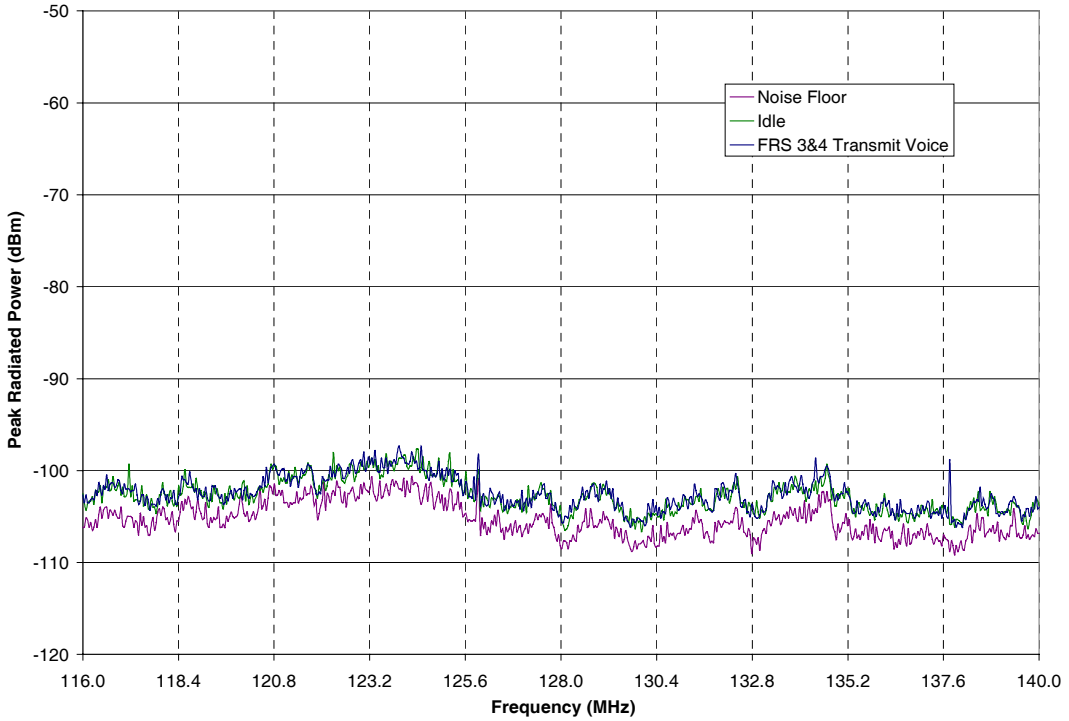

Figure A20: FRS 3 and 4.

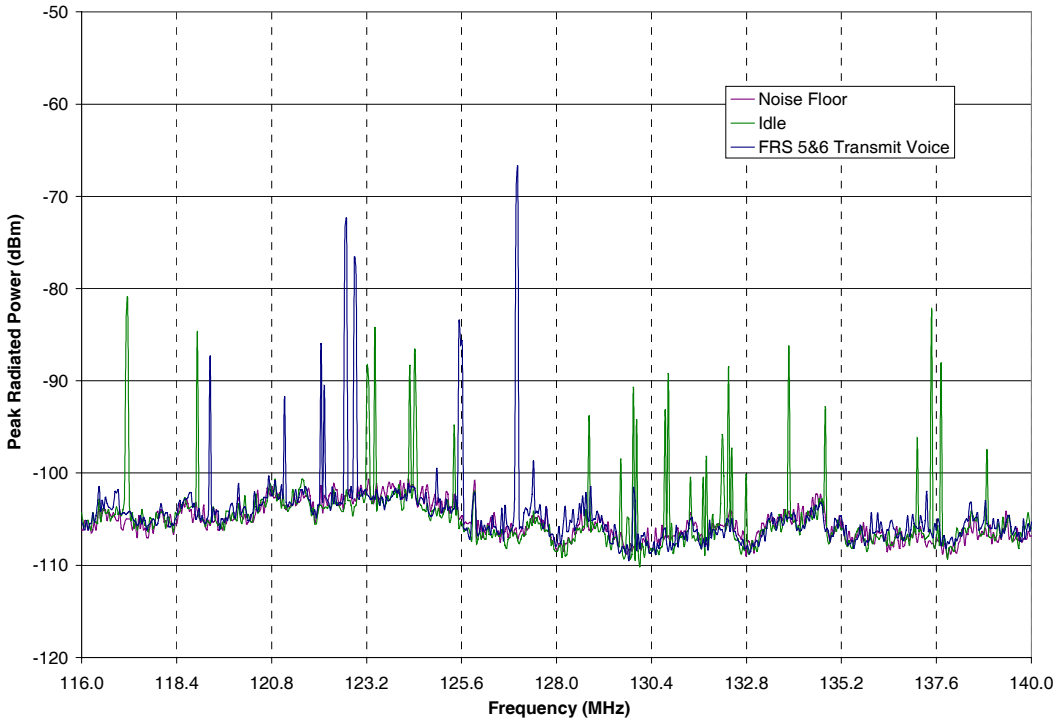

Figure A21: FRS 5 and 6.

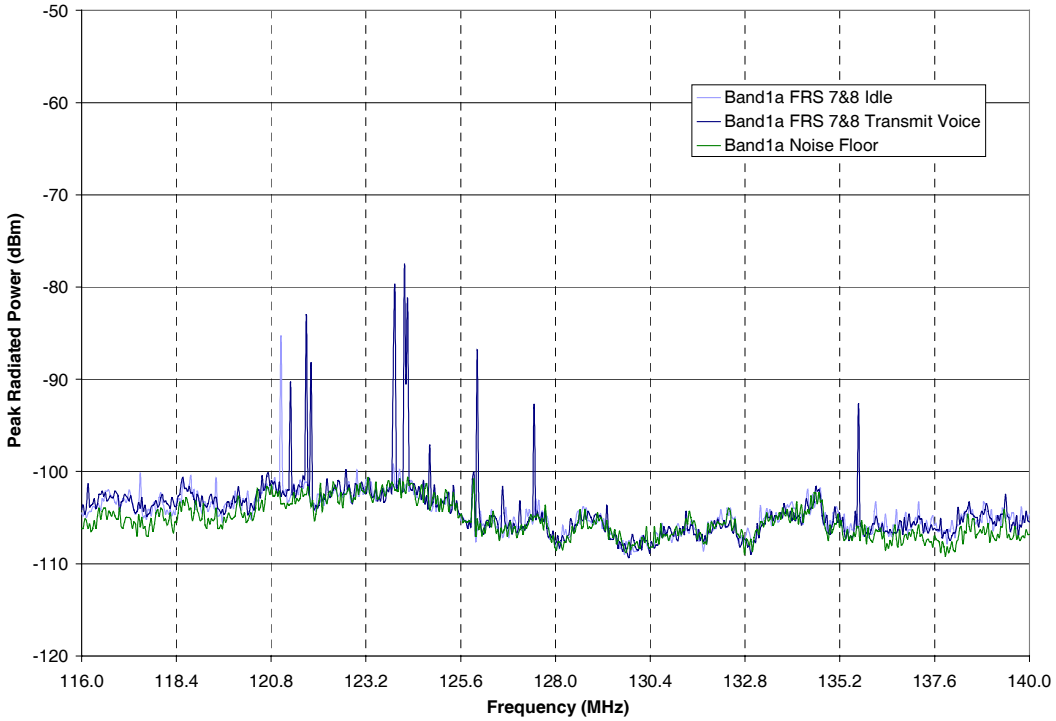

Figure A22: FRS 7 and 8.

A.5 GMRS Radios

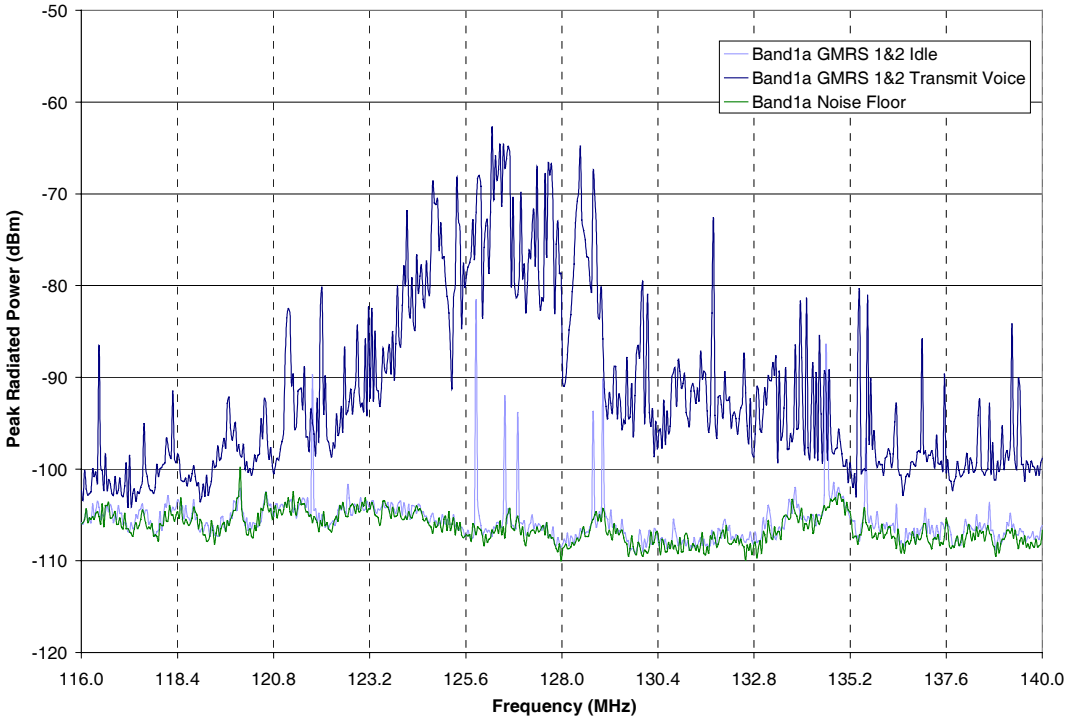

Figure A23: GMRS 1 and 2.

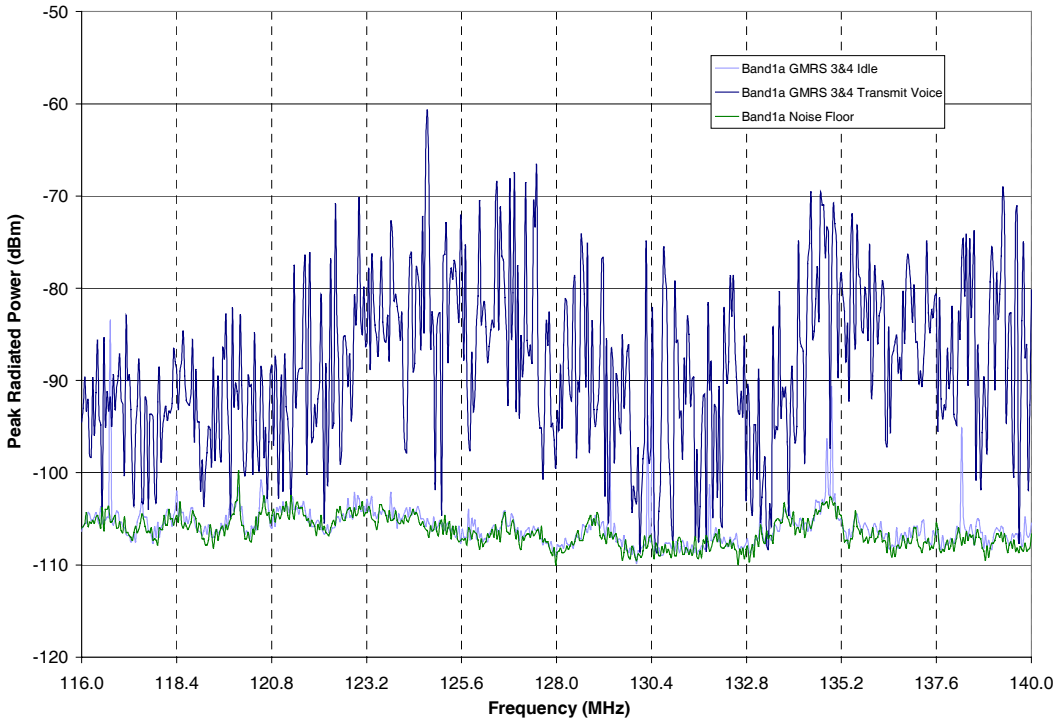

Figure A24: GMRS 3 and 4.

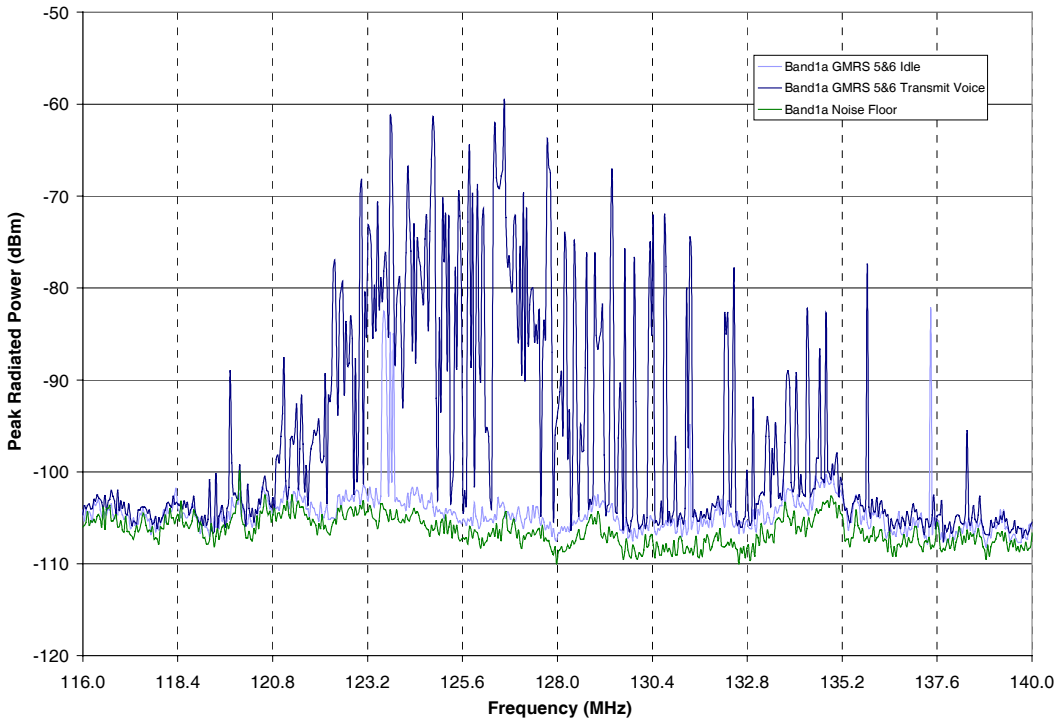

Figure A25: GMRS 5 and 6.

Appendix B: Measurements and Results of Non-Intentional Transmitters Including Computer Laptops and Personal-Digital-Assistants

The following charts show the results of individual modes tested for each non-intentional transmitter, which revealed the best host for each measurement frequency band. These charts were reduced further to achieve the maximum radiated emissions envelope for each host device, as discussed and seen in Section 3.4. Once again the equivalent noise floor was added to the charts to show emissions from the devices were above the calibrated noise floor from the measuring instrument.

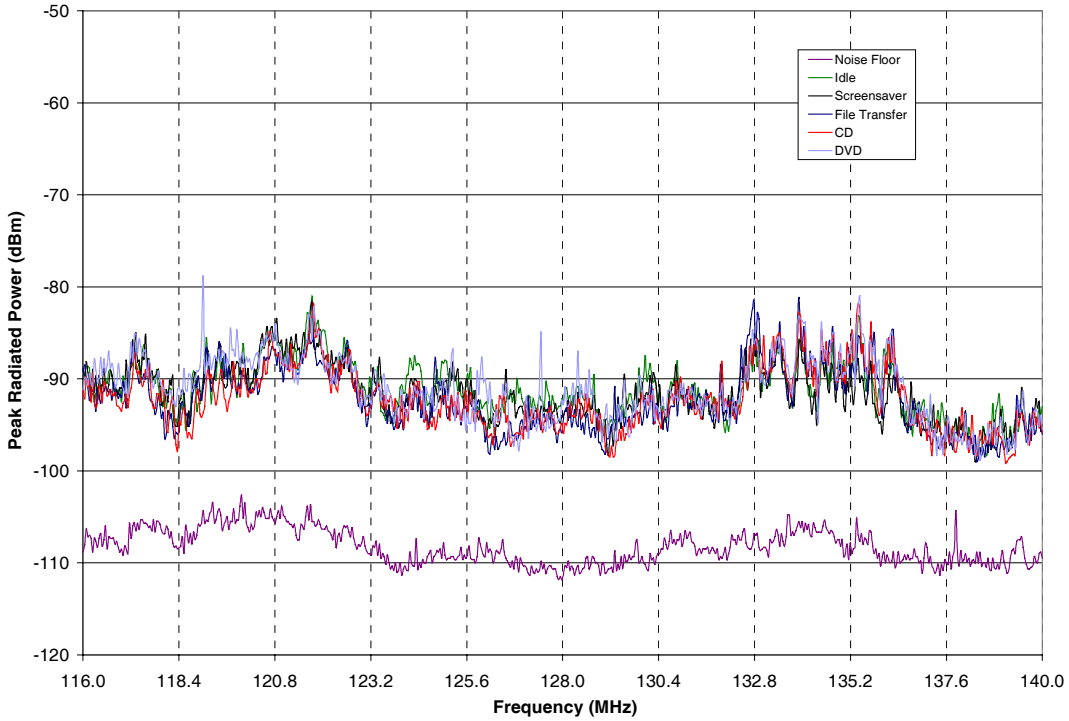

Figure B1: Laptop-1.

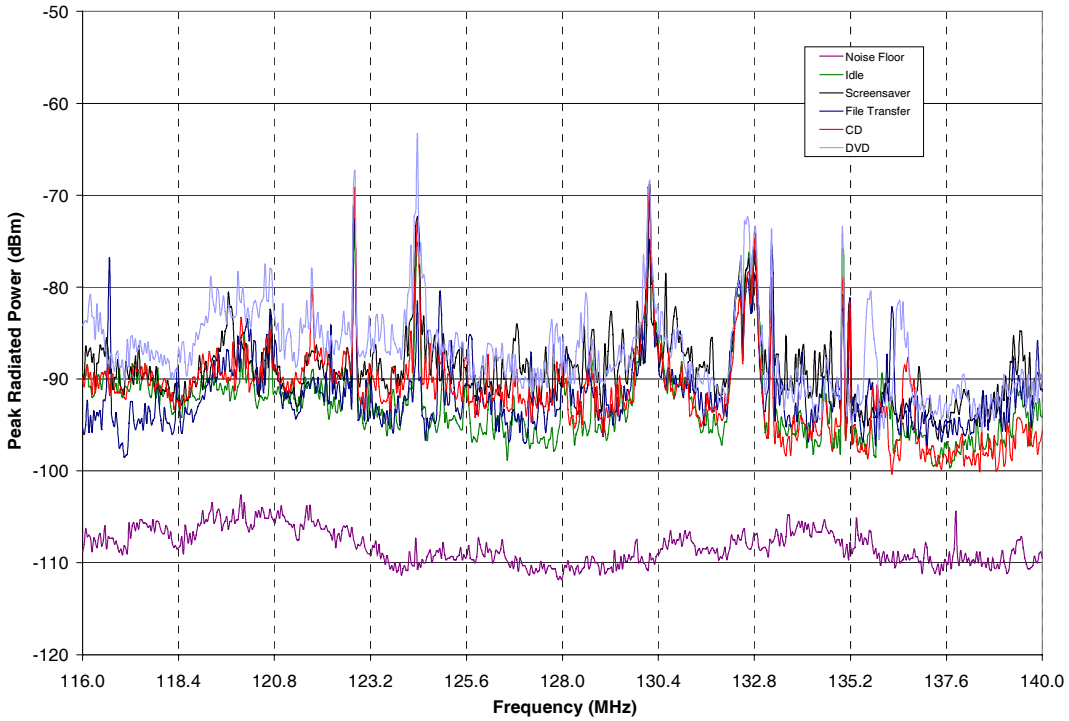

Figure B2: Laptop-2.

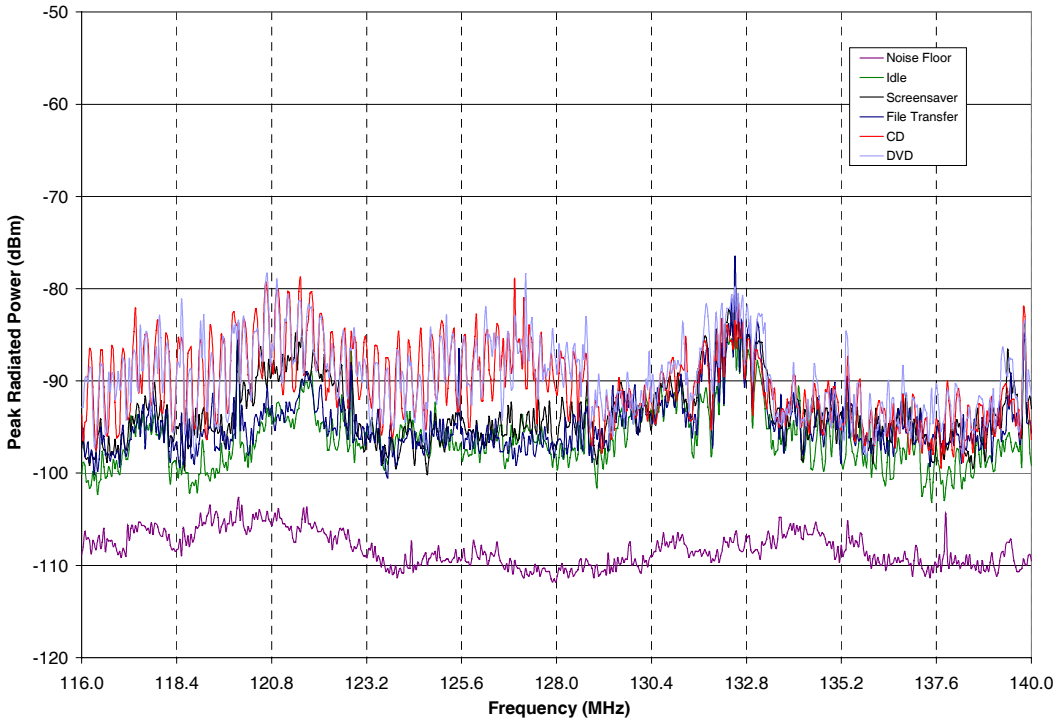

Figure B3: Laptop-3.

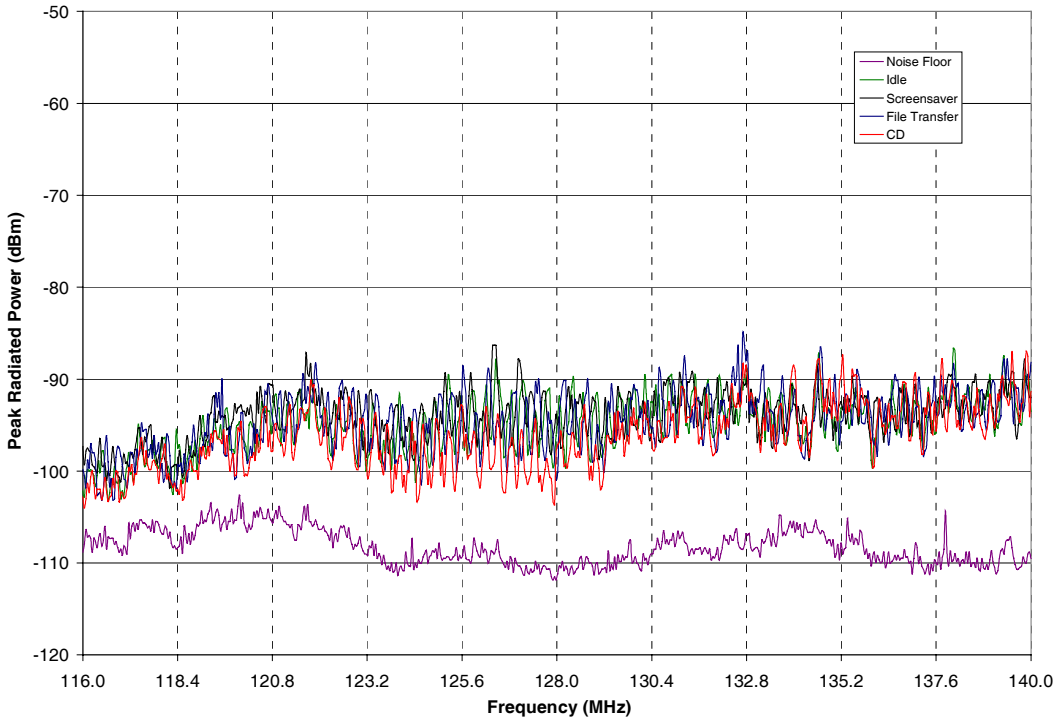

Figure B4: Laptop-4.

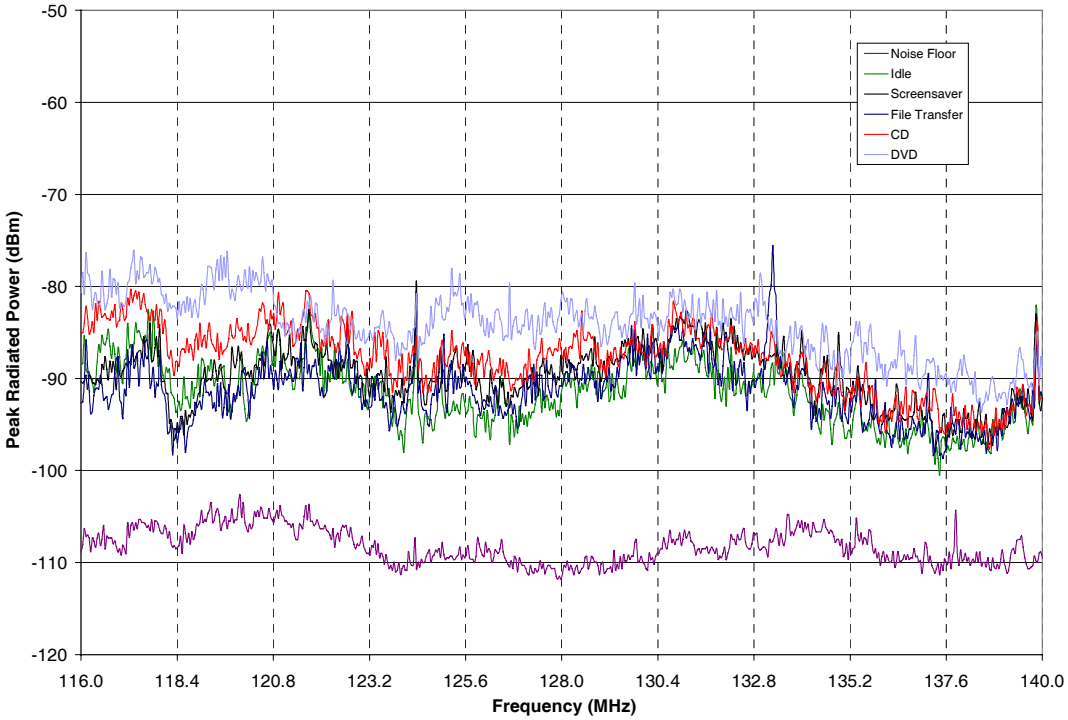

Figure B5: Laptop-5.

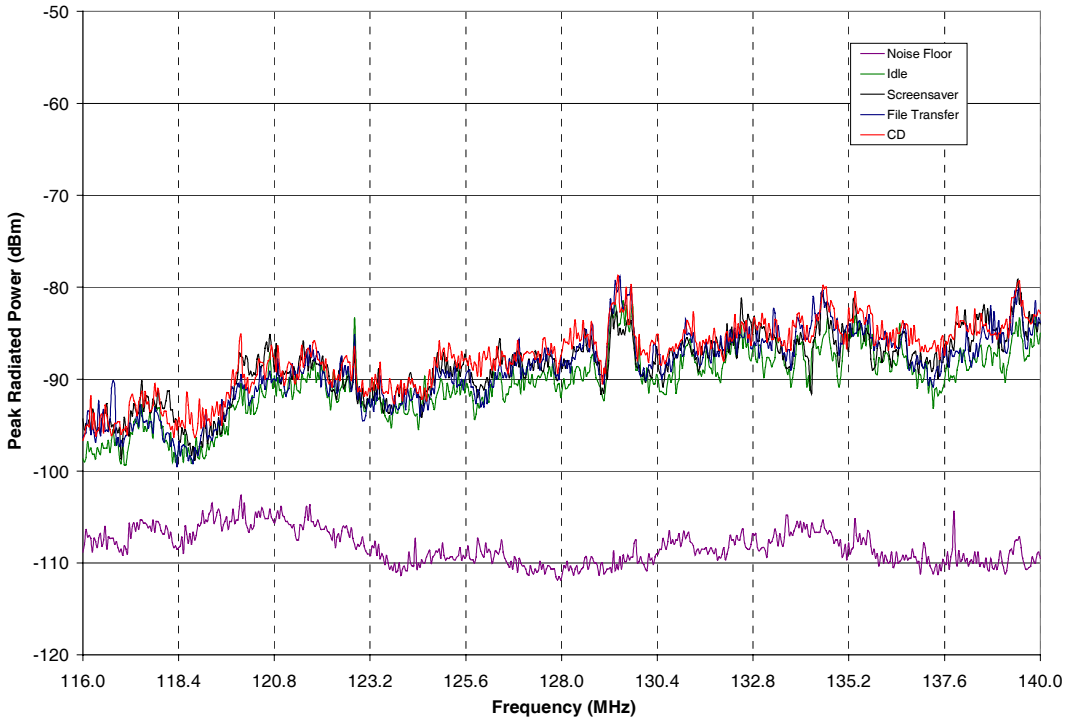

Figure B6: Laptop-6.

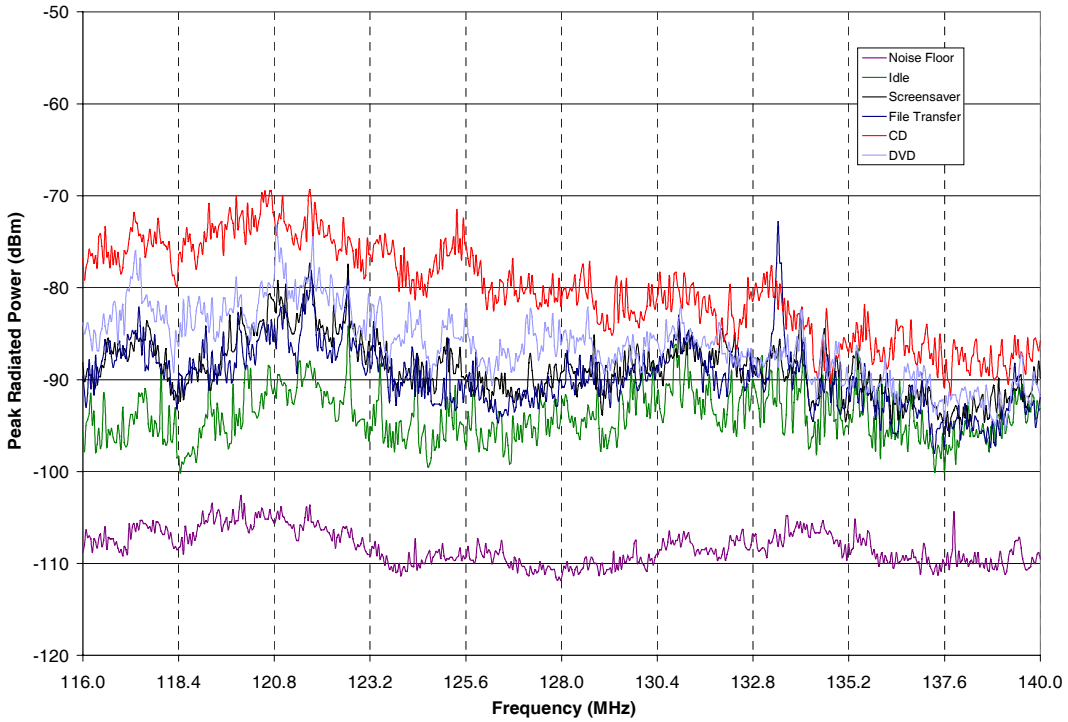

Figure B7: Laptop-7.

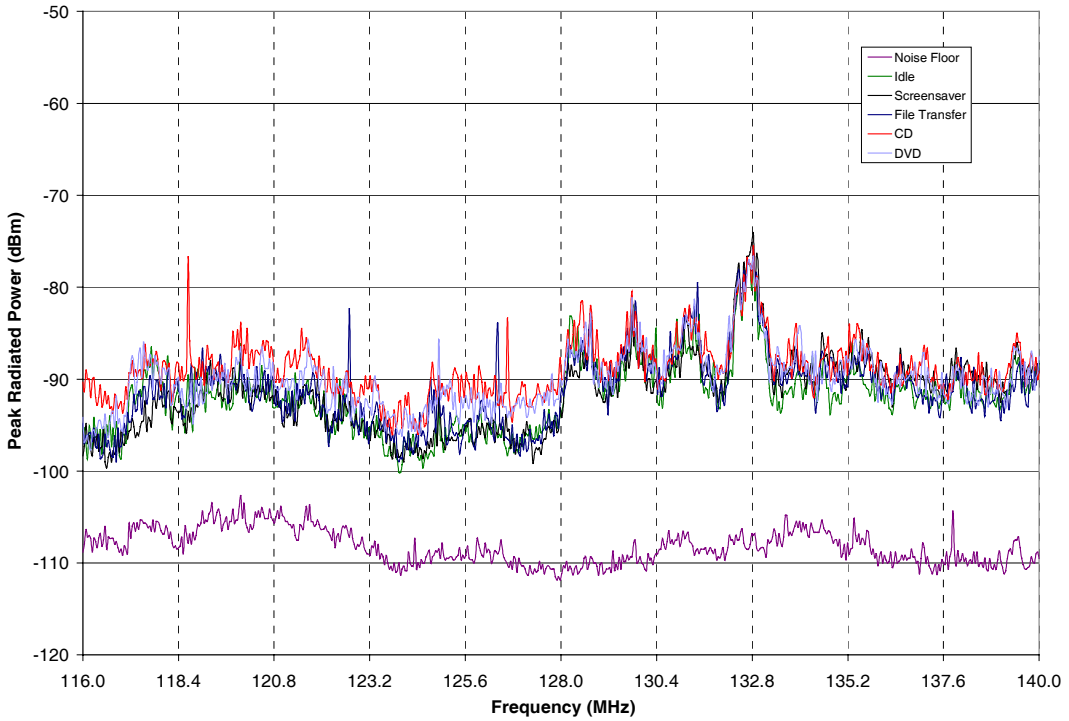

Figure B8: Laptop-8.

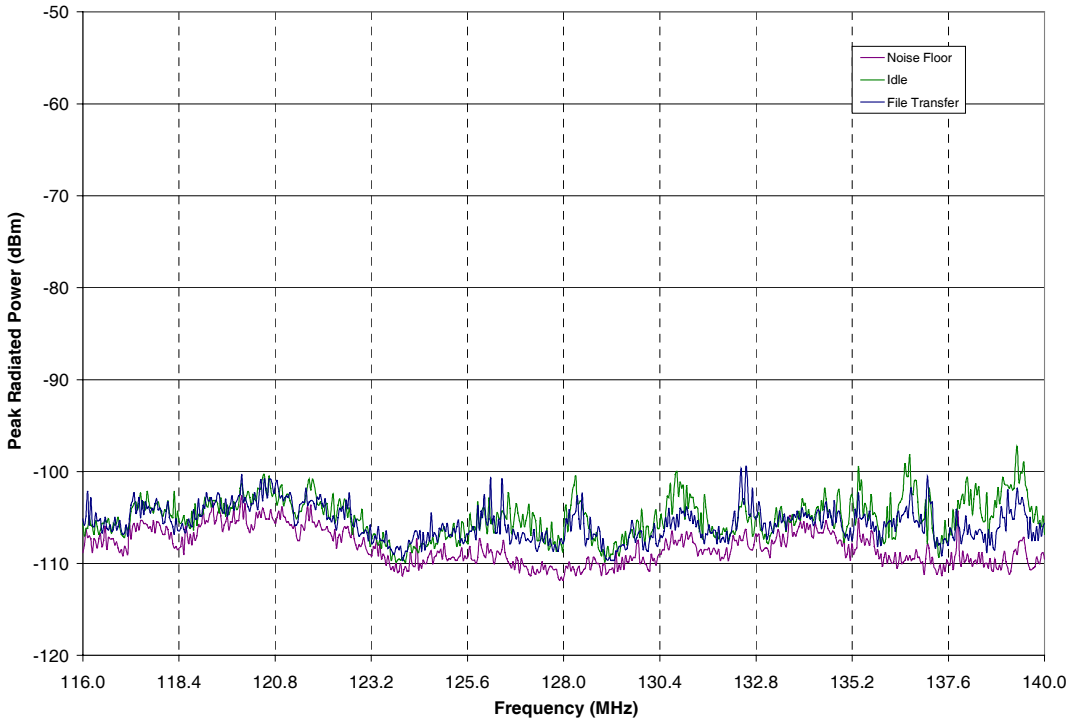

Figure B9: PDA-1.

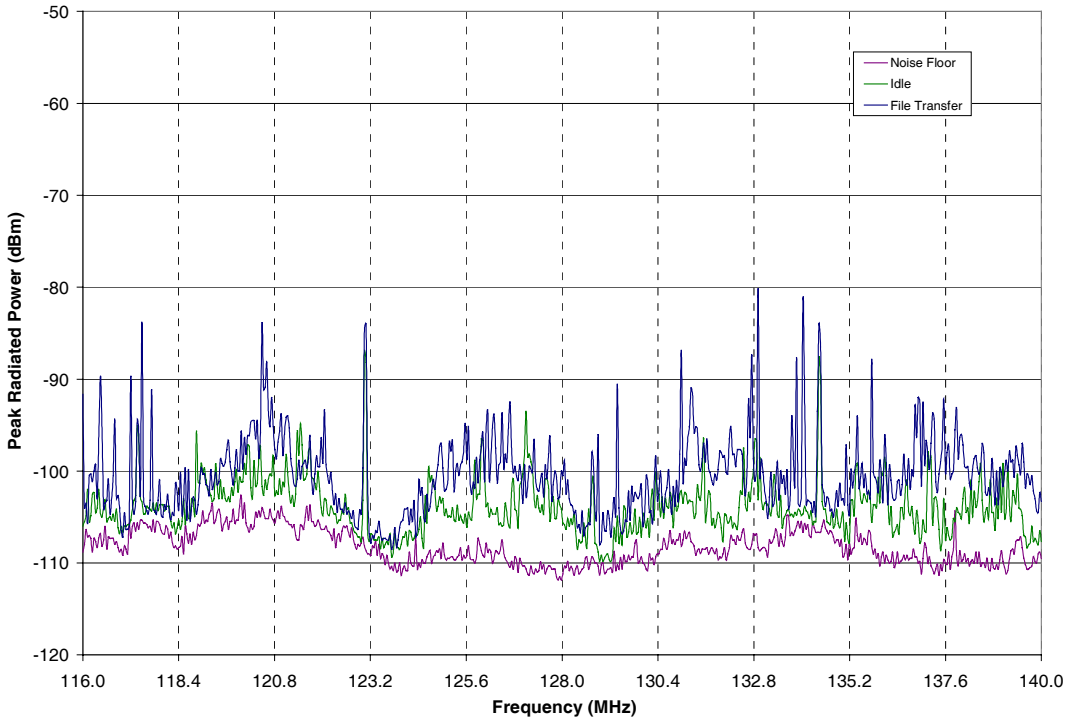

Figure B10: PDA-2.

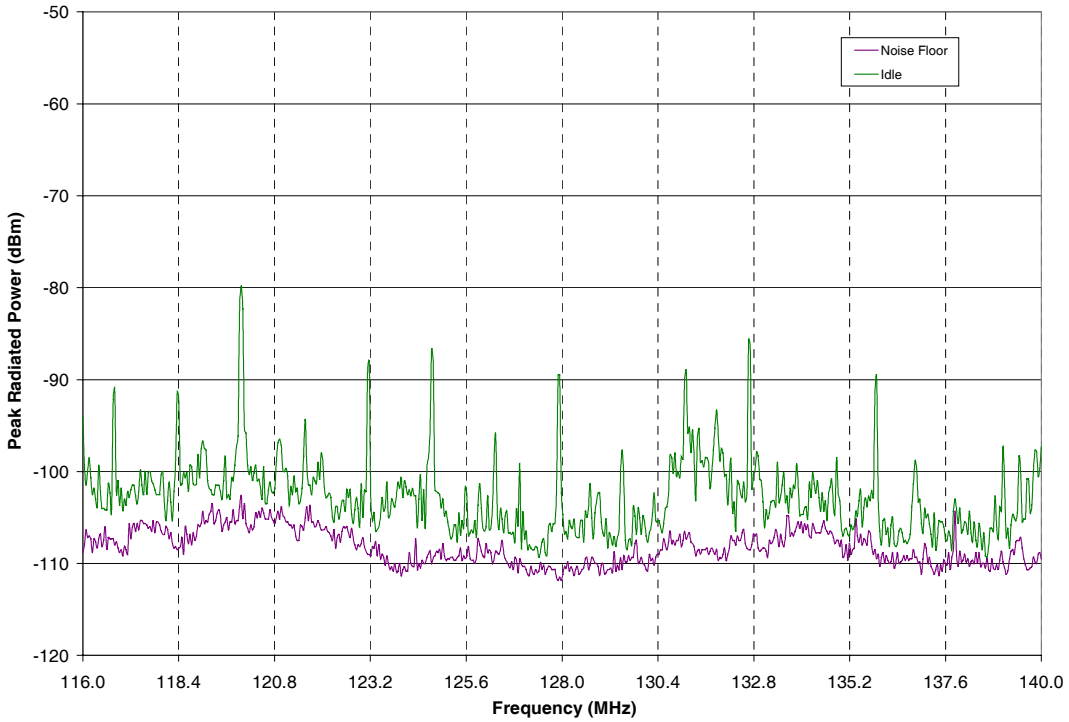

Figure B11: Printer.

REPORT DOCUMENTATION PAGE

Form Approved
OMB No. 0704-0188

1. REPORT DATE *(DD-MM-YYYY)*	2. REPORT TYPE	3. DATES COVERED *(From - To)*
01- 03 - 2004	Technical Memorandum	

4. TITLE AND SUBTITLE

Portable Wireless LAN Device and Two-Way Radio Threat Assessment for Aircraft VHF Communication Radio Band

5a. CONTRACT NUMBER

5b. GRANT NUMBER

5c. PROGRAM ELEMENT NUMBER

6. AUTHOR(S)

Nguyen, Truong X.; Koppen, Sandra V.; Ely, Jay J.; Williams, Reuben A.; Smith, Laura J.; and Salud, Maria Theresa P.

5d. PROJECT NUMBER

5e. TASK NUMBER

5f. WORK UNIT NUMBER

23-728-30-10

7. PERFORMING ORGANIZATION NAME(S) AND ADDRESS(ES)

NASA Langley Research Center
Hampton, VA 23681-2199

8. PERFORMING ORGANIZATION REPORT NUMBER

L-18362

9. SPONSORING/MONITORING AGENCY NAME(S) AND ADDRESS(ES)

National Aeronautics and Space Administration
Washington, DC 20546-0001

10. SPONSOR/MONITOR'S ACRONYM(S)

NASA

11. SPONSOR/MONITOR'S REPORT NUMBER(S)

NASA/TM-2004-213010

12. DISTRIBUTION/AVAILABILITY STATEMENT

Unclassified - Unlimited
Subject Category 33
Availability: NASA CASI (301) 621-0390 Distribution: Standard

13. SUPPLEMENTARY NOTES

An electronic version can be found at http://techreports.larc.nasa.gov/ltrs/ or http://ntrs.nasa.gov

14. ABSTRACT

Measurement processes, data and analysis are provided to address the concern for Wireless Local Area Network devices and two-way radios to cause electromagnetic interference to aircraft Very High Frequency (VHF) Voice Communication system. In this study, spurious radiated emissions in the VHF band from various wireless network devices and two-way radios are characterized using a reverberation chamber. The results are compared against baseline measurement results from standard laptop computers and personal-digital-assistants as these devices are currently allowed for use during parts of flight. Also reported are aircraft interference path loss data and in-band on-channel interference threshold in the VHF band. From these data, interference risk is assessed for the aircraft VHF communication system.

15. SUBJECT TERMS

Electromagnetic, Compatibility, Interference, Susceptibility, VHF, Avionics Pathloss, Emission, PED, Wireless, WLAN, Two-Way Radio, FRS, GMRS

16. SECURITY CLASSIFICATION OF:			17. LIMITATION OF ABSTRACT	18. NUMBER OF PAGES	19a. NAME OF RESPONSIBLE PERSON
a. REPORT	b. ABSTRACT	c. THIS PAGE			STI Help Desk (email: help@sti.nasa.gov)
					19b. TELEPHONE NUMBER *(Include area code)*
U	U	U	UU	93	(301) 621-0390